A THEORETICAL AND EXPERIMENTAL INVESTIGATION OF THE THERMAL BUCKLING OF FLAT RECTANGULAR PLATES

by

Ronald W. Jackson, B.Sc. (Eng.), A.M.I.Mech.E.

A Thesis presented to the University of Glasgow

for the Degree of Doctor of Philosophy

September 1960

ABSTRACT

The thesis presents a theoretical and experimental investigation of the buckling of flat rectangular plates when subjected to symmetrical and asymmetrical temperature distributions over their lateral surfaces. These temperature distributions induce thermal stresses. Under certain conditions the compressive component of the induced thermal stresses causes the plate to buckle out of its own plane.

The evaluation of the critical temperature, which initiates buckling, is carried out in two successive steps.

1. A solution of the biharmonic equation that governs the distribution of thermal stresses under stable conditions is obtained.
2. This stable state distribution of thermal stresses is utilised to obtain an approximate solution of the equation governing the stability of flat plates with internal varying stresses. This gives the value of the critical temperature at the onset of buckling.

The subject matter of the thesis is divided into four parts:-

PART I is a review of the published literature covering rigorous and approximate methods which have been used to determine the stable state

distribution of thermal stresses and the evaluation of the critical buckling temperature. It also includes considerations of plate deflections in the post-buckling range with particular reference to the growth of the plate centre deflection with increasing values of plate temperature differential.

PART II deals exclusively with the theoretical analysis and evaluation of the critical buckling temperature.

It includes, as its first consideration, the determination of the steady state distribution of thermal stresses in the plate. An approximate solution of the biharmonic equation, governing the distribution of stresses is presented using the Kantorovitch Method. This is followed by an original application of the Rayleigh-Ritz Method, to obtain an approximate solution of the biharmonic equation giving the thermal stresses in a polynomial form.

This is followed by an investigation of the effects of plate aspect ratio and the degree of asymmetry of the temperature distributions on the value of critical temperature. The cases considered have, to the author's knowledge, not been investigated hitherto.

The numerical work associated with the theoretical analysis was carried out on a 'Deuce' Computer using Alpha Code and General Interpretive Programmes.

PART III presents the experimental work carried out in substantiation of the theoretical methods used in Part II. This covers the

determination of the critical buckling temperatures and deformations of aluminium alloy plates, of aspect ratios ranging from one to three, subjected to symmetrical and asymmetrical temperature distributions.

PART IV discusses, critically examines and summarises the comparison and correspondence obtained between the theoretically predicted and experimentally determined values of critical temperatures and deformations. It is shown that good agreement exists.

The thesis concludes with six appendices which present detailed analyses and calculations followed by a bibliography.

LIST OF SYMBOLS

a	half-plate length in x direction, in.
a_{mn}	coefficients or vectors in series expansion for plate deflections.
b	half-plate width in y direction, in.
D	plate flexural stiffness, $\frac{Et^3}{12(1-\nu^2)}$
E	Young's modulus of plate material, lb./in.^{2}
j	$\sqrt{-1}$, unless defined otherwise.
t	plate thickness, in.
m,n,p,q	integers
T	temperature distribution in plate, ^{o}C.
T_o	temperature differential, difference between centre and edge temperature in 'tent-like' temperature distribution (see figure 23), difference between maximum and edge temperature (see figure 24), ^{o}C.
T_1	temperature difference between centre and edge of plate of reference 6 (see figure 3).
T_{st}	temperature coefficient in a Fourier series.
T_{ocr}	critical value of T_o, ^{o}C.
U^*	complementary energy of heated plate, in.-lb.
V	potential energy of an initially flat, buckled plate, in.-lb.
w	plate deflection, in.
W_i	initial plate deflection, in.

W_{ic}	initial plate centre deflection, in.
W_c	plate centre deflection measured from the x-y plane of plate, in.
x,y	coordinate axes.
a/b	plate aspect ratio.
e_o/e_{cr}	ratio of middle plane strain to the buckling strain.
$\frac{E\alpha T_o b^2 t}{\pi^2 D}$	temperature differential parameter.
$\frac{E\alpha T_{ocr} b^2 t}{\pi^2 D}$	critical temperature differential parameter.
R_T	ratio of T_o to T_{ocr}
α	coefficient of thermal expansion in./in. ^oC.
β	non-dimensional coefficients.
γ	coefficients in stress function ϕ.
ε_x, ε_y	normal strains in plane of plate in x and y directions respectively.
σ_x, σ_y	normal stresses in plane of plate in x and y directions respectively, lb./in.^{2}
τ_{xy}	shear stress in plane of plate, lb./in.^{2}
δ	incremental operator.
η	variable of integration.
ϕ	stress function.
ν	Poisson's ratio.

∇^2 differential operator, $\frac{\partial^2}{\partial x^2} + \frac{\partial^2}{\partial y^2}$

∇^4 differential operator, $\frac{\partial^4}{\partial x^4} + \frac{2\partial^4}{\partial x^2 \partial y^2} + \frac{\partial^4}{\partial y^4}$

Σ summation operator.

Numbers in brackets in the text refer to the publications listed in the Bibliography.

CONTENTS

PART I CRITICAL REVIEW

The determination of thermal stresses and deformations plays an important part in the design of nuclear reactors, turbines, supersonic aircraft and other types of structural components operating at elevated temperatures. This has lead to renewed interest in the subject of thermo-elasticity which dates back to the first half of the last century when Duhamel[1] modified the equations of elasticity to allow for thermal effects.

Elastic thermal stresses in a body can be produced either by non-uniform temperature distributions throughout the body, or by restraints at boundaries which restrict the free thermal expansions. Thermal stresses can also arise when a composite structure consisting of members with different coefficients of expansion is subjected to a uniform rise of temperature.

In general, thermal stresses can be treated as a steady state problem, since even under temperature distributions varying with time, the thermal inertia effects can often be neglected.

Aircraft structures designed for supersonic speeds are subject to aerodynamic heating. This is caused by the rapid slowing down of the air through the boundary layer which generates heat. Thus the external surfaces of the aircraft are heated. The induced thermal stresses in plate elements resulting from non-uniform heating may have a significant effect on the aerodynamic performance of the aircraft.

Lateral deflections of a plate element can arise as soon as heating takes place if the temperature varies across the thickness but is constant over its surface. If, however, the temperature is constant across the thickness of an idealized flat plate element but varies in a non-linear manner over its surfaces, then the induced compressive components of the thermal stresses will cause lateral deflections of the plate to occur only when a critical temperature is reached.

The behaviour of a plate with initial imperfections will differ from that of an idealized flat plate. In the latter case, no lateral deflections occur until the critical temperature is exceeded. A plate with initial imperfections will deflect as soon as heat is applied. These deflections will increase rapidly at a non-linear rate as the critical temperature (a characteristic of the applied temperature distributions) is approached.

The subject matter of the thesis is this instability phenomenon induced in rectangular flat plates by non-linear temperature distributions over the lateral surfaces of the plates.

The published literature of theoretical stress and deformation effects is very extensive. It is felt that a thesis review will serve a more useful purpose if it attempts to cover in relative detail, a rationally restricted range rather than provide brief resumes of a large number of papers.

Generally, the papers dealing with the thermal stress problem have been restricted to cases where the induced stresses are self equilibrating.

That is to say, the stresses on any overall cross-section produce zero resultant direct and shear load and zero bending moment.

An object has been to show, in some detail, typical methods used in analysis rather than particular aspects of plate behaviour under non-linear temperature fields.

The first section of the review (1) deals with the steady state plane stress problem arising from non-uniform heating. In this section, the review includes exact solutions of the governing differential equation. It is relevant to comment here that while Duhamel's[1] analogy enables a thermo-elastic problem to be formulated as an ordinary elastic problem using fictitious boundary and body forces, only a few problems with body forces have been solved which are of direct relevance to the problem considered. Owing to the inherent difficulty of applying this analogy, various approximate methods have been used to obtain a solution. These are presented in the remaining part of section (1).

The second section (2) of the review is concerned with the instability of a rectangular plate induced by the compressive component of the induced thermal stresses. It is essentially a characteristic value problem if small deflection plate equations are used in the theoretical analysis for an idealized flat plate.

The final section (3) of the review is concerned with the behaviour of an actual plate with initial imperfections and where the stretching of the mid plane is taken into account in the analysis. Of particular interest is the growth of plate centre deflection with increasing value of temperature differential across the surface of the plate.

(1) Thermal Stresses in Plates under Stable Conditions

The basic equations of elasticity, modified to include temperature effects, were deduced independently by Duhamel[1] and Neumann[2] in 1838. The equations were later modified by Hopkinson[3] in 1879 who gave the equations in the form used to-day[4].

If the plate is thin and subjected to arbitrary temperature distributions over its lateral surfaces then the differential equation governing the distribution and magnitude of the stresses in the plate is given by:-

$$\nabla^4 \phi = -E\alpha\nabla^2 T(x,y) \quad \ldots\ldots\ldots \quad 1.1$$

where ϕ is the Airy stress function such:-

$$\sigma_x = \frac{\partial^2 \phi}{\partial y^2} \; ; \quad \sigma_y = \frac{\partial^2 \phi}{\partial x^2} \; ; \quad \tau_{xy} = -\frac{\partial^2 \phi}{\partial x \partial y} \quad \ldots\ldots\ldots \quad 1.1a$$

At this point it is convenient to divide the published literature on the subject of thermal stresses into two categories:-

(a) Those giving a mathematically rigorous solution of the biharmonic equation for a particular temperature distribution.

(b) Those using approximate methods to arrive at a solution accurate enough for engineering purposes.

(a) Rigorous solutions of the biharmonic equation

A solution of the biharmonic equation has been obtained by Timoshenko and Goodier[4] for the case of a long thin rectangular plate subjected to a temperature distribution constant in the longitudinal direction but varying in the transverse direction. The longitudinal stress, σ_x, set up in the plate was deduced as follows. Each element in the plate was subjected to a compressive stress of magnitude $-E\alpha T$ in order to suppress its free thermal expansion. This procedure resulted in compressions of magnitude $-E\alpha T$ acting, in this case, on the transverse ends of the plate. If tensions of magnitude $+E\alpha T$ are applied to the transversed edges in order that there is no resultant force acting at the edges, then the thermal stresses in the plate are obtained by superposing the effect of these boundary tensile stresses at points removed from the ends, on the original compressive stress, $-E\alpha T$ at that point.

If the temperature is not symmetrical about the longitudinal axis (x) then the tensile forces applied at the ends will not only have a resultant force, $t \int_{-b}^{b} E\alpha T dy$, but a resultant couple $t \int_{-b}^{b} E\alpha T y dy$ for the coordinate system shown in figure 23. Therefore, the longitudinal stress at a point remote from the ends is given by

$$\sigma_x = \sigma_x' + \sigma_x'' + \sigma_x''' \qquad \ldots\ldots\ldots \quad 1.2$$

where σ_x' is the compressive stress, $-E\alpha T$; σ_x'' is the uniform tensile

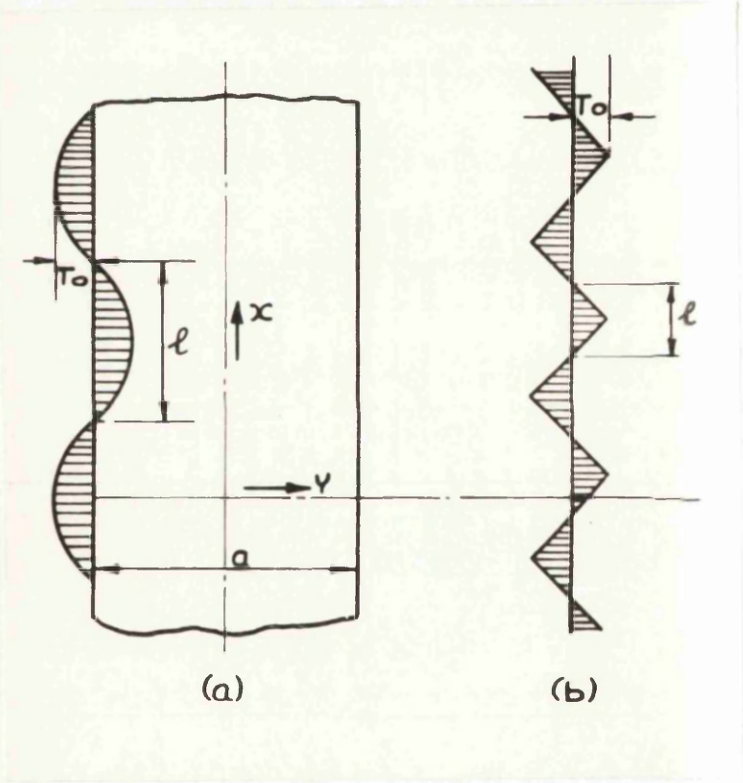

Figure 1(a) and 1(b): Temperature distributions assumed in Reference 5.

stress across the section given by $\sigma_x'' = \frac{1}{2b}\int_{-b}^{+b} E\alpha T dy$ due to the resultant tensile forces on the ends, and σ_x''' is the bending stress $\sigma_x''' = \frac{3y}{b^3}\int_{-b}^{b} E\alpha T y dy$ due to the resultant moment on the ends.

Den Hartog[5] considered the case of a plate of width 'a' and infinitely long subjected to a sinusoidal temperature distribution along its longitudinal edges of the form:- $T = T_o \sin \frac{\pi x}{l}$ and constant on lines across the width of the plate. This type of temperature distribution is shown in figure 1a, where l is one half wave length.

For this particular temperature distribution, the biharmonic equation can be written as:-

$$\nabla^4 \phi = -E\alpha T_o \omega^2 \sin \omega x \qquad \ldots\ldots\ldots \quad 1.3$$

where $\omega = x/l$.

Den Hartog, using classical methods, shows that a solution to this equation is any biharmonic function plus a particular integral. In this case, the particular integral satisfying equation 1.3 is:-

$$\phi_{particular} = \frac{E\alpha T_o \sin \omega x}{\omega^2} \qquad \ldots\ldots\ldots \quad 1.4$$

and that the complementary function could be assumed as:-

$$\phi_{compl.} = f(y) \sin \omega x \qquad \ldots\ldots\ldots \quad 1.4a$$

If the complementary function is substituted in equation 1.3, the biharmonic equation is reduced to an ordinary linear differential equation:-

$$f'''' - 2\omega^2 f'' + \omega^4 f = 0 \qquad \ldots\ldots\ldots \quad 1.5$$

where the primes indicate differentiation of the function with respect to y.

The complete solution of this equation which includes four arbitrary constants of integration, can be expressed as:-

$$\phi = \sin \omega x \left[(C_1 y + C_2) e^{\omega y} + (C_3 y + C_4) e^{-\omega y} - \frac{E\alpha T_o}{\omega^2} \right] \qquad \ldots\ldots \quad 1.6$$

The constants $C_1 - C_4$ can be found from the boundary conditions at $y = \pm a/2$, where $\tau_{xy} = \sigma_y = 0$.

Den Hartog also solved the case of a triangular temperature distribution along the longitudinal edges, as shown in figure 1(b), by expanding the temperature wave in a Fourier Series of the form:-

$$T = \frac{8T_o}{\pi^2} \sum_{1,3,5}^{n} \frac{1}{n^2} \cos \frac{n\pi x}{l} \qquad \ldots\ldots\ldots \quad 1.7$$

In a paper published by Klosner and Forray[6] an investigation was made into the thermal stresses set up in an aircraft wing due to kinetic heating. They assumed that the temperature over the surface of the wings varied in both the chordwise and spanwise directions, as shown in figure 3, and that the wings could be approximated to flat cover

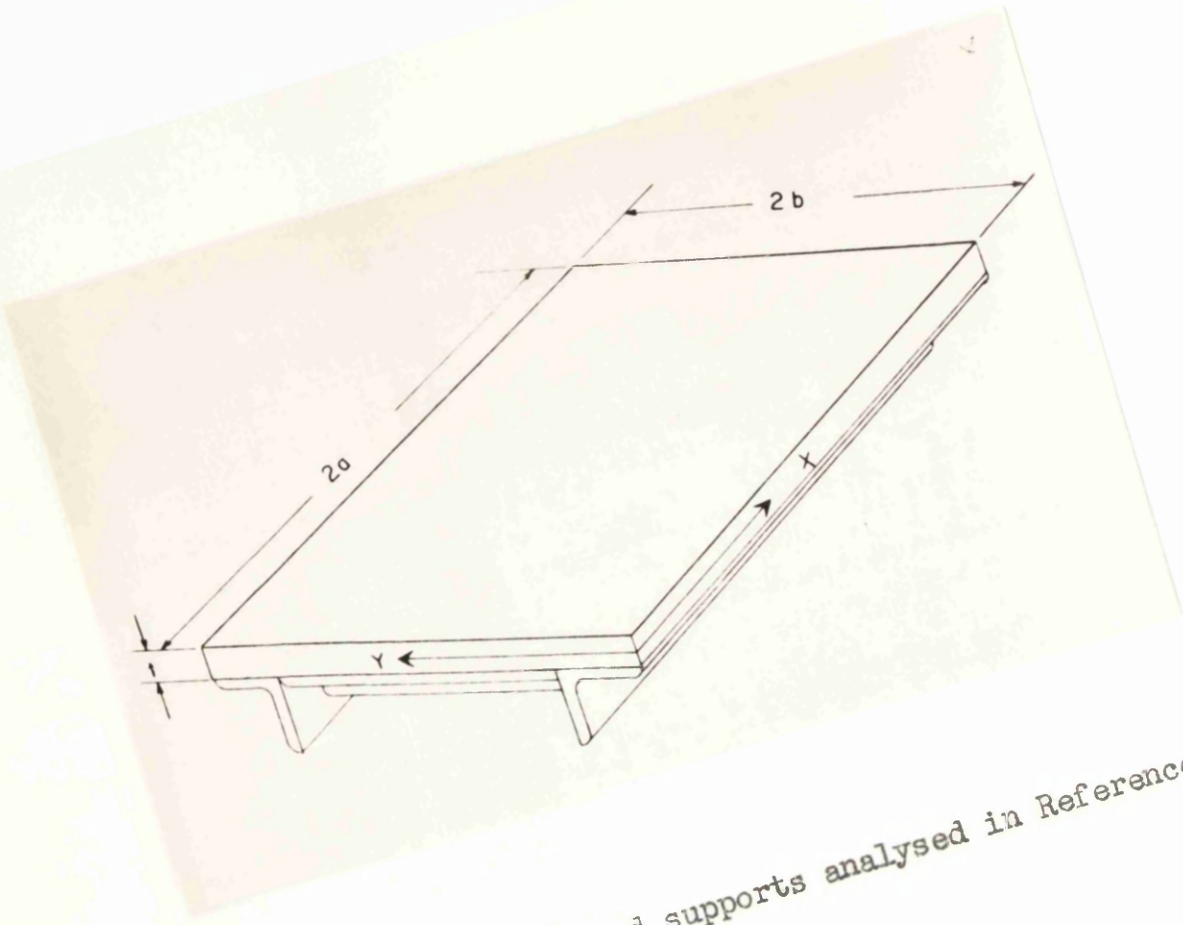

Figure 2: Plate and supports analysed in Reference 6.

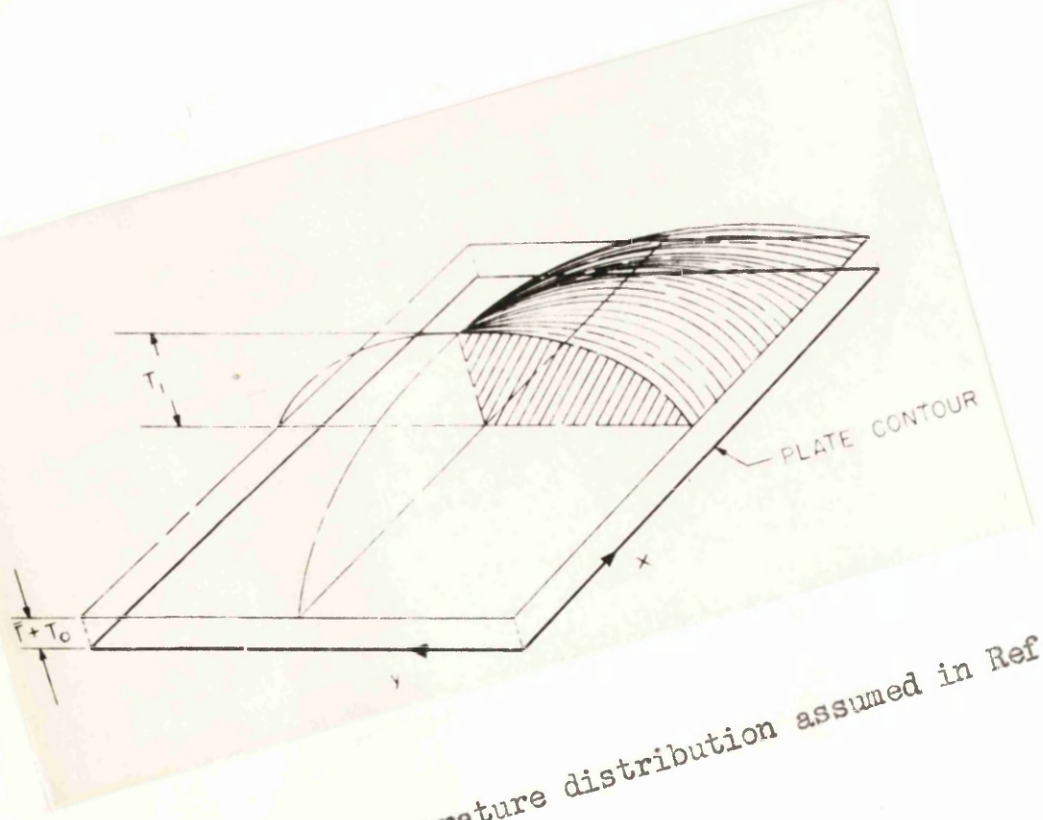

Figure 3: Temperature distribution assumed in Reference 6.

plates supported at the boundaries by flexible webs which offer no rotational resistance but remain straight with no transverse deflection.

If the plate is subjected to a temperature distribution represented by the Fourier Series,

$$T = \bar{T} + T_o + \sum_{s=o}^{\infty} \sum_{t=o}^{\infty} T_{st} \cos \frac{s\pi x}{a} \cdot \cos \frac{t\pi y}{b} \qquad \ldots\ldots\ldots \quad 1.8$$

where $\bar{T}$ = difference between average temperature of the supporting structure and room temperature and T_o is the difference between temperature at the edge of the plate and the average temperature of the supports, then a rigorous solution of the biharmonic equation can be obtained by taking the stress function in the form:-

$$\phi = K_1 \frac{y^2}{2} + K_2 \frac{x^2}{2} + \sum_{s=1}^{\infty} t_{so} \cos \frac{s\pi x}{a} + \sum_{t=1}^{\infty} t_{ot} \cos \frac{t\pi y}{b}$$

$$+ \sum_{s=1}^{\infty} \sum_{t=1}^{\infty} t_{st} \cos \frac{s\pi x}{a} \cdot \cos \frac{t\pi y}{b} \qquad \ldots\ldots\ldots \quad 1.9$$

where

$$t_{so} = \frac{E\alpha T_{so}}{\left(\frac{s\pi}{a}\right)^2} \; ; \; t_{ot} = \frac{E\alpha T_{ot}}{\left(\frac{t\pi}{b}\right)^2} \; ; \; t_{st} = \frac{E\alpha T_{st}}{\left(\frac{s\pi}{a}\right)^2 + \left(\frac{t\pi}{b}\right)^2}$$

It can be shown that equation 1.9 satisfies the biharmonic equation and the boundary conditions when all the edges remain straight and the average strain along the edge equals the strain in the support,

$$\text{i.e.} \quad \bar{\varepsilon}_x = \varepsilon_{x\,av} = \frac{1}{2a}\int_0^{2a} \varepsilon_x dx \qquad \ldots\ldots\ldots \quad 1.10$$

Hence, the stresses in the plate are given by:-

$$\sigma_x = \frac{\partial^2 \phi}{\partial y^2} \; ; \; \sigma_y = \frac{\partial^2 \phi}{\partial x^2} \; ; \; \tau_{xy} = -\frac{\partial^2 \phi}{\partial x \partial y} \qquad \ldots\ldots\ldots \quad 1.11$$

for the coordinate system shown in figure 2.

The constants K_1 and K_2 are found from the conditions that the strain in the supports equals the average strain in the plate along the edges. Thus the resultant force on any cross-section parallel to the x and y axes respectively, is:-

$$t\int_0^{2b} \sigma_x dy = 2K_1 bt \quad \text{and} \quad t\int_0^{2a} \sigma_y dx = 2K_2 at \qquad \ldots\ldots\ldots \quad 1.12$$

These forces must correspond to the forces in the supports,

$$\text{i.e.} \quad \bar{P}_x = -K_1 bt \quad \text{and} \quad \bar{P}_y = -K_2 at \qquad \ldots\ldots\ldots \quad 1.13$$

Therefore the average strains in the supports are:-

$$\bar{\varepsilon}_x = -\frac{K_1 bt}{\bar{A}_x \bar{E}} + \bar{\alpha}\bar{T}$$

$$\bar{\varepsilon}_y = -\frac{K_2 at}{\bar{A}_y \bar{E}} + \bar{\alpha}\bar{T} \qquad \ldots\ldots\ldots \quad 1.14$$

where the bar denotes support conditions and, in particular, $\bar{A}_x$ and $\bar{A}_y$ are the cross-sectional area of the webs.

Along the edges, $y = 0$, $y = 2b$, the average strain can be found from the condition that

$$\varepsilon_{xav} = \frac{1}{2a} \int_0^{2a} \varepsilon_x dx \qquad \ldots\ldots\ldots \quad 1.15$$

and along the edges $x = 0$, $x = 2a$

$$\varepsilon_{yav} = \frac{1}{2b} \int_0^{2b} \varepsilon_y dy \qquad \ldots\ldots\ldots \quad 1.16$$

Making use of the stress-strain relationships and equating strains in the webs to the average strains along the edges of the plate, then the equations for K_1 and K_2 are:-

$$K_1 = \frac{E\alpha(T_o + T_{oo}) + E(\alpha - \bar{\alpha})\bar{T}}{\nu^2 - K_x K_y} (\nu + K_y) \qquad \ldots\ldots\ldots \quad 1.17$$

$$K_2 = \frac{E\alpha(T_o + T_{oo}) + E(\alpha - \bar{\alpha})\bar{T}}{\nu^2 - K_x K_y} (\nu + K_x) \qquad \ldots\ldots\ldots \quad 1.17$$

where $K_x = 1 + \frac{btE}{\bar{A}_x \bar{E}}$; $K_y = 1 + \frac{atE}{\bar{A}_y \bar{E}}$

After K_1 and K_2 have been evaluated the stresses in the plate can be found by using equations 1.9 and 1.11.

In this particular case the method is primarily based on the

solution of a two-dimensional stress problem in which the loads can be expressed in the form of a Fourier Series. This method for the solution of the biharmonic equation is discussed in detail by Timoshenko and Goodier[16].

(b) Approximate solutions of the biharmonic equation

In many practical problems of thermoelasticity it is difficult or impossible to obtain a rigorous solution of the biharmonic equation. Therefore approximate methods have been developed accurate enough for engineering purposes. One such method used by Mendelson and Hirschberg[7] makes use of an approximate polynomial form for the stress function in order to reduce the biharmonic equation to an ordinary differential equation with constant coefficients. The method used is essentially a 'collocation procedure' applied to the biharmonic equation.

Reference (7) is of interest since it gives numerical examples of the stresses set up in flat rectangular plates due to spanwise and chordwise temperature distributions over the lateral surfaces of the plate.

In this approximate method the stress function is assumed to have the form

$$\phi = \sum_{j=1}^{n} P_j(y)\, \phi_j(x) \qquad \ldots\ldots\ldots \quad 1.18$$

in which $P_j(y)$ is a polynomial in y only, associated with the j^{th} station

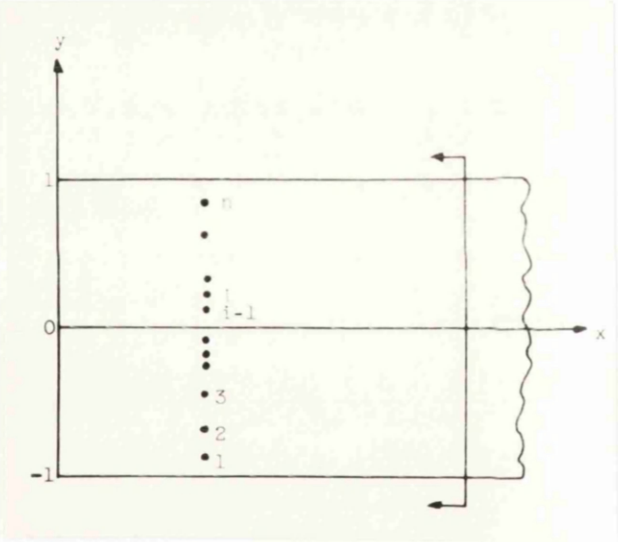

Figure 4: Coordinate system used in Reference 7, and the stations where the differential equation is satisfied.

and satisfying the conditions:-

$$P_j(y_j) = 1 \; ; \; P_j(y_i) = 0, \quad j \neq i. \qquad \ldots\ldots\ldots \quad 1.19$$

At the edges of the plate, $y = \pm 1$, shown in figure 4 where $\sigma_y = \tau_{xy} = 0$,

$$P_{(j)}(\pm 1) = 0 \quad \text{and} \quad P'_{(j)}(\pm 1) = 0 \qquad \ldots\ldots\ldots \quad 1.20$$

must be satisfied to ensure that $\sigma_y = \frac{\partial^2 \phi}{\partial x^2}$ and $\tau_{xy} = -\frac{\partial^2 \phi}{\partial x \partial y}$ holds for any $\phi_j(x)$. Polynomials for $P_{(j)}$ satisfying conditions expressed in equations 1.19 and 1.20 for even functions in y (i.e. symmetry about $y = 0$) can be obtained and are of the form:-

$$P_j(y) = \frac{\dfrac{(y^2 - 1)^2}{(y_j^2 - 1)^2} \prod_{i \neq j} (y^2 - y_i^2)}{\prod_{i \neq j} (y_j^2 - y_i^2)} \qquad \ldots\ldots\ldots \quad 1.21$$

and for odd functions of y (i.e. anti-symmetry about $y = 0$) the polynomials are of the form:-

$$P_j(y) = \frac{\dfrac{(y^2 - 1)^2}{(y_j^2 - 1)^2} \prod_{i \neq j} y(y^2 - y_i^2)}{\prod_{i \neq j} (y_j^2 - y_i^2)} \qquad \ldots\ldots\ldots \quad 1.22$$

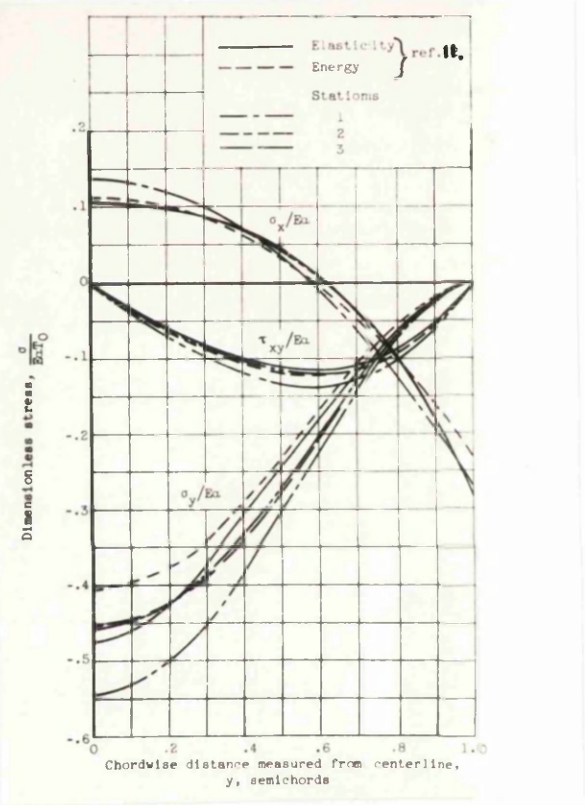

Figure 5: Comparison of dimensionless stress for several methods of solution. Chordwise stress σ_y plotted at free end, x = o; spanwise stress σ_x and τ_{xy} plotted at $\frac{1}{4}$ chord from free end, $x = \frac{1}{2}$, plate thickness constant; $T = T_o(y^2 - \frac{1}{3})$.

where $\prod$ indicates the product for all values of i except i = j.

Substituting equation 1.21 or 1.22 in the biharmonic equation leads to a set of simultaneous differential equations:-

$$\Sigma_{j=1}^{n}\left[P_j(y_i)\phi_j'''' + 2P_j''(y_i)\phi_j'' + P_j''''(y_i)\phi_j\right] = -\nabla^2\left[E\alpha T(x,y_i)\right] \quad \ldots\ldots\ldots \quad 1.23$$

Mendelson and Hirschberg have evaluated the thermal stresses in a semi-infinite thin rectangular plate subjected to a symmetrical temperature distribution $T = T_o(y^2 - \frac{1}{3})$ for the coordinate system shown in figure 4. This particular temperature distribution has a zero mean and first moment about the x-axis.

The stresses remote from the end[4] are:-

$$\sigma_x = E\alpha T_o(\tfrac{1}{3} - y^2) \; ; \; \sigma_y = 0 \; ; \; \tau_{xy} = 0 \quad \ldots\ldots\ldots \quad 1.24$$

At points near the free end (x = 0) the stress distribution is modified by the condition that the edge, x = 0, remains stress free.

The stresses near the free end can be obtained if the stress function is assumed to be:-

$$\phi = P_1\phi_1 + P_2\phi_2 \quad \ldots\ldots\ldots \quad 1.25$$

i.e. a two station solution.

The stations were chosen at the points $y_1 = \frac{1}{4}$ and $y_2 = \frac{3}{4}$

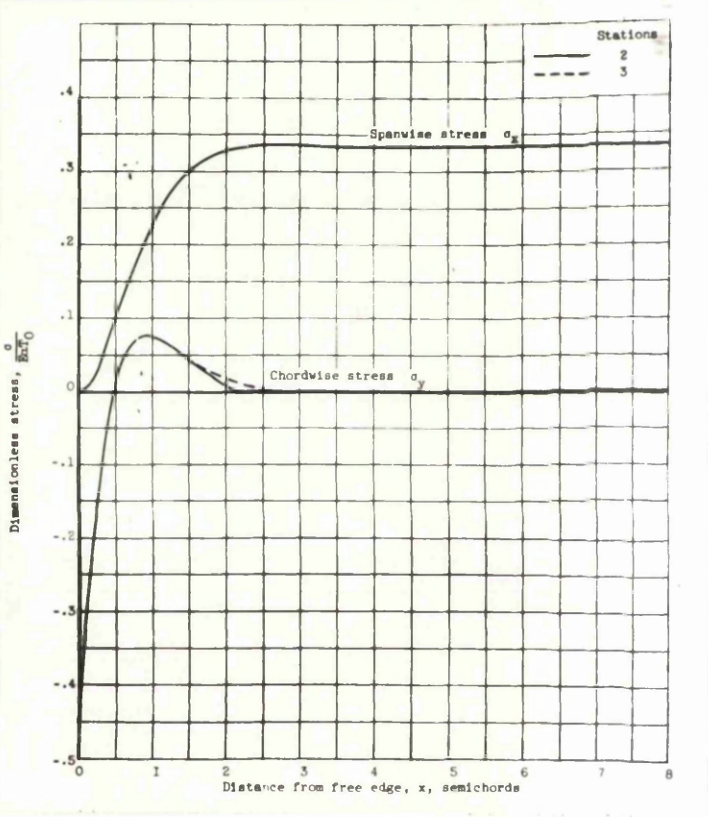

Figure 6: Comparison at mid-chord for two and three station solutions. Stresses for parabolic temperature distribution, $T = T_o(y^2 - \frac{1}{3})$.

and the polynomials associated with these points are:-

$$P_1 = \frac{(y^2-1)^2(y^2-\frac{9}{16})}{(\frac{1}{16}-1)^2(\frac{1}{16}-\frac{9}{16})} = -\frac{512}{225}(y^2-1)^2(y^2-\frac{9}{16}) \quad \ldots\ldots \quad 1.26$$

$$P_2 = \frac{(y^2-1)^2(y^2-\frac{1}{16})}{(\frac{9}{16}-1)^2(\frac{9}{16}-\frac{1}{16})} = \frac{512}{225}(y^2-1)^2(y^2-\frac{1}{16})$$

The values of P_1 and P_2 and their derivations, at $y = \frac{1}{4}$ and $y = \frac{3}{4}$, are:-

$y_1 = \frac{1}{4}$		$y_2 = \frac{3}{4}$	
P_1	= 1	P_1	= 0
P_1''	= -5.564	P_1''	= 8.089
P_1''''	= 88.75	P_1''''	= -320.8
P_2	= 0	P_2	= 1
P_2''	= 8.571	P_2''	= -22.78
P_2''''	= -282.1	P_2''''	= 1599

$\ldots\ldots\ldots$ 1.27

Substituting these values into equation 1.23 two linear

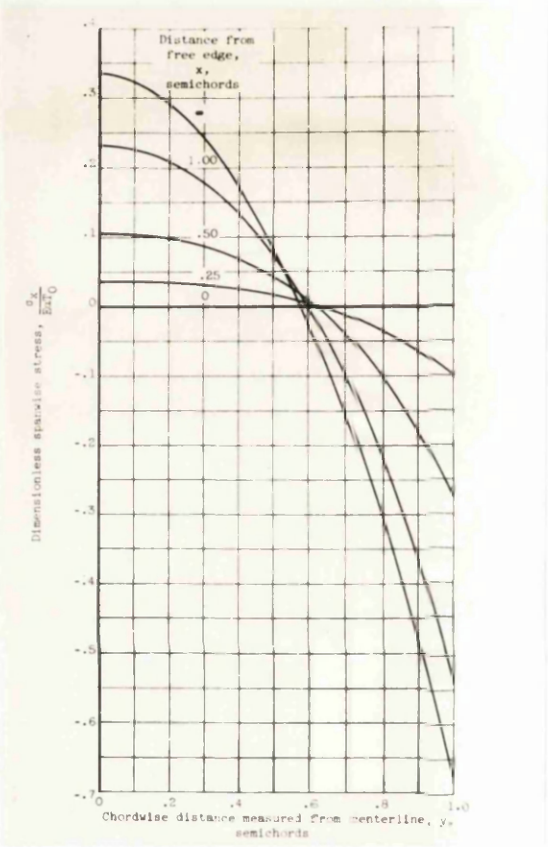

Figure 7: Spanwise stress, σ_x; two station solution, plate subject to parabolic temperature distribution, $T = T_o(y^2 - \frac{1}{3})$.

simultaneous differential equations are obtained:-

$$\phi_1'''' - 11.12\phi_1'' + 88.75\phi_1 + 17.14\phi_2'' - 282.1\phi_2 = -2E\alpha T_o$$

$$16.18\phi_1'' - 320.8\phi_1 + \phi_2'''' - 45.55\phi_2'' + 1599\phi_2 = -2E\alpha T_o$$

..... 1.28

The particular integrals of this set of equations are:-

$$\phi_{1p} = -0.07324\, E\alpha T_o \quad ; \quad \phi_{2p} = 0.01595\, E\alpha T_o \quad ..... \quad 1.29$$

and the complementary function is obtained by the usual exponential substitution. Thus the complete solution is:-

$$\phi_1 = \sum_{k=1}^{\infty} A_k e^{\lambda_k x} - 0.07324\, E\alpha T_o$$

..... 1.30

$$\phi_2 = \sum_{k=1}^{\infty} B_k e^{\lambda_k x} - 0.01595\, E\alpha T_o$$

where λ_k are the roots of the determinental equation and are equal to

$$\lambda_1 = -2.120 + j\,1.117 \qquad \lambda_3 = -5.682 + j\,2.681$$
$$\lambda_2 = \bar{\lambda}_1 \qquad \lambda_4 = \bar{\lambda}_3$$
$$\lambda_5 = -\lambda_1 \qquad \lambda_7 = -\lambda_3$$
$$\lambda_6 = \bar{\lambda}_5 \qquad \lambda_8 = \bar{\lambda}_7$$

the bar signifying complex conjugate quantities. B_k is given in terms

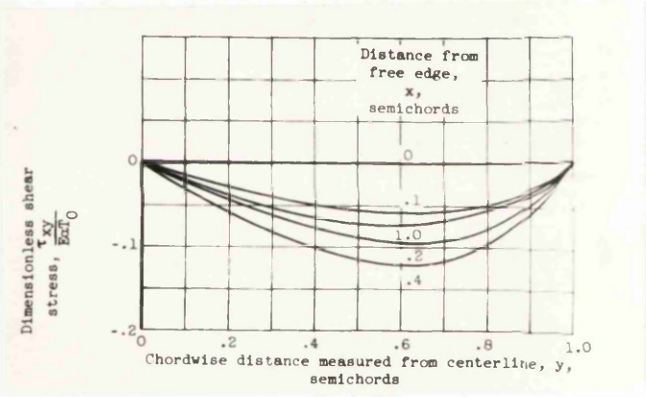

Figure 8: Shear stress, τ_{xy}; two station solution, plate subjected to parabolic temperature distribution, $T = T_o(y^2 - \frac{1}{3})$.

of A_k as follows:-

$$B_k = -\frac{\lambda_k^4 - 11.13\,\lambda_k^2 + 88.75}{17.14\,\lambda_k^2 - 282.1} A_k \qquad \ldots\ldots\ldots \quad 1.32$$

The values of the A_k's can be found from the boundary conditions:-

$$\sigma_x = \tau_{xy} = 0 \quad \text{at} \quad x = 0,$$

which implies:

$$\phi_1(0) = \phi_1'(0) = \phi_2(0) = \phi_2'(0) = 0 \qquad \ldots\ldots\ldots \quad 1.33$$

The conditions at the end of a finite plate of length 2a are:-

$$\sigma_x = \tau_{xy} = 0$$

which again implies that:

$$\phi_1(2a) = \phi_1'(2a) = \phi_2(2a) = \phi_2'(2a) = 0 \qquad \ldots\ldots\ldots \quad 1.34$$

From these conditions the eight values of A_k can be found.

If the plate is infinitely long in the 'x' direction then A_5, A_6, A_7 and A_8 must vanish in order that the stresses remain finite.

Thus the values of the A_k's are:-

$$A_1 = (0.0365 - j\,0.07114)\,E\alpha T_o \;;\; A_2 = \bar{A}_1$$

$$\ldots\ldots\ldots \quad 1.35$$

$$A_3 = (0.0003671 + j\,0.0001926)\,E\alpha T_o \;;\; A_4 = \bar{A}_3$$

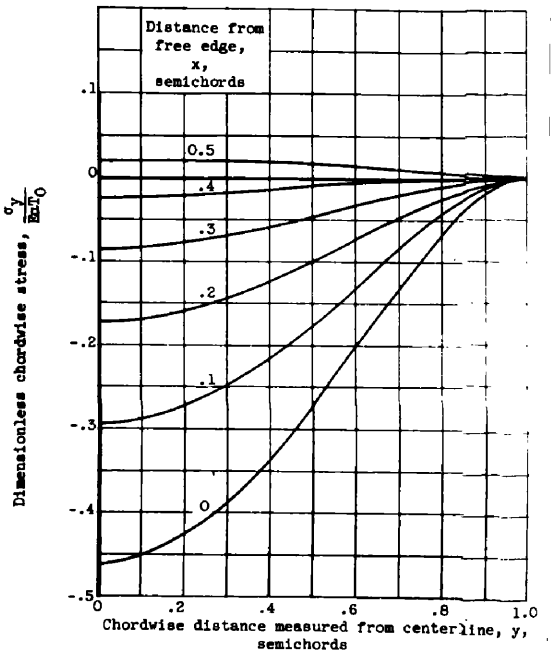

Figure 9: Chordwise stress, σ_y; two station solution, plate subjected to parabolic temperature distribution, $T = T_o(y^2 - \frac{1}{3})$.

After adding all the complex conjugates the imaginary parts drop out. The final solution is:-

$$\phi_1 = 2e^{-2.120x}\left[0.03625\cos 1.117x + 0.07114\sin 1.117x\right] E\alpha T_o + 2e^{-5.682x}\left[0.008941\cos 2.681x - 0.0001926\sin 2.681x\right] E\alpha T_o - 0.01595\, E\alpha T_o$$

$$\phi_2 = 2e^{-2.120x}\left[0.008941\cos 1.117x + 0.01294\sin 1.117x\right] E\alpha T_o + 2e^{-5.682x}\left[0.0009662\cos 2.681x + 0.0001790\sin 2.681x\right] E\alpha T_o - 0.01595\, E\alpha T_o$$

..... 1.36

and the stresses given by:-

$$\sigma_x = P_1''\phi_1 + P_2''\phi_2 \;;\; \sigma_y = P_1\phi_1'' + P_2\phi_2'' \;;\; \tau_{xy} = -P_1'\phi_1' - P_2'\phi_2'$$

..... 1.37

The authors show that at $x = \infty$,

$$\phi_1 = -0.07324\, E\alpha T_o \;;\; \phi_2 = -0.01595\, E\alpha T_o$$

and $\phi_1' = \phi_1'' = \phi_2' = \phi_2'' = 0$, giving $\sigma_y = \tau_{xy} = 0$

and $\sigma_x = E\alpha T_o\left(\frac{1}{3} - y^2\right)$, which is identical to the expression for the longitudinal stresses in a plate at a point far removed from the

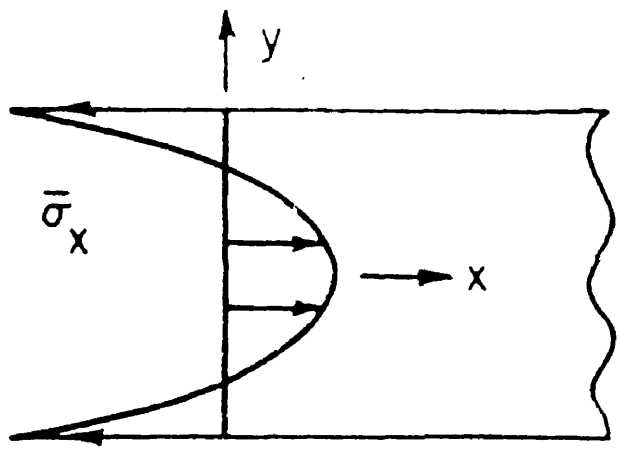

Figure 10: Coordinate system and edge loadings (Ref. 8).

ends using methods of reference (4). This distribution of stresses in a flat plate, subject to a parabolic distribution $T = T_o(y^2 - \frac{1}{3})$ over its lateral surfaces is shown in figures 5, 6, 7, 8 and 9. These figures have been reproduced from reference (7).

In a paper published on the end problem of rectangular strips[8], Horvay points out that variational methods developed by Timoshenko and others in the 1920's give only average stress values. Regions of rapid stress variations and stress concentrations cannot, because of the averaging properties of the method, be adequately dealt with.

In his paper Horvay shows that the problem of a flat plate subjected to temperature distributions, varying in the y-direction but constant in the x-direction, can be reduced to the problem of the stresses set up in an infinite plate given by the equation

$$\sigma_{x\infty} = -E\alpha T + \frac{1}{2}\int_{-1}^{1} E\alpha T\, dy + \frac{3}{2}y\int_{-1}^{1} E\alpha T y\, dy \quad \ldots\ldots\ldots \quad 1.38$$

together with the stresses, σ_{x_1}, σ_{y_1} and τ_{xy_1} set up by the boundary stresses that must be applied to ensure the transverse edge is stress free. Thus the problem is reduced to a long plate, as shown in figure 10, loaded on the transverse edge by stresses $-\sigma_{x_\infty}$. A solution for the stresses in the plate can be obtained using the method of self-equilibrating polynomials.

Horvay assumes that the stress function ϕ, satisfying the biharmonic equation $\nabla^4\phi = 0$, can be expressed as:-

$$\phi_{(x.y)} = \sum_{k=2}^{n} C_k f_k(y).g_k(x) \qquad \ldots\ldots\ldots \quad 1.39$$

and that the complementary energy of a heated plate may be written as:-

$$U^* = \frac{1}{2E} \int_0^x \int_{-1}^{1} \left[\left(\frac{\partial^2\phi}{\partial y^2}\right)^2 + \left(\frac{\partial^2\phi}{\partial x^2}\right)^2 - 2\nu \frac{\partial^2\phi}{\partial x^2}.\frac{\partial^2\phi}{\partial y^2} + 2(1+\nu)\left(\frac{\partial^2\phi}{\partial x \partial y}\right)^2 \right.$$

$$\left. + 2E\alpha T \left(\frac{\partial^2\phi}{\partial y^2} + \frac{\partial^2\phi}{\partial x^2}\right) \right] dx.dy \qquad \ldots\ldots\ldots \quad 1.40$$

Substituting equation 1.39 in 1.40, n - 2 equations are obtained which after minimising by means of the calculus of variation yields a differential equation for the K^{th} term of ϕ :-

$$g_k'''' - 2g_k'' \int_{-1}^{1} (f_k')^2 \, dy + g_k \int_{-1}^{1} (f_k'')^2 \, dy = 0 \qquad \ldots\ldots \quad 1.41$$

The stresses due to the boundary loadings are therefore given by:-

$$\sigma_{x_1} = \sum_2^n C_k f_k'' g_k \; ; \quad \sigma_{y_1} = \sum_2^n C_k f_k g_k'' \; ; \quad \tau_{xy_1} = -\sum_2^n C_k f_k' g_k' \qquad 1.42$$

At the free edge x = 0, g_k is made equal to unity. The stress function at the edge (bar above quantity denotes edge value for x = 0) becomes

$$\bar{\phi} = \sum_2^n C_k f_k(y) \, g_k = \sum_2^n C_k f_k(y) \qquad \ldots\ldots\ldots \quad 1.43$$

The y functions, f_k, are chosen as polynomials which constitute an orthonormal and orthogonal set:-

$$\text{i.e.} \quad \int_{-1}^{1} (f_k)^2 dy = 1 \qquad \text{and} \qquad \int_{-1}^{1} f_k . f_{k+1} dy = 0$$

and at the boundaries, $y = \pm 1$, satisfy the conditions

$$f_k(\pm 1) = 0 \qquad \text{and} \qquad f_k'(\pm 1) = 0 \qquad \ldots\ldots \quad 1.44$$

Also, the even polynomials have the property that

$$\int_{-1}^{1} f_k'' dy = 0 \qquad \ldots\ldots\ldots \quad 1.45$$

which gives zero stress resultant along the edge $x = 0$ and zero resultant moment since f_k is an even function in y. The odd polynomials have the property that

$$\int_{-1}^{1} y f_k'' dy = 0 \qquad \ldots\ldots\ldots \quad 1.46$$

which gives zero resultant moment and the odd properties of the function ensures a zero stress resultant.

Horvay has established that this set of self-equilibrating functions satisfies the differential equation

$$(1-y^2)^2 f'''' - 10y(1-y^2)f''' + (\lambda - 24)(1-y^2)f'' + (12-4\lambda)yf' - 2\lambda f = 0$$

$$\text{where} \quad \lambda = (n+2)(n+3) \qquad \ldots\ldots\ldots \quad 1.47$$

The properties of f_k have been investigated and tables can be found in reference 9.

The expansion coefficients, $C_2, C_4 \ldots C_n$, can be determined by considering the self-equilibrating boundary stress system which can be equated after integrating twice, to the stress function $\bar{\phi}(y) = \Sigma_2^n C_k f_k$ at the free end. Thus:

$$\bar{\phi}_{(even)} = \int_{-1}^{y} d\eta \int_{o}^{\eta} \bar{\sigma}_{x_{(even)}}(\eta_1)d\eta_1 = \beta_o + \beta_2 y^2 \ldots \beta_k y^k$$

$$= C_2 f_2 + C_4 f_4 \ldots C_n f_n \quad \ldots\ldots\ldots \quad 1.48$$

and

$$\bar{\phi}_{(odd)} = \int_{o}^{y} d\eta \int_{-1}^{\eta} \sigma_{x_{(odd)}}(\eta_1)d\eta_1 = \beta_1 y + \beta_3 y^3 \ldots \beta_{k-1} y^{k-1}$$

$$= C_3 f_3 + C_5 f_5 \ldots C_{n-1} f_{n-1}$$

The same result can be obtained by integrating the boundary stresses on the free end and satisfying the boundary conditions, $\bar{\phi} = \bar{\phi}' = 0$, at $y = \pm 1$. The stress function can then be resolved into its odd and even components to give the same results as above. Thus the expansion coefficients, $C_2, C_3 \ldots C_n$, can be determined from the condition that

$$C_n = \int_{-1}^{1} \bar{\phi}_{even} f_n dy \quad \text{and} \quad C_{n-1} = \int_{-1}^{1} \bar{\phi}_{odd} f_{n-1} dy \quad \ldots\ldots \quad 1.49$$

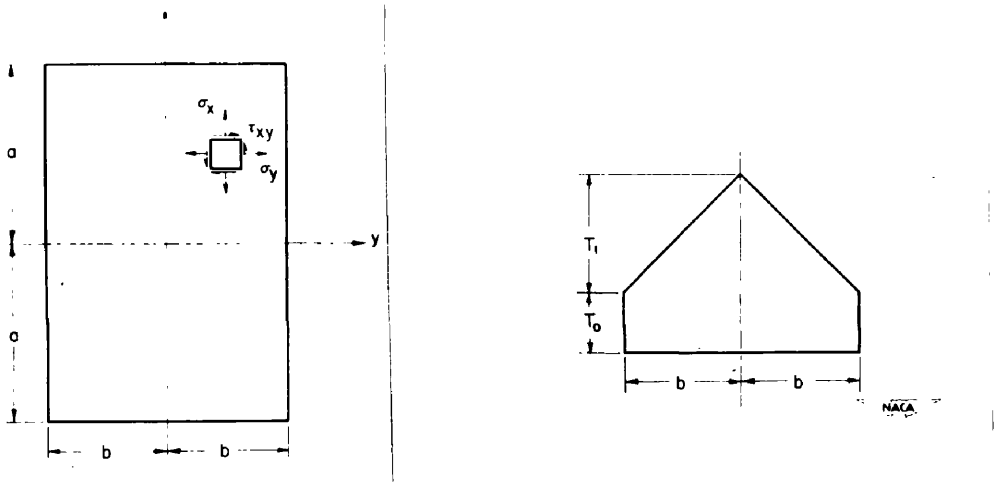

Figure 11: Plate dimensions, coordinate system and 'tent-like' temperature distrubution, analysed in Reference 10.

This can easily be proved by multiplying equation 1.43 on both sides by f_n and then integrating between limits:-

$$\text{i.e.} \quad \int_{-1}^{1} \bar{\phi}_{even} f_n dy = \int_{-1}^{1} C_2 f_2 f_n dy \ldots\ldots \int_{-1}^{1} C_n f_n^2 dy \quad \ldots\ldots\ldots \quad 1.50$$

The condition of orthogonality ensures that the cross product terms $\int_{-1}^{1} C_2 f_2 f_n dy = 0$ and the condition of orthonormality ensures that

$$\int_{-1}^{1} f_n^2 dy = 1 \quad \ldots\ldots\ldots \quad 1.60$$

Thus

$$C_n = \int_{-1}^{1} \bar{\phi}_{even} f_n \, dy$$

Likewise for the odd components.

These expansion coefficients have been evaluated with respect to $\langle y^k f_n \rangle$ and tabulated for k, 0 to 11 and n, 2 to 9 in Table 1B of reference 9. It should be noted that the coefficients are zero for k + n = odd number. Reference 9 also gives the tabulated values of $f_n(y)$ and $g_n(x)$ and their derivatives.

According to Horvay these tables permit rapid solutions in numerical form to be found for flat plates with self-equilibrating end loads acting in the plane of the plate providing the end load can be expressed in polynomial form up to and including the ninth power.

Another method of approach to the solution of the biharmonic equation, the Kantorovitch method developed by Heldenfels and Roberts[10],

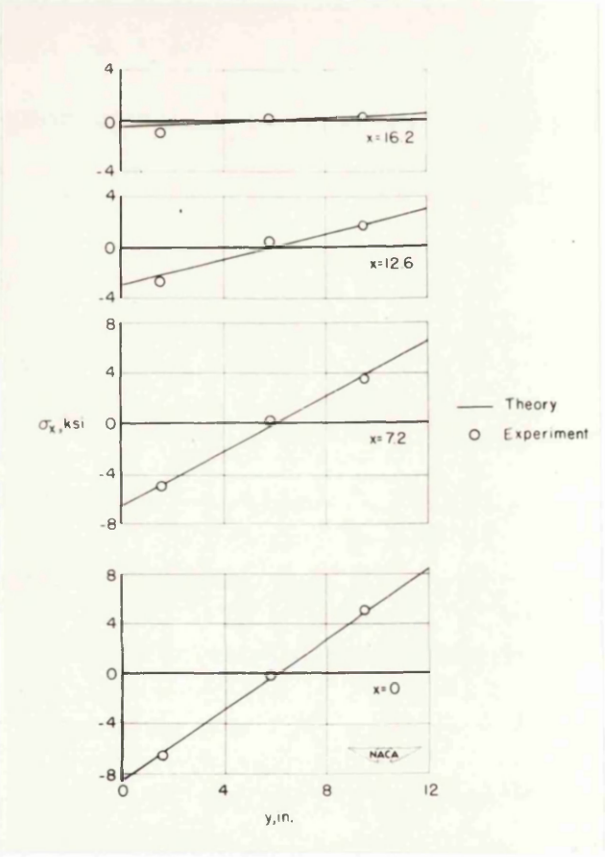

Figure 12: Longitudinal direct stresses, σ_x, induced by temperature distribution of figure 11.

assumes that the stress function can be expressed as $\phi = f.g.$, where f is a function of y only and g is a function of x only. An approximate solution of the biharmonic equation can be obtained by selecting a function f and then using the principle of minimum complementary energy to obtain the best approximation for the function g.

Heldenfels and Roberts[10] have used this method to determine the thermal stresses set up in flat rectangular plates subject to 'tent like' temperature distributions over their lateral surfaces. Using this method, the stress function is obtained in a fairly simple functional form. This is useful when the buckling of flat plates by the induced compressive components of the thermal stresses is to be investigated. As this is the principal method used for the determination of the stress function, detailed analyses and calculations are given in Part II and in Appendices 1, 2 and 3 of the thesis.

The results of the above approximate theoretical analysis have been verified experimentally by Heldenfels and Roberts using Baldwin-Lima AB7-$\frac{1}{4}$" length bakelite-bonded strain gauges attached to a 3' x 2' x $\frac{1}{4}$" aluminium alloy plate. Reference 10 states that agreement between measured and computated stresses are within $\pm$ 500 lb./in.^{2} and that good agreement exists between the experimental and computated longitudinal stress, σ_x. Only fair agreement was found between the computated and experimental transverse and shear stresses.

Reference 10 indicates that the error in the later cases can be attributed to approximations in the analysis rather than errors of measurement.

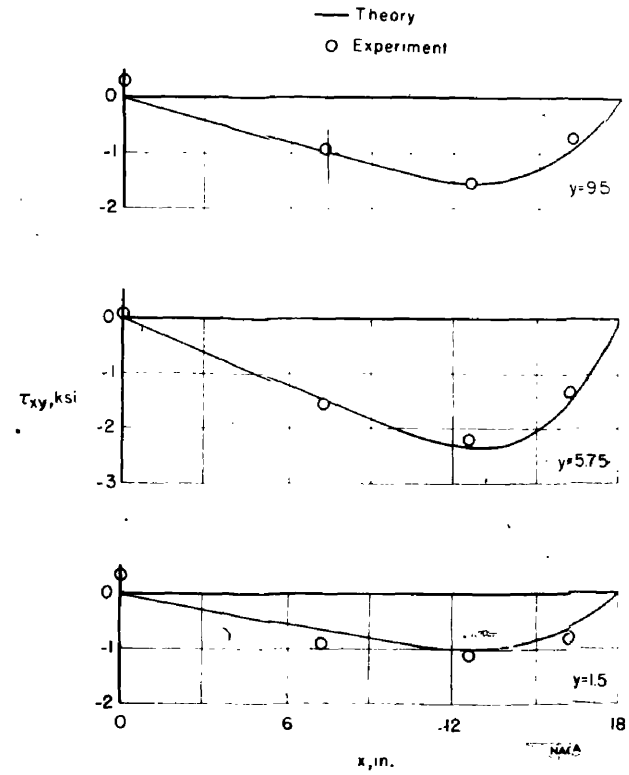

Figure 13: Longitudinal distribution of shear stress, τ_{xy}.

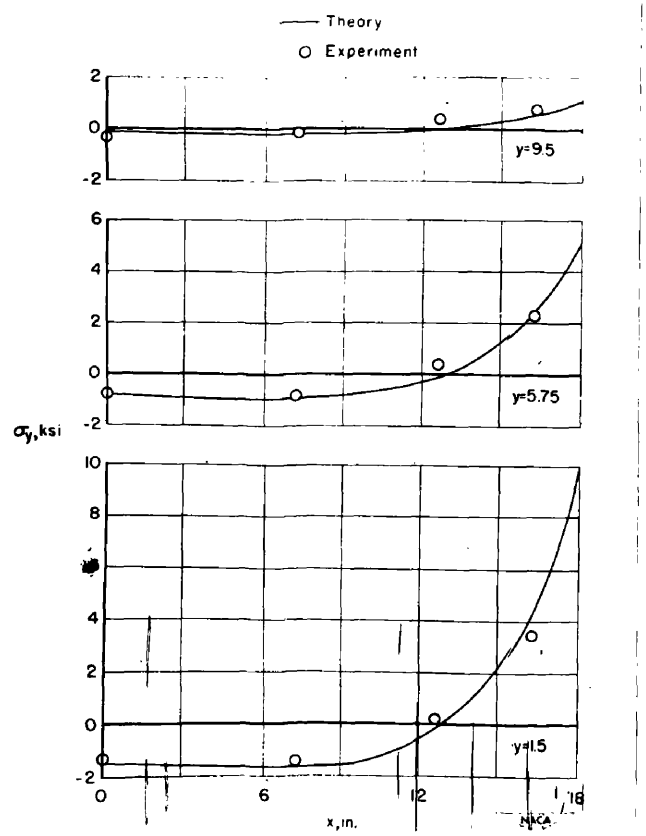

Figure 14: Longitudinal distribution of stress, σ_y.

Theoretical and experimental results are shown graphically in figures 12, 13 and 14.

(c) Critical discussion

It has been shown that only in particular cases can an exact solution of the biharmonic equation be obtained. A typical example is the case of a semi-infinite plate treated by Timoshenko and Goodier[4] in which the stresses in a flat rectangular plate are given at points far removed from the free ends.

Approximate methods must be used if the value of the stresses near the stress free transverse edges are required. Reference 7, using the collocation method, shows graphically the variation of stresses in a plate subjected to a parabolic temperature distribution $T = T_o(y^2 - \frac{1}{3})$. Using only one station in the collocation method, the stresses are not grossly in error compared with the two and three station solution.

A comparison is also made with solutions in which the stress function is expressed in terms of an infinite series. If two terms are taken, Reference 7 states that the boundary conditions are satisfied only in an average manner. Nevertheless the agreement between the two methods is remarkably good. Also shown in figure 5 is the solution of the biharmonic equation using energy methods. Agreement with the other two methods is generally poor, especially at points near the transverse ends. This bears out the remarks of Horvay in reference 8 in which he states that energy methods give only average values; the values of

stresses in regions of rapid stress variations are usually underestimated.

Horvay's method for the solution of the biharmonic equation is similar to the method developed for the particular case of thermal stresses in flat plates by Heldenfels and Roberts. The difference lies in the choice of f(y) part of the stress function. Heldenfels and Roberts use for their f(y) function, a function proportional to the stress function for an infinite plate, whereas Horvay takes the f(y) function in the form of a series of self-equilibrating polynomials. Singer[12] points out that in the method of Horvay, the variation of complementary energy is carried out with respect n - 2 parameters. This method should therefore give a more accurate result than the method of Heldenfels and Roberts in which there is only one variational equation.

Singer says that this statement must be qualified by two remarks. Firstly, the calculation of the complementary energy implies orthogonality of the derivatives of the function f(y), i.e. $f'(y)$ and $f''(y)$. However, only the functions f(y) are orthogonal. Horvay, however, assumes that the coupling terms, $\int_{-1}^{1} f_k' f_{k+2}' dy$ and $\int_{-1}^{1} f_k'' f_{k+2}'' dy$ are negligible for engineering purposes.

Secondly, Singer points out that Horvay's solution is not valid for short plates since the effect of self-equilibrating loads on the far end become noticeable when the penetration length is of the same order as the half-length of the plate. Generally this solution is in error for plates of aspect ratio less than 2.

Using both the Horvay and the Heldenfels and Roberts method,

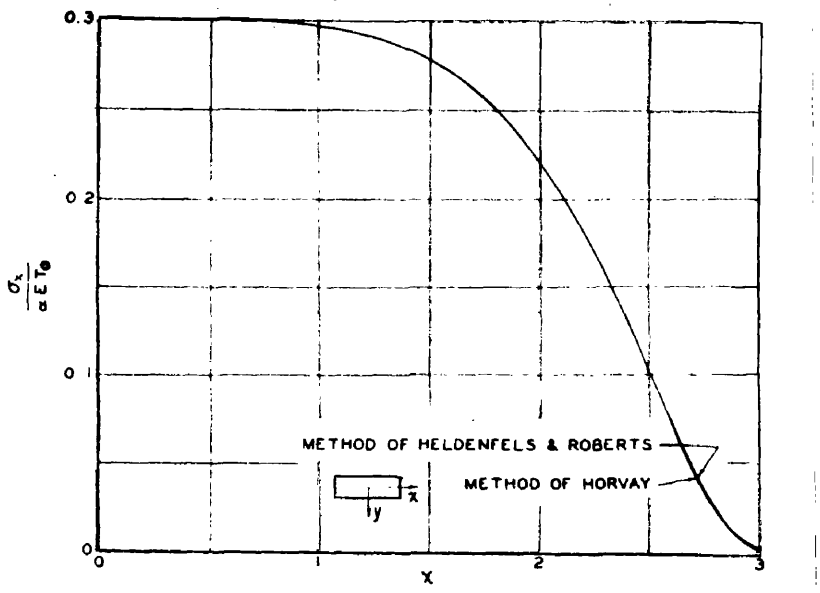

Figure 15: Spanwise distribution of σ_x at $y = 0.8$ for a plate of constant thickness, and temperature distribution $T = T_o(1-y)$ for $0 \leq y \leq 1$ and $T = T_o(1+y)$ for $-1 \leq y \leq 0$.

Singer[12] has evaluated the stresses in a flat rectangular plate subjected to a 'tent-like' temperature distribution:-

$$T = T_o (1 - y) \quad \text{valid for} \quad 0 \leq y \leq 1$$

$$T = T_o (1 + y) \quad \text{valid for} \quad -1 \leq y \leq 0$$

A comparison of the stresses is shown graphically in figure 15. It is presumed that Singer expressed the end loads (i.e. $-\sigma_{x_\infty}$) in a polynomial form by making use of Legendre Polynomial Expansion to ensure a continuous function over the range, $y = \pm 1$. This overcomes the difficulty of the discontinuity in the edges stresses at $y = 0$ resulting from the 'tent-like' temperature distribution.

The conclusion that can be drawn from the methods reviewed is that the method developed by Heldenfels and Roberts and the collocation method are suitable if the stresses are required in a functional form. On the other hand, if the numerical stress distribution is required rapidly, it appears that the method of Horvay shows up to the best advantage, providing the aspect ratio of the plate is greater than 2.

The collocation method becomes complicated if more than a two station solution is used. Therefore, the method of Heldenfels and Roberts which gives a solution in simple functional form has much to commend. It is for this reason that this method has been used in the theoretical analysis (Part II) where applicable.

2. Thermal Buckling of Flat Rectangular Plates

One of the first papers to investigate the thermal buckling of flat plates was published in 1952[13] by Gossard, Seide and Roberts.

They considered a flat rectangular plate simply supported along its edges and subjected to a 'tent-like' temperature distribution over its lateral surfaces. Although this type of temperature distribution is rarely encountered in practice (usually of exponential form), the analysis is applicable to any type of temperature loading.

As the temperature differential between the cooled longitudinal edges and longitudinal line source of heat increases, a value will be reached when the plate will buckle out of its own plane due to the compressive component of the induced thermal stresses.

If small deflection theory is used, and the stress distribution does not change at the onset buckling, the critical temperature can be found by methods appropriate to the stability of flat plates with varying internal stresses.

The deflection of the plate is governed by the differential equation:-

$$\nabla^4 \omega = \frac{D}{t}\left[\sigma_x \frac{\partial^2 \omega}{\partial x^2} + \sigma_y \frac{\partial^2 \omega}{\partial y^2} + 2\tau_{xy} \frac{\partial^2 \omega}{\partial x \partial y}\right] \qquad \ldots\ldots\ldots \quad 1.61$$

and the internal stresses given by the stress function using the method

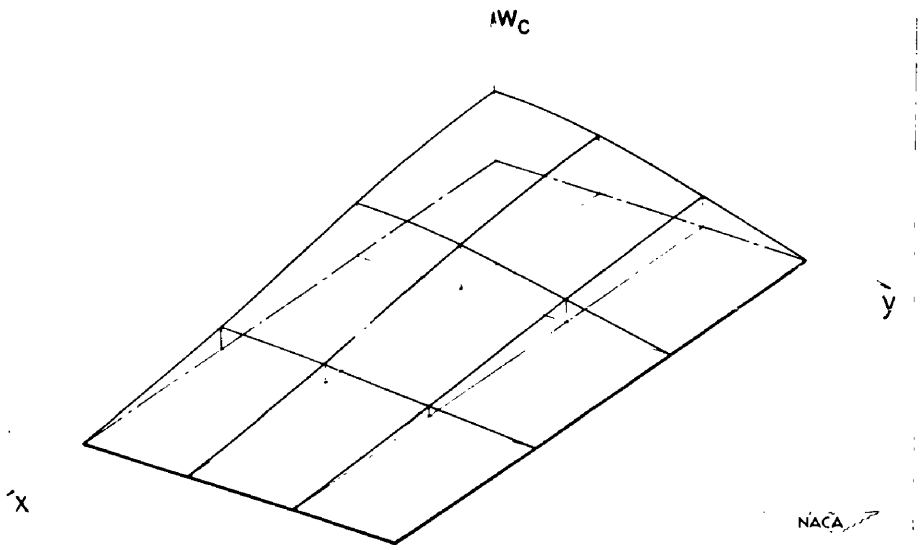

Figure 17: Coordinate system and assumed buckle pattern used in reference 13.

of reference 10 is:-

$$\phi = \frac{b^2 E\alpha T_o}{12}\left[1 - 3\left(\frac{y}{b}\right)^2 + 2\left(\frac{y}{b}\right)^3\right]\left[B_1 \sinh R_1 \frac{x}{a} \sin R_2 \frac{x}{a} + B_2 \cosh R_1 \frac{x}{a} \cos R_2 \frac{x}{a} + 1\right] \quad \ldots\ldots\ldots \quad 1.62$$

where B_1, B_2 and R_1, R_2 are defined in reference 13 and Appendix 4.

Using the principle of minimum potential energy, in conjunction with the Rayleigh-Ritz method, the critical buckling temperature can be found at the point of instability of the plate. To obtain a solution, reference 13 assumes a symmetrical buckle pattern about the centre of the plate:-

$$\omega = \sum_{m=1,3,5}^{\infty} \sum_{n=1,3,5}^{\infty} a_{mn} \cos \frac{m\pi x}{2a} \cos \frac{n\pi y}{2b} \quad \ldots\ldots\ldots \quad 1.63$$

and that the potential energy of the plate is:-

$$V = \frac{D}{2} \int_{-a}^{a} \int_{-b}^{b} \left\{(\nabla^2\omega)^2 - 2(1-\nu)\left[\frac{\partial^2\omega}{\partial x^2}\frac{\partial^2\omega}{\partial y^2} - \left(\frac{\partial^2\omega}{\partial x \partial y}\right)^2\right]\right\} dx.dy$$

$$+ \frac{t}{2} \int_{-a}^{a} \int_{-b}^{b} \left[\sigma_x\left(\frac{\partial^2\omega}{\partial x^2}\right)^2 + \sigma_y\left(\frac{\partial^2\omega}{\partial y^2}\right)^2 + 2\tau_{xy}\frac{\partial\omega}{\partial x}.\frac{\partial\omega}{\partial y}\right] dx.dy$$

$$\ldots\ldots\ldots \quad 1.64$$

Since the variation of potential energy is stationary at the onset of buckling then:-

$$\frac{\partial V}{\partial a_{mn}} = 0 \quad (\text{for } m = 1,3,5 \; ; \; n = 1,3,5) \qquad \ldots\ldots\ldots \quad 1.65$$

This procedure leads to a set of linear homogeneous simultaneous equations of the form:-

$$\frac{1}{b^2 E a T_{ocr}{}^t/\pi^2 D} K_{pq} a_{pq} + \sum_{m=1,3,5}^{\infty} \sum_{n=1,3,5}^{\infty} K_{pqmn} a_{mn} = 0 \qquad \ldots\ldots \quad 1.66$$

$$p = 1,3,5 \; ; \quad q = 1,3,5$$

where $K_{pq} = \left[\frac{1}{4}\left(p^2 \frac{b}{a} + q^2 \frac{a}{b}\right)\right]^2$

$$K_{pqmn} = p\left[m A_{nq}\left(B_1 D_{mp} + B_2 E_{mp} + F_{mp}\right)\right]$$

$$+ n B_{nq}\left(D_3 G_{mp} + D_4 H_{mp}\right)$$

$$+ q\left[n C_{nq}\left(D_1 I_{mp} + D_2 J_{mp}\right) + m B_{qn}\left(D_3 G_{pm} + D_4 H_{pm}\right)\right]$$

and B_1, B_2, D_1 to D_4 are defined in Appendix 4.

Gossard, Seide and Roberts found for a plate of aspect ratio 1.57, the lowest value of the critical temperature parameter to be:-

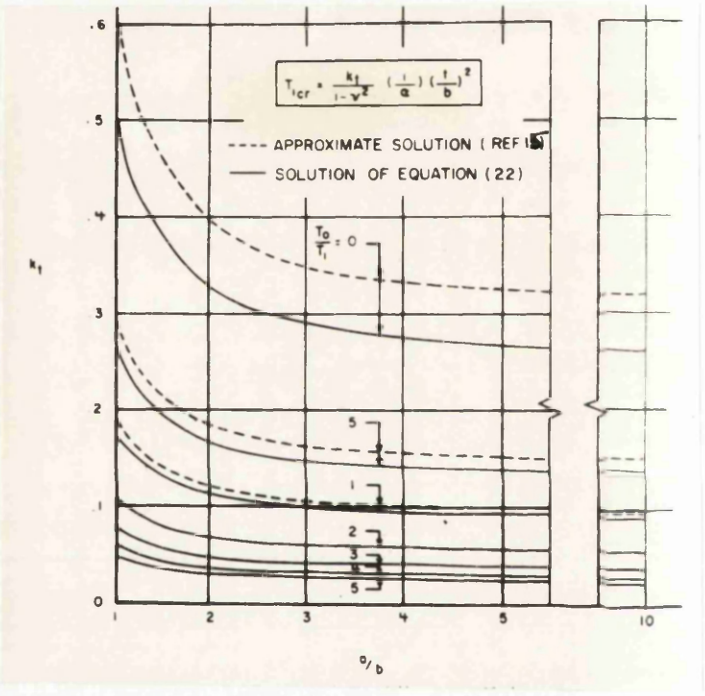

Figure 18: Variation of thermal buckling coefficient, K_t, with aspect ratio where $T_{1cr} = \dfrac{K_t}{(1-\nu^2)a}\left(\dfrac{t}{b}\right)^2$.

$$\frac{b^2 E \alpha T_{ocr} t}{\pi^2 D} = 5.39 \qquad \ldots\ldots\ldots\ldots \quad 1.67$$

Klosner and Forray[6] have investigated the buckling of a flat rectangular plate simply supported by webs at the edges which remain straight and do not deflect laterally and offer no rotational support. In particular, they investigated the case of a plate with parabolic variation of temperature over the plate of the form:-

$$T = T_o + T_1 \left[1 - \left(\frac{x - a}{a}\right)^2\right]\left[1 - \left(\frac{y - b}{b}\right)^2\right] \qquad \ldots\ldots\ldots\ldots \quad 1.68$$

where T_1 is the difference of temperature between the centre and edge of the plate, and T_o is the difference of temperature between the webs and the edge of the plate. A further simplification was introduced by making the cross-sectional area of the webs large compared with the cross-sectional area of the plate.

Under the action of the induced compressive component of the thermal stresses, the plate, at some value of critical temperature, will buckle out of its plane. Using methods similar to those used by reference 13, Klosner and Forray have evaluated the critical buckling temperature for the above problem, using the stress function in a form defined by equation 1.9. The results of their analysis are shown graphically in figure 18.

It can be seen that if T_o is large compared to T_1, then the

effect of the self-equilibrating stresses in the plate are negligible; the plate acts as if it were uniformly heated but restrained at the boundaries from expanding freely. The results agree with the method used in reference 15. When the ratio of T_o/T_1 is less than 2, then the effect of the self-equilibrating stresses in the plate becomes dominant and the analysis of reference 15 is no longer applicable.

3. Post-Buckling Analysis

It is well known that a plate after buckling will in many cases carry, without failure, loads several times greater than that to initiate buckling. In an analogous manner, a plate will sustain a temperature differential greater than that to initiate thermal buckling before failure occurs.

If the lateral deflection of a plate becomes large, i.e. becomes comparable with the thickness, then the assumption that the mid-plane remains unstressed, no longer holds. In this case the Von Kármán large deflection plate equations must be used to evaluate the stresses and deflections. They are of the form:-

$$\nabla^4 \phi = -E\alpha\nabla^2 T + E\left[\left(\frac{\partial^2\omega}{\partial x \partial y}\right)^2 - \frac{\partial^2\omega}{\partial x^2}\cdot\frac{\partial^2\omega}{\partial y^2}\right] \quad \ldots\ldots\ldots \quad 1.69$$

$$\nabla^4 \omega = \frac{t}{D}\left[\sigma_x \frac{\partial^2\omega}{\partial x^2} + \sigma_y \frac{\partial^2\omega}{\partial y^2} + 2\tau_{xy}\frac{\partial^2\omega}{\partial x \partial y}\right] \quad \ldots\ldots\ldots \quad 1.70$$

where the terms in the square brackets in equation 1.69 arise from the stretching of the mid-plane.

Equations 1.69 and 1.70 must therefore be solved simultaneously to obtain the stresses and deflections. Reference 13 has obtained an approximate solution of these equations using the Galerkin[14] method. A simplification was introduced to reduce the amount of numerical work to reasonable proportions by assuming that the shape of the large

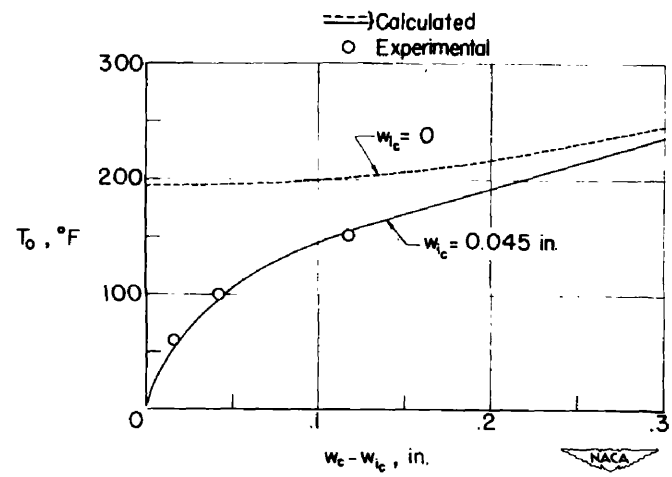

Figure 19: Comparison of calculated and experimental plate centre deflections.

deflections were of similar form as that predicted by the small deflection theory.

After a large amount of involved numerical work, reference 13 obtained the variation of plate centre deflection with the plate temperature differential. Taking initial plate deflections into account reference 13 obtained the following equation:-

$$\frac{E\alpha T_o b^2 t}{\pi^2 D} = 5.39\left(1 - \frac{W_{ic}}{W_c}\right) + 1.12\left(1 - \nu^2\right)\left(\frac{W_c^2 - W_{ic}^2}{t^2}\right) \quad \ldots\ldots \quad 1.71$$

from which the growth of centre deflection with increase in temperature differential for a plate of aspect ratio, 1.566, can be obtained.

Figure 19 reproduced from reference 13 shows the experimental and theoretical plate centre deflections, $W_c - W_{ic}$, plotted as a function of temperature differential, T_o. The values of α, ν, t, b and W_{ic} used in reference 13 to plot the theoretical curve were:-

$$\alpha = 0.127 \times 10^{-4}/^{\circ}F., \qquad \nu = 0.33$$

$$t = 0.25 \text{ in.}, \quad b = 11.5 \text{ in.}, \quad W_{ic} = 0.045 \text{ in.}$$

Gatewood[18] has suggested that it may not be necessary to solve the large deflection equations for the thermal buckling and deflection problem. In reference 18, equation 1.71 has been re-arranged into the form:-

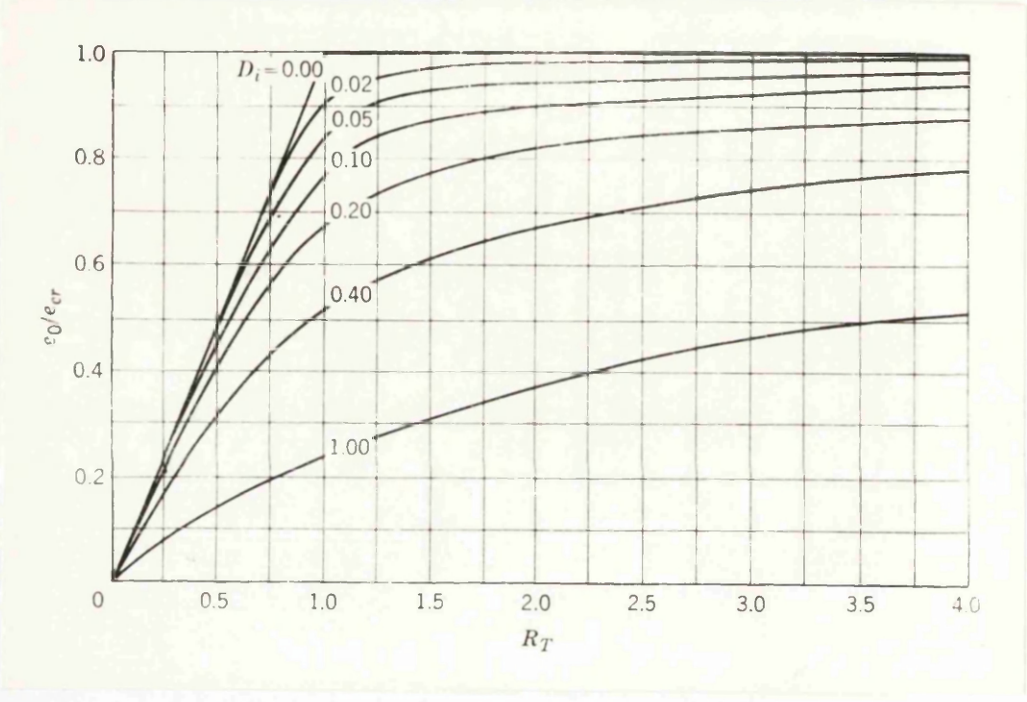

Figure 20: The ratio of e_o/e_{cr} plotted as a function of R_T with D_i as parameter.

$$R_T = \frac{T_o}{T_{ocr}} = \frac{e_o}{e_{cr}} + \left[\frac{D_i}{1 - e_o/e_{cr}}\right]^2 - D_i^2 \quad \ldots\ldots\ldots \quad 1.72$$

where $D_i = \frac{W_{ic}}{2.32t}$.

Except for a different value of D_i, reference 18 shows that this equation is identical to an equation derived in this reference, based on mid-plane thermal strains. The method of reference 18 using the mid-plane strain approach results in the value of D_i as:-

$$D_i = \frac{W_{ic}}{2.42t} \quad \ldots\ldots\ldots \quad 1.73$$

Thus the determination of the growth of plate centre deflection with increasing temperature differential requires only the evaluation of the critical temperature and the value of e_o/e_{cr} from equation 1.72 for particular values of T_o/T_{ocr}. Using this result in the following equation:-

$$W_c = \frac{W_{ic}}{1 - e_o/e_{cr}}, \quad \ldots\ldots\ldots \quad 1.74$$

the value of the plate centre deflection can be obtained for a plate with an initial centre deflection W_{ic} for values of temperature differential p to the critical buckling temperature.

Gatewood has suggested that the simplest method of solution is to graph equation 1.72 with D_i as parameter. This graph, reproduced from reference 18, is shown in figure 20. For particular values of R_T

and D_i, the value of e_o/e_{cr} can be read directly off this graph, and hence the plate centre deflection can be found.

The preceding pages have outlined briefly the method used in the thermal stress and buckling problems. At this point is is of interest to outline some of the cases that have not been fully investigated hitherto.

It appears that little work has been carried out on the influence of the aspect ratio on the critical buckling temperature of plates, particularly short plates. For plates of this size, the condition that the edges remain stress-free necessitates a modification of the longitudinal direct stress which introduces transverse and shear stresses. Undoubtedly, this will affect the critical temperature initiating instability in the plate and might have some practical significance.

To complete the buckling investigation it will be of interest to show the effects of the degree of asymmetry of the temperature distributions on the value of critical temperature. Finally the method proposed by Gatewood for the determination of the growth of plate centre deflection can be verified experimentally. Providing that this simple method gives results in agreement with the experimental values, and values obtained from a solution of the large deflection equations, then its use is justified for practical calculations.

PART II. THEORETICAL ANALYSES

In this part of the thesis the effect of plate aspect ratio and the degree of asymmetry of the temperature distributions on the critical buckling temperature of plates is investigated.

The evaluation of the critical temperature is carried out in steps corresponding to the stages through which a plate passes as the temperature differential increases.

They are:

(1) Distribution of induced thermal stresses.

(2) Thermal buckling of flat rectangular plates.

The first step (1) is concerned with the distribution of the thermal stresses due to a steady state 'tent-like' temperature distribution before the onset of buckling.

The Kantorovitch method[14] developed by Heldenfels and Roberts[10] has been used to determine the thermal stresses and has been extended to deal with asymmetrical 'tent-like' temperature distributions. Since the Rayleigh-Ritz method[14] is frequently used in elastic problems it was thought worthwhile to investigate the use of this method for the determination of the thermal stresses induced in a plate as a result of a 'tent-like' temperature distribution. The fact that the results obtained agree with results of the previous analysis, as will be shown later, provides some indication that both

methods give satisfactory results.

The second step (2), the evaluation of the critical temperature, has been carried out using an original application of the Galerkin method in which both forms for the distribution of thermal stresses have been used.

The final part of the theoretical analyses is concerned with the use of an electronic digital computer (English Electric 'Deuce') to carry out the numerical analyses of some of the cases investigated.

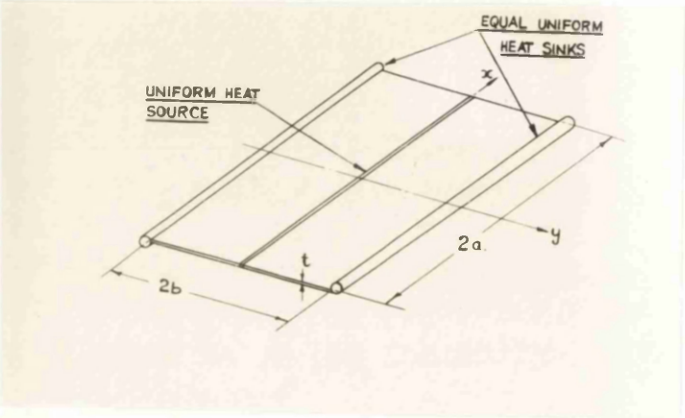

Figure 21: Coordinate system for symmetrical heating of the plate.

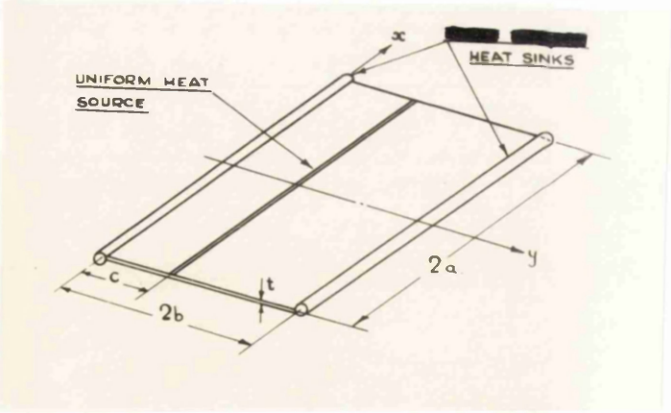

Figure 22: Coordinate system for asymmetrical heating of the plate.

1. Thermal Stress Analysis

(a) Kantorovitch method - single product solution

Consider a flat rectangular plate heated along a longitudinal line and cooled along its longitudinal edges, as shown in figures 21 and 22.

In the analysis for the induced thermal stresses the following assumptions are made:-

(1) The plate is free to expand in its own plane.

(2) There are no external forces acting on the plate.

(3) The plate is thin and may be considered to be in a state of plane stress.

(4) The material properties of the plate are constant in the temperature range of interest.

(5) The stresses are within the elastic range of the plate material.

(6) The plate does not buckle out of its original plane.

Using the Airy stress function, the stresses in the plate can be expressed as:-

$$\sigma_x = \frac{\partial^2 \phi}{\partial y^2} \; ; \; \sigma_y = \frac{\partial^2 \phi}{\partial x^2} \text{ and } \tau_{xy} = -\frac{\partial^2 \phi}{\partial x \partial y} \quad \ldots\ldots\ldots \quad 2.1$$

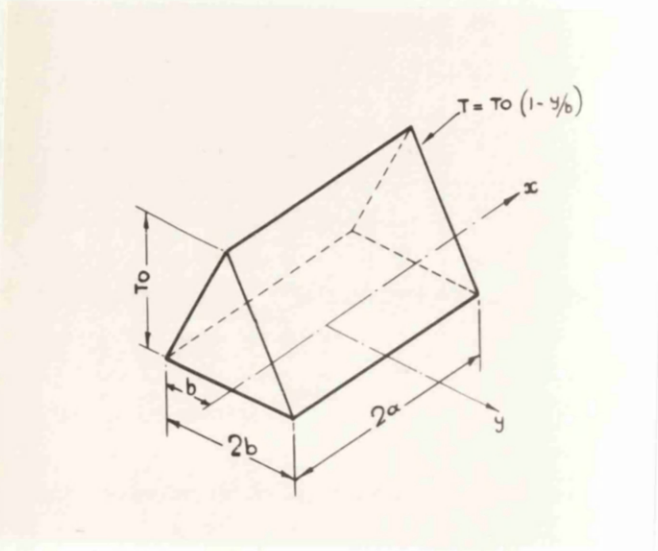

Figure 23: Temperature distributions, symmetrical cases.

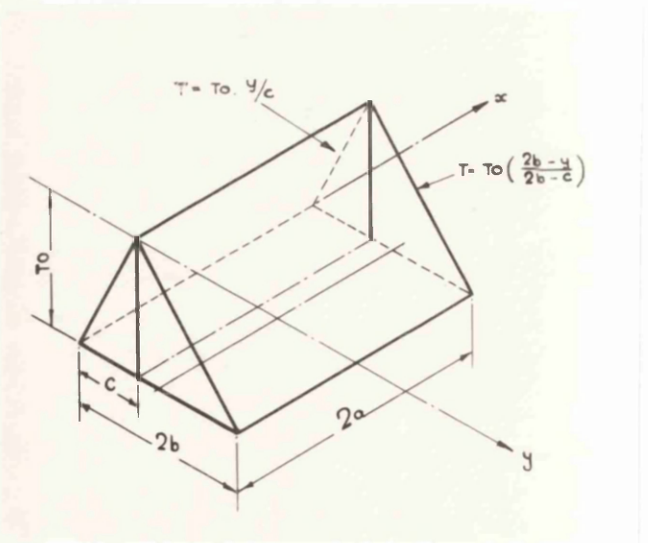

Figure 24: Temperature distributions - asymmetrical cases.

and are governed by the differential equation:-

$$\nabla^4 \phi = -E\alpha \nabla^2 T(x.y) \quad \ldots\ldots\ldots \quad 2.2$$

If a 'tent-like' temperature distribution is chosen (figures 23 and 24), then equation 2.2 can be simplified to

$$\nabla^4 \phi = -E\alpha \frac{d^2T}{dy^2} \quad \ldots\ldots\ldots \quad 2.3$$

The following analysis to determine an approximate solution of the biharmonic equation is similar to the method developed by Heldenfels and Roberts[10]. An approximate solution of equation 2.3 is based on the assumption that the stress function ϕ can be expressed in the single product form:-

$$\phi = f(y).g(x) \quad \ldots\ldots\ldots \quad 2.4$$

where f is a function of y only and g is a function of x only. The stresses in the plate, using the Airy stress function, are:-

$$\sigma_x = gf'' \; ; \; \sigma_y = g''f \text{ and } \tau_{xy} = -g'f' \quad \ldots\ldots\ldots \quad 2.5$$

where the primes indicate differentiation with respect to the appropriate variable.

An approximate solution of the biharmonic equation can be found, as shown in the analysis, by selecting a functionf(y) and then using the principle of minimum complementary energy to determine the

best value for function g(x). The accuracy of the solution is necessarily dependent on the original choice for the function f(y).

The complementary energy of a heated plate[21] can be written as:-

$$U^* = \frac{1}{2E} \int_{-a}^{a} \int_{-b}^{b} \left[\sigma_x^2 + \sigma_y^2 - 2\nu\, \sigma_x \sigma_y + 2(1+\nu)\tau_{xy} + 2E\alpha T(\sigma_x + \sigma_y) \right] dxdy \qquad \ldots\ldots\ldots \quad 2.6$$

If the temperature distribution across the surfaces of the plate is taken as $T = X.Y$, where X is a function of x only and Y is a function of y only, then substituting equations 2.5 and 2.7 in equation 2.6, the complementary energy becomes:

$$U^* = \frac{1}{2E} \int_{-a}^{a} \{A_1 g^2 + A_2 g''^2 - 2\nu\, A_3 g g'' + 2(1+\nu)\, A_4 g'^2 + 2E\alpha\, (A_6 X g + A_8 X g'')\}\, dx \qquad \ldots\ldots\ldots \quad 2.8$$

where

$$A_1 = \int_{-b}^{b} (f'')^2 dy \qquad A_4 = \int_{-b}^{b} (f')^2 dy$$

$$A_2 = \int_{-b}^{b} f^2 dy \qquad A_6 = \int_{-b}^{b} Y f''\, dy$$

$$A_3 = \int_{-b}^{b} f f''\, dy = \left[f f' \right]_{-b}^{b} - A_4 = -A_4 \qquad A_8 = \int_{-b}^{b} Y f\, dy$$

$$\ldots\ldots\ldots \quad 2.9$$

The complementary energy can now be minimised by means of the calculus of variations. This leads to the following linear differential equation for the function g for the particular case of X = constant. (Full details are given in Appendix 1).

$$A_2 g'''' - 2A_4 g'' + A_1 g = -E\alpha A_6 X \qquad \ldots\ldots\ldots \quad 2.10$$

In the cases considered, the temperature distributions across the plate vary in the transverse direction but are constant in the longitudinal direction (figures 23 and 24). This can be represented by the equation

$$T = T_o Y(y) \qquad \ldots\ldots\ldots \quad 2.11$$

A suitable choice for the function f is the stress function for an infinite plate[4].

$$\text{i.e.} \quad f'' = \sigma_{x_\infty} \quad \text{where}$$

$$\sigma_{x_\infty} = -E\alpha T + \frac{1}{2b}\int_{-b}^{b} E\alpha T dy + \frac{3}{2}\frac{y}{b^3}\int_{-b}^{b} E\alpha T y.dy \qquad \ldots\ldots\ldots \quad 2.12$$

Integrating equation 2.12 twice yields:-

$$f = \int\int \sigma_{x_\infty} dy.dy + S_1 y + S_2 \qquad \ldots\ldots\ldots \quad 2.13$$

The constants of integration can be determined from the boundary conditions at $y = \pm b$, where $f = f' = 0$. Making use of these conditions,

the constants of integration can be evaluated and also integrals represented by A_1, A_2, A_4 and A_6.

The complementary function, g_c, of equation 2.10 can be expressed as

$$g_c = C_1 \sinh rx \sin sx + C_2 \cosh rx \cos sx + C_3 \cosh rx \sin sx + C_4 \sinh rx \cos sx \quad \ldots\ldots\ldots \quad 2.14$$

where $\pm(r + js)$ and $(r - js)$ are the roots of the auxiliary equation:-

$$A_2 m^4 - 2A_4 m^2 + A_1 = 0 \quad \ldots\ldots\ldots \quad 2.15$$

The particular integral of equation 2.10 is

$$g_p = -\frac{E \alpha A_6}{A_1} = 1 \quad \ldots\ldots\ldots \quad 2.16$$

since $-E \alpha A_6 = A_1$, as shown in Appendix 2. Therefore, the complete solution of equation 2.10 is

$$g = g_c + g_p \quad \ldots\ldots\ldots \quad 2.17$$

i.e. $$g = 1 + C_1 \sinh rx \sin sx + C_2 \cosh rx \cos sx + C_3 \cosh rx \sin sx + C_4 \sinh rx \cos sx$$

where the constants C_1, C_2, C_3 and C_4 are constants to be determined

from the boundary conditions at $x = \pm a$ where $g = g' = 0$. Using these conditions, the values of these constants are:-

$$C_1 = \frac{r \sinh(ra) \cos(sa) - s \cosh(ra) \sin(sa)}{r \sin(sa) \cos(sa) + s \sinh(ra) \cosh(ra)}$$

$$C_2 = -\frac{r \cosh(ra) \sin(sa) + s \sinh(ra) \cos(sa)}{r \sin(sa) \cos(sa) + s \sinh(ra) \cosh(ra)}$$

$$C_4 = C_3 = 0 \qquad \ldots\ldots\ldots \quad 2.18$$

Thus the distribution of stresses in the plate is given by the following equations:-

$$\sigma_x = \sigma_{x_\infty} \{1 + C_1 \sinh(rx) \sin(sx) + C_2 \cosh(rx) \cos(sx)\}$$

$$\sigma_y = \{\int\int \sigma_{x_\infty} dy.dy + S_1 y + S_2\} \{C_7 \sinh(rx) \sin(sx) + C_8 \cosh(rx) \cos(sx)\}$$

$$\tau_{xy} = -\{\int \sigma_{x_\infty} dy + S_1\} \{C_5 \sinh(rx) \cos(sx) + C_6 \cosh(rx) \sin(sx)\}$$

where $C_5 = C_1 s + C_2 r$; $C_6 = C_1 r - C_2 s$; $C_7 = C_1(r^2 - s^2) - 2C_2 r.s.$;

$$C_8 = 2C_1 rs + C_2(r^2 - s^2) \qquad \ldots\ldots\ldots \quad 2.19$$

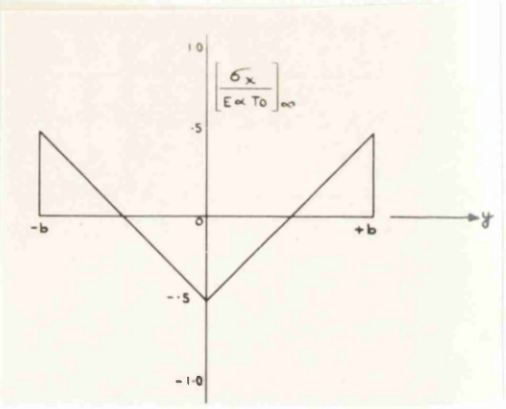

Figure 25: Primary stress distribution, σ_x: symmetrical case, c = b.

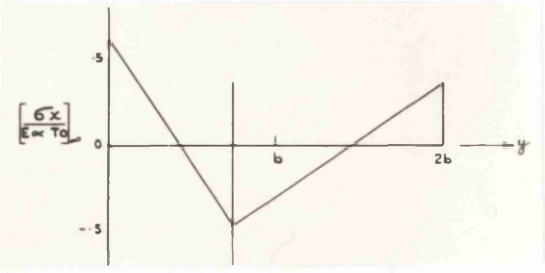

Figure 26: Primary stress distribution, σ_x: asymmetrical case, c = $^3/_4$b.

In the case of asymmetrical 'tent-like' temperature distributions, as shown in figure 24, the temperature can be expressed as:-

$$T = XY \qquad \ldots\ldots\ldots \quad 2.20$$

where $X = T_o$(constant) ; $Y = {}^{y}/_{c}$ for $0 < y < c$

and $Y = \dfrac{2b - y}{2b - c}$ for $c < y < 2b$.

At the point $y = c$, for the coordinate system shown in figure 24, a discontinuity occurs in the temperature function. This requires that the integrals A_1, A_2, A_4 and A_6 must in this case be evaluated over the two sets of limits, 0 to c and c to 2b respectively, and then added together to give the integral between the boundaries 0 and 2b.

For the same reason the f(y) part of the stress function will, in general, have different forms in each domain. The derivation of the stress function for all the cases considered is given in Appendix 3.

To simplify the algebraic analysis, the stress function can be evaluated for particular values of $c = b$, ${}^{3}/_{4}b$, ${}^{b}/_{2}$ and ${}^{b}/_{4}$ which corresponds to various degrees of asymmetry of the temperature distribution.

Figures 25 to 28 show the variation of the primary stress, σ_{x_∞}, for the above four cases considered in the investigation.

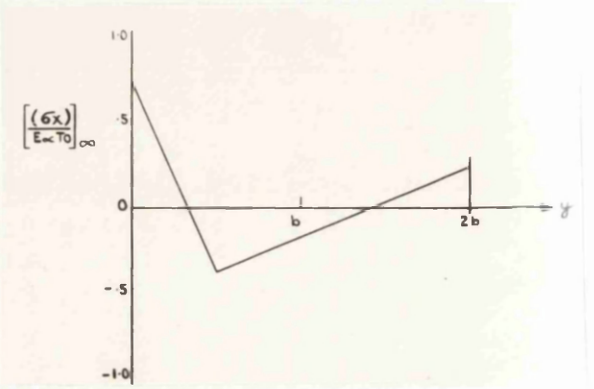

Figure 27: Primary stress distribution, σ_x: asymmetrical case, c = b/2.

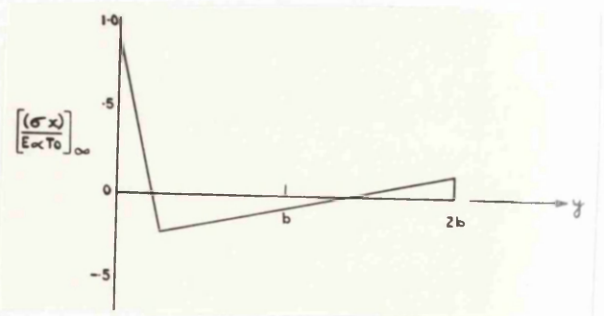

Figure 28: Primary stress distribution, σ_x: asymmetrical case, c = b/4.

Symmetrical case, c = b

For $0 < y < b$ (Coordinate system shown in figure 21)

$$\phi = \frac{b^2 E \alpha T_o}{12} \{1 - 3(\frac{y}{b})^2 + 2(\frac{y}{b})^3\}\{1 + C_1 \sinh(rx) \sin(sx) + C_2 \cosh(rx) \cos(sx)\} \quad \ldots\ldots\ldots 2.21$$

Asymmetrical case, c = $^3/_4$b

For $0 < y < {}^3/_4 b$

$$\phi = b^2 E \alpha T_o \{\frac{5}{16} (\frac{y}{b})^2 - \frac{35}{144} (\frac{y}{b})^3\}\{1 + C_1 \sinh(rx) \sin(sx) + C_2 \cosh(rx) \cos(sx)\} \quad \ldots\ldots\ldots 2.22$$

For $^3/_4 b < y < 2b$

$$\phi = b^2 E \alpha T_o \{-\frac{3}{20} + \frac{3}{5} (\frac{y}{b}) - \frac{39}{80} (\frac{y}{b})^2 + \frac{9}{80} (\frac{y}{b})^3\}\{1 + C_1 \sinh(rx) \sin(sx) + C_2 \cosh(rx) \cos(sx)\}$$

Asymmetrical case, $c = b/2$

For $0 < y < b/2$

$$\phi = b^2 E \alpha T_o \left\{\frac{3}{8}\left(\frac{y}{b}\right)^2 - \frac{9}{24}\left(\frac{y}{b}\right)^3\right\}\left\{1 + C_1 \sinh(rx)\sin(sx) + C_2 \cosh(rx)\cos(sx)\right\} \qquad 2.23$$

For $b/2 < y < 2b$

$$\phi = b^2 E \alpha T_o \left\{-\frac{1}{18} + \frac{1}{3}\left(\frac{y}{b}\right) - \frac{7}{24}\left(\frac{y}{b}\right)^2 + \frac{5}{72}\left(\frac{y}{b}\right)^3\right\}\left\{1 + C_1 \sinh(rx)\sin(sx) + C_2 \cosh(rx)\cos(sx)\right\}$$

Asymmetrical case, $c = b/4$

For $0 < y < b/4$

$$\phi = b^2 E \alpha T_o \left\{\frac{7}{16}\left(\frac{y}{b}\right)^2 - \frac{35}{48}\left(\frac{y}{b}\right)^3\right\}\left\{1 + C_1 \sinh(rx)\sin(sx) + C_2 \cosh(rx)\cos(sx)\right\} \qquad 2.24$$

For $b/4 < y < 2b$

$$\phi = b^2 E \alpha T_o \left\{-\frac{4}{336} + \frac{1}{7}\left(\frac{y}{b}\right) - \frac{15}{112}\left(\frac{y}{b}\right)^2 + \frac{11}{336}\left(\frac{y}{b}\right)^3\right\}\left\{1 + C_1 \sinh(rx)\sin(sx) + C_2 \cosh(rx)\cos(sx)\right\}$$

(b) Rayleigh-Ritz method - polynomial form of solution

Another variational approach to the solution of the biharmonic equation governing the distribution of thermal stresses in a plate can be made using the classical Rayleigh-Ritz method in conjunction with the principle of minimum complementary energy. It will be shown that the results obtained agree with the results of the previous analysis. This provides some indication, though not a proof, that both methods give satisfactory results.

For a plate subjected to symmetrical temperature distributions about the longitudinal axis, the assumed form of the stress function satisfying these conditions can be written as:-

$$\phi = E\alpha T_o(x^2-a^2)^2(y^2-b^2)^2(\gamma_1+\gamma_2x^2+\gamma_3y^2+\gamma_4x^2y^2) \quad \ldots\ldots \quad 2.25$$

where γ_1, γ_2, γ_3 and γ_4 are parameters to be determined.

It can be shown that the assumed form satisfies the boundary conditions of a plate free from external loads. These conditions are:-

$$\sigma_x = \tau_{xy} = 0 \quad \text{at } x = \pm a$$

$$\sigma_y = \tau_{xy} = 0 \quad \text{at } y = \pm a$$

for the coordinate system shown in figure 21.

The Rayleigh-Ritz method applied to a plate subjected to a

'tent-like' temperature distribution gives the stress function in a continuous form over the entire surface of the plate. Further, it is possible to take into account variations of temperature in both the longitudinal and transverse directions.

The condition for minimum complementary energy can be expressed as:-

$$\frac{\partial U^*}{\partial \gamma_n} = 0, \text{ where } n = 1,2,3 \text{ and } 4 \qquad \ldots\ldots\ldots \quad 2.26$$

Applying this condition to equation 2.6, four simultaneous equations are obtained which determine the values of the parameters γ_1, γ_2, γ_3 and γ_4. The derivation of these equations is given in detail in Appendix 5. For the convenience of non-dimensional plotting of the stress distributions, and also for buckling calculations, equation 2.25 can be expressed in the form:-

$$\phi = b^2 E\alpha T_o \left[\left(\frac{x}{a}\right)^2 - 1\right]^2 \left[\left(\frac{y}{b}\right)^2 - 1\right]^2 \left[\beta_1 + \beta_2\left(\frac{x}{a}\right)^2 + \beta_3\left(\frac{y}{b}\right)^2 + \beta_4\left(\frac{xy}{ab}\right)^2\right] \ldots \quad 2.27$$

where β_1, β_2, β_3 and β_4 are non-dimensional coefficients related to γ_1 etc. by the following equations:-

$$E\alpha T_o\beta_1 = \gamma_1 a^4 b^2 \qquad E\alpha T_o\beta_3 = \gamma_3 a^4 b^4$$

$$E\alpha T_o\beta_2 = \gamma_2 a^6 b^2 \qquad E\alpha T_o\beta_4 = \gamma_4 a^6 b^4$$

$$\ldots\ldots\ldots \quad 2.28$$

The stresses in the plate are then:-

$$\sigma_x = \frac{\partial^2 \phi}{\partial y^2} = E\alpha T_o b^2 \Bigg[30 \frac{x^6}{a^6}\frac{y^4}{b^4} + 12 \frac{x^6}{a^6}\frac{y^2}{b^4}(\beta_2 - 2\beta_4)$$

$$+ 2\frac{x^6}{a^6 b^2}(-2\beta_2 + \beta_4) + 30 \frac{x^4}{a^4}\frac{y^4}{b^6}(\beta_3 - 2\beta_4)$$

$$+ 30 \frac{x^4}{a^4}\frac{y^4}{b^6}(\beta_3 - 2\beta_4) + 12 \frac{x^4}{a^4}\frac{y^2}{b^4}(\beta_1 - 2\beta_2 - 2\beta_3 + 4\beta_4)$$

$$+ 2\frac{x^4}{a^4 b^2}(-2\beta_1 + 4\beta_2 + \beta_3 - 2\beta_4) + 30 \frac{x^2}{a^2}\frac{y^4}{b^6}(-2\beta_3 + \beta_4)$$

$$+ 12\frac{x^2}{a^2}\frac{y^2}{b^4}(-2\beta_1 + \beta_2 + 4\beta_3 - 2\beta_4) + 2\frac{x^2}{a^2 b^2}(4\beta_1 - 2\beta_2 - 2\beta_3 + \beta_4)$$

$$+ 30\frac{y^4}{b^6}\beta_3 + 12\frac{y^2}{b^4}(\beta_1 - 2\beta_3) + \frac{2}{b^2}(-2\beta_1 + \beta_3) \Bigg]$$

$$\sigma_y = \frac{\partial^2 \phi}{\partial x^2} = E\alpha T_o b^2 \Bigg[30\frac{x^4}{a^6}\frac{y^6}{b^6}\beta_4 + 30\frac{x^4}{a^6}\frac{y^4}{b^4}(\beta_2 - 2\beta_4) + 30\frac{x^4}{a^6}\frac{y^2}{b^2}(-2\beta_2 + \beta_4)$$

$$+ 30\frac{x^4}{b^6}\beta_2 + 12\frac{x^2}{a^4}\frac{y^6}{b^6}(\beta_3 - 2\beta_4) + 12\frac{x^2}{a^4}\frac{y^4}{b^4}(\beta_1 - 2\beta_2 - 2\beta_3 + 4\beta_4)$$

$$+ 12\frac{x^2}{a^4}\frac{y^2}{b^2}(-2\beta_1 + 4\beta_2 + \beta_3 - 2\beta_4) + 12\frac{x^2}{a^4}(\beta_1 - 2\beta_2)$$

$$+ 2\frac{y^6}{a^2b^6}(-2\beta_3 + \beta_4) + 2\frac{y^4}{a^2b^4}(-2\beta_1 + \beta_2 + 4\beta_3 - 2\beta_4)$$

$$+ 2\frac{y^2}{a^2b^2}(4\beta_1 - 2\beta_2 - 2\beta_3 + \beta_4) + \frac{2}{a^2}(-2\beta_1 + \beta_2)\Bigg]$$

$$\tau_{xy} = \frac{-\partial^2\phi}{\partial x\partial y} = -E\alpha T_o b^2\Bigg[36\frac{x^5}{a^6}\frac{y^5}{b^6}\beta_4 + 24\frac{x^5}{a^6}\frac{y^3}{b^4}(\beta_2 - 2\beta_4) + 12\frac{x^5y}{a^6b^2}(-2\beta_2 + \beta_4)$$

$$+ 24\frac{x^3}{a^4}\frac{y^5}{y^6}(\beta_3 - 2\beta_4) + 16\frac{x^3}{a^4}\frac{y^3}{b^4}(\beta_1 - 2\beta_2 - 2\beta_3 + 4\beta_4)$$

$$+ 8\frac{x^3}{a^4}\frac{y}{b^4}(-2\beta_1 + 4\beta_2 + \beta_3 - 2\beta_4) + 12\frac{xy^5}{a^2b^6}(-2\beta_3 + \beta_4)$$

$$+ 8\frac{xy^3}{a^2b^4}(-2\beta_1 + \beta_2 + 4\beta_3 - 2\beta_4) + 4\frac{xy}{a^2b^2}(4\beta_1 - 2\beta_2 - 2\beta_3 + \beta_4)\Bigg]$$

..... 2.29

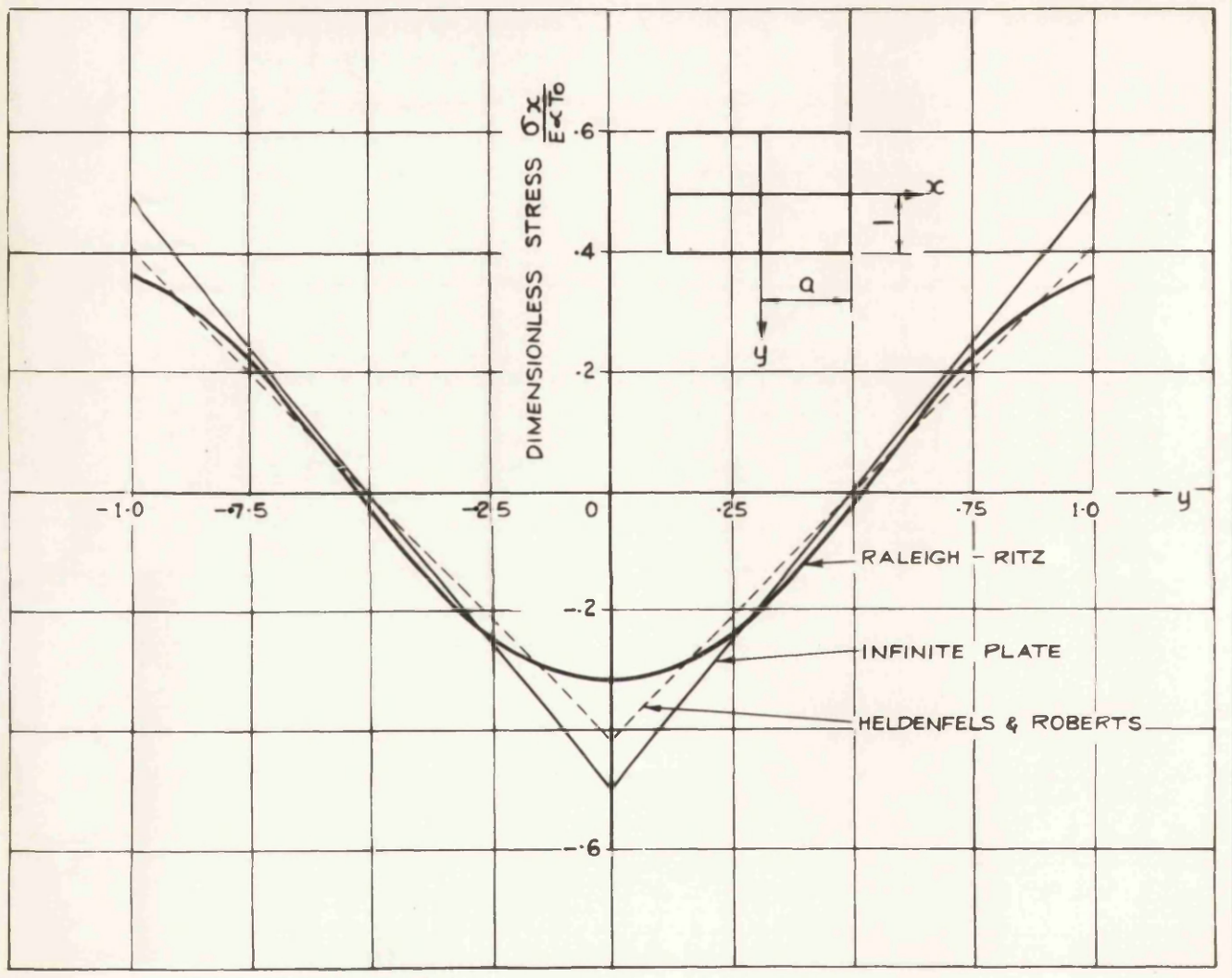

Figure 29: Comparison of the transverse distribution of longitudinal stress (σ_x) at x = 0 for a plate subjected to a symmetrical 'tent-like' temperature distribution, plate aspect ratio 1.566.

Figure 29 compares the distribution of the non-dimensional longitudinal stress obtained by the Rayleigh-Ritz and the Kantorovitch method developed by Heldenfels and Roberts.

For this comparison a plate of aspect ratio 1.567 subjected to a tent-like distribution

$$T = T_o\left(1 + \frac{y}{b}\right) \quad \text{for} \quad -b < y < 0$$

$$T = T_o\left(1 - \frac{y}{b}\right) \quad \text{for} \quad 0 < y < b \qquad \text{.....} \quad 2.30$$

was chosen.

The particular value of the parameters β_1 etc., are in this case:-

$$\beta_1 = 0.0708721 \qquad \beta_2 = 0.066080$$

$$\beta_3 = -0.0207127 \qquad \beta_4 = -0.0712483$$

The agreement between the value of stresses given by the two methods is close at all points except at the origin, $x = 0$, $y = 0$.

Since the Rayleigh-Ritz method is essentially an averaging process, the smoothing out of the distribution of longitudinal stress at the origin where a discontinuity occurs in the temperature function is hardly surprising.

Nevertheless, it will be shown in the analysis for the

buckling of the plate, that this 'rounding-off' in the distribution of stresses has no significance if the overall buckling of a plate is considered.

2. Thermal Buckling Analysis

(a) Evaluation of the critical temperature using the single product form for the stress distributions

As the temperature differential T_o increases, a value will be reached in an idealized flat plate when the plate will buckle out of its own plane due to the compressive component of the induced thermal stresses.

Assuming that the plate deflections are small, which implies that the mid-plane does not stretch, and that the stress distribution does not change after the onset of buckling, then the critical buckling temperature can be found from the equation governing the stability of flat plates with varying internal stresses.

The relevant differential equation is:-

$$\frac{D}{t} \nabla^4 \omega = \sigma_x \frac{\partial^2 \omega}{\partial x^2} + \sigma_y \frac{\partial^2 \omega}{\partial y^2} + 2\tau_{xy} \frac{\partial^2 \omega}{\partial x \partial y} \qquad \ldots\ldots\ldots \quad 2.31$$

where the stresses σ_x, σ_y and τ_{xy} are given by the equations:-

$$\sigma_x = \sigma_{x_\infty} \left(1 + B_1 \sinh R_1 \frac{x}{a} \sin R_2 \frac{x}{a} + B_2 \cosh R_1 \frac{x}{a} \cos R_2 \frac{x}{a} \right)$$

$$\sigma_y = \left(\iint \sigma_{x_\infty} dy.dy + S_1 y + S_2 \right) \left(D_1 \sinh R_1 \frac{x}{a} \sin R_2 \frac{x}{a} + D_2 \cosh R_1 \frac{x}{a} \cos R_2 \frac{x}{a} \right)$$

$$\tau_{xy} = (-\int \sigma_{x_\infty} dy + S_1)(D_3 \sinh R_1 \frac{x}{a} \cos R_2 \frac{x}{a} + D_4 \cosh R_1 \frac{x}{a} \sin R_2 \frac{x}{a})$$

It should be noted that the constants, B_1, B_2, D_1, D_2, D_3, D_4, R_1 and R_2, defined in Appendix 4, are similar to those defined in equation 2.19.

The Galerkin method[14] is convenient for determining the critical temperature differential providing that the assumed form of the deflection pattern satisfies the boundary conditions for simply supported edges in the cases considered, term by term.

For simply supported edges the boundary conditions are:-

$$\omega = 0, \quad M_x = 0 = \frac{\partial^2 \omega}{\partial x^2} + \nu \frac{\partial^2 \omega}{\partial y^2} \quad \text{at } x = \pm a$$

$$\omega = 0, \quad M_y = 0 = \frac{\partial^2 \omega}{\partial y^2} + \nu \frac{\partial^2 \omega}{\partial x^2} \quad \text{at } y = \pm b \qquad \ldots\ldots\ldots \quad 2.32$$

It can be shown that the condition of minimum potential energy can be expressed as

$$\iiint \left[(D.E)\ \delta f \right] dx.dy.dz = 0 \qquad \ldots\ldots\ldots \quad 2.33$$

where D.E is the governing differential equation and δf the small variation of a particular chosen function contained in the differential equation.

The minimum energy condition is therefore expressible directly from the governing differential equation and does not require the

formulation of the energy expression itself.

Experimental results indicate that the buckle pattern may be taken as:-

$$(a)\quad \omega = \sum_{m=1,3,5}^{\infty} \sum_{n=1,3,5}^{\infty} a_{mn} \cos \frac{m\pi x}{2a} \cos \frac{n\pi y}{2b}$$

$$(b)\quad \sum_{m=2,4,6}^{\infty} \sum_{n=1,3,5}^{\infty} a_{mn} \sin \frac{m\pi x}{2a} \cos \frac{n\pi y}{2b} \qquad \ldots\ldots\ldots \quad 2.34$$

The above forms apply to the symmetrical case only; and, in particular, form (a) covers the case of 1, 3 and 5 half waves and form (b) covers the case of 2, 4 and 6 half waves in the x direction.

In the asymmetrical case, a better approximation to the deflected form can be obtained by taking

$$\omega = \sum_{m=1,3,5}^{\infty} \sum_{n=1,2,3} a_{mn} \cos \frac{m\pi x}{2a} \sin \frac{n\pi y}{2b} \qquad \ldots\ldots\ldots \quad 2.35$$

for the coordinate system shown in figure 22.

If the relevant differential equation is substituted in equation 2.33, the condition of minimum potential energy can be expressed as:-

$$\int_0^a \int_0^{b \text{ or } 2b} \left(\frac{D}{t} \nabla^4 \omega - \sigma_x \frac{\partial^2 \omega}{\partial x^2} - \sigma_y \frac{\partial^2 \omega}{\partial y^2} - 2\tau_{xy} \frac{\partial^2 \omega}{\partial x \partial y}\right) \frac{\partial \omega}{\partial a_{mn}} = 0 \quad \ldots\ldots \quad 2.36$$

the integration being carried out over one quadrant for the symmetrical case, and over one half of the plate for the asymmetrical case.

This procedure leads to a set of linear simultaneous equations which constitutes a characteristic value problem from which the lowest critical temperature differential can be found together with the corresponding ratio between the coefficients, a_{mn}.

In the symmetrical case, the simultaneous equations for an odd number of half waves are of the form:-

$$\frac{1}{E\alpha T_{ocr} b^2 t / \pi^2 D} \; a_{pq} \left[\frac{1}{4} \left(q^2 \frac{a}{b} + p^2 \frac{b}{a} \right) \right]^2$$

$$= a_{mn} \sum_{m=1,3,5} \sum_{n=1,3,5} \Big[- A_{nq} m^2 (B_1 I_{mp} + B_2 J_{mp} + F_{mp})$$

$$- C_{nq} n^2 \frac{a^2}{b^2} (D_1 I_{mp} + D_2 J_{mp})$$

$$+ 2 B_{nq} m.n. \frac{a}{b} (D_3 G_{mp} + D_4 K_{mp} \Big] \quad \ldots\ldots \quad 2.37$$

where p = 1, 3, 5, q = 1, 3, 5; and the form for even number of half waves, symmetrical case:-

$$\frac{1}{E\alpha T_{ocr} b^2 t/\pi^2 D} \; a_{pq} \left[\frac{1}{4}\left(q^2 \frac{a}{b} + p^2 \frac{b}{a}\right)\right]^2$$

$$= a_{mn} \sum_{m=2,4,6} \sum_{n=1,3,5} \Bigg[- A_{nq} m^2 \left(B_1 D_{mp} + B_2 E_{mp} + F_{mp}\right)$$

$$- C_{nq} n^2 \frac{a^2}{b^2} \left(D_1 D_{mp} + D_2 E_{mp}\right)$$

$$- 2_{nq} m.n.\frac{a}{b} \left(D_3 G'_{mp} + D_4 K'_{mp}\right) \Bigg] \quad \ldots\ldots \quad 2.38$$

where p = 2, 4, 6, q = 1, 3, 5; and for the asymmetrical case:-

$$\frac{2}{E\alpha T_{ocr} b^2 t/\pi^2 D} \; a_{pq} \left[\frac{1}{4}\left(p^2 \frac{b}{a} + q^2 \frac{a}{b}\right)\right]^2$$

$$= a_{mn} \sum_{m=1,3,5} \sum_{n=1,2,3} \Bigg[- A'_{nq} m^2 \left(B_1 I_{mp} + B_2 J_{mp} + F_{mp}\right)$$

$$- C'_{nq} n^2 \frac{a^2}{b^2} \left(D_1 I_{mp} + D_2 J_{mp}\right)$$

$$- 2B'_{nq} m.n.\frac{a}{b} \left(D_3 G_{mp} + D_4 K_{mp}\right) \Bigg] \quad \ldots\ldots \quad 2.39$$

where p = 1, 3, 5, q = 1, 2, 3 and A_{nq}, A'_{nq}, B_{nq}, B'_{nq}, C_{nq}, C'_{nq}, D_{mp}, E_{mp}, G_{mp}, G'_{mp}, I_{mp}, J_{mp}, K_{mp}, K'_{mp}, B_1, B_2, D_1, D_2, D_3 and D_4 are defined in Appendix 4.

$$\begin{bmatrix} 15.719 & 14.861 & -7.526 & 22.457 & -5.821 & 1.958 & 1.141 & .67710 & -.2031 \\ 1.347 & 7.433 & 5.4870 & 3.527 & 7.695 & 1.0137 & .2115 & .802 & .386 \\ -.119 & .953 & 3.483 & -.339 & 1.890 & 3.501 & -.017 & .131 & .385 \\ .504 & .869 & -.481 & 1.426 & .374 & -.476 & 1.424 & -.406 & -.021 \\ -.072 & 1.045 & 1.475 & .206 & .438 & .648 & .878 & 1.262 & -.155 \\ .011 & .060 & 1.190 & -.114 & .282 & .189 & -.251 & 1.098 & 1.229 \\ .003 & .007 & -.003 & .196 & .219 & -.143 & .536 & .211 & -.177 \\ .0016 & .021 & .020 & -.043 & .246 & .492 & .103 & .187 & .316 \\ -.0003 & .006 & .039 & -.0001 & -.020 & .365 & -.092 & .209 & .062 \end{bmatrix} \begin{bmatrix} a_{11} \\ a_{31} \\ a_{51} \\ a_{13} \\ a_{33} \\ a_{53} \\ a_{15} \\ a_{35} \\ a_{55} \end{bmatrix} = \frac{100}{E\alpha T_{ocr} b^2 t/\pi^2 D} \begin{bmatrix} a_{11} \\ a_{31} \\ a_{51} \\ a_{13} \\ a_{33} \\ a_{53} \\ a_{15} \\ a_{35} \\ a_{55} \end{bmatrix}$$

..... 2.40

In order that the coefficients, a_{mn}, have values other than zero, the determinant of the above set of equations must be zero. This condition gives the values of the critical temperatures, the lowest value being the only one of importance.

If nine terms are retained in the deflected form, it is convenient to express the above set of equations in matrix form. For the particular case of a plate of aspect ratio 1.566, buckling into an odd number of half waves in the longitudinal direction, the nine simultaneous equations are as shown on the accompanying sheet.

The numerical evaluation of such matrices to give the largest eigen value can be carried out using an iterative method[17]. This gives the largest value of

$$\frac{100}{E\alpha T_{ocr} b^2 t/\pi^2 D}$$

and by inversion the smallest value of

$$E\alpha T_{ocr} b^2 t/\pi^2 D = \frac{\alpha}{12\pi^2(1-\nu^2)} (b/t)^2 T_{ocr} \quad \ldots\ldots\ldots \quad 2.41$$

Besides giving the smallest value of the critical temperature, the above method also gives the relative values of the coefficients, a_{mn}. The value of the critical temperature parameter and the relative values of the coefficients, a_{mn}, was found to be, for a plate of aspect ratio, 1.566,

$$\frac{E\,\alpha T_{ocr} b^2 t}{\pi^2 D} = 5.39423 \qquad \ldots\ldots\ldots \quad 2.42$$

and

$$\begin{bmatrix} a_{11} \\ a_{31} \\ a_{51} \\ a_{13} \\ a_{33} \\ a_{53} \\ a_{15} \\ a_{35} \\ a_{55} \end{bmatrix} = \begin{bmatrix} 1.0000 \\ 0.13646 \\ 0.000703 \\ 0.03648 \\ 0.00444 \\ 0.000914 \\ 0.000693 \\ 0.000249 \\ 0.000047 \end{bmatrix} \qquad \ldots\ldots\ldots \quad 2.43$$

Using these coefficients the deflection of the buckled plate can be written as:-

$$\omega = a_{11} \left\{ \cos \frac{\pi x}{2a} \cos \frac{\pi y}{2b} + 0.13646 \cos \frac{3\pi x}{2a} \cos \frac{\pi y}{2b} \right.$$

$$\left. + 0.000703 \cos \frac{5\pi x}{2a} \cos \frac{\pi y}{2b} + 0.03648 \cos \frac{\pi y}{2a} \cos \frac{3\pi x}{2b} \right.$$

$$+ 0.00444 \cos \frac{3\pi x}{2a} \cos \frac{3\pi y}{2b} + 0.000911 \cos \frac{5\pi x}{2a} \cos \frac{3\pi y}{2b}$$

$$+ 0.000693 \cos \frac{\pi x}{2a} \cos \frac{5\pi y}{2b} + 0.000249 \cos \frac{3\pi x}{2a} \cos \frac{5\pi y}{2b}$$

$$+ 0.000047 \cos \frac{5\pi x}{2a} \cos \frac{5\pi y}{2b} \} \qquad \ldots\ldots\ldots \quad 2.44$$

In order to show the importance of terms retained in the deflected form, the critical temperature parameter has been evaluated taking various numbers of terms of equation 2.34 into account.

The convergence of the critical temperature parameter with respect to the number of terms taken in the deflected form is shown in Table 1. It can be seen that only the first four terms are of significance.

Tables 2, 3 and 4 present the results for all the cases investigated. In particular, Tables 2 and 3 show the variation of the value of critical-temperature parameter with respect to aspect ratio of the plate. In these cases it should be remembered that the temperature distribution is symmetrical about the transverse axis.

Table 4 shows the variation of the critical temperature parameter with the degree of asymmetry of the temperature distributions. Finally, Tables 6, 7 and 8 present the theoretical buckle patterns in tabular form corresponding to the critical temperature parameters given in Tables 2, 3 and 4.

TABLE 1

Terms taken into account	$\frac{E\alpha T_{ocr} b^2 t}{\pi^2 D}$
a_{11}	6.317
a_{11} a_{31}	5.657
a_{11} a_{31} a_{51}	5.657
a_{11} a_{31} a_{51} a_{13}	5.396
a_{11} a_{31} a_{51} a_{13} a_{33}	5.394
a_{11} a_{31} a_{51} a_{13} a_{33} a_{53}	5.394
a_{11} a_{31} a_{51} a_{13} a_{33} a_{53} a_{15}	5.394
a_{11} a_{31} a_{51} a_{13} a_{33} a_{53} a_{15} a_{35}	5.394
a_{11} a_{31} a_{51} a_{13} a_{33} a_{53} a_{15} a_{35} a_{55}	5.394

TABLE 2

Odd case, m = 1, 3, 5

Aspect Ratio a/b	Buckling Mode in 'x' direction	$\frac{E\alpha T_{ocr} b^2 t}{\pi^2 D}$	T_{ocr} * °C.
0.5	One half wave	72.497	1350
.75	"	16.949	315
1.0	"	8.12894	151.0
1.5	"	5.41837	100.5
1.57	"	5.39430	100
2.0	"	5.720195	106.5
2.5	Three half waves	5.52141	102.5
3.0	"	5.05113	93.9
3.5	"	4.90547	91.1
4.0	"	4.95655	92.0
4.5	"	5.06861	94.1

* Based on a plate, b = 11.5 in., $\nu = 0.313$, $\alpha = 23.2 \times 10^{-6}/°C.$

TABLE 3

Even case, m = 2, 4, 6

Aspect Ratio a/b	Buckling Mode in 'x' direction	$\frac{E\alpha T_{ocr} b^2 t}{\pi^2 D}$	T^*_{ocr} °C.
2.0	Two half waves	5.45747	101
2.5	"	5.019108	93.1
3.0	"	5.10438	94.6
3.5	Four half waves	5.11992	95.0
4.0	"	4.927736	91.5
4.5	"	4.85645	90

* Based on a plate, b = 11.5 in., ν = 0.313, α = 23.2 x 10^{-6}/°C.

TABLE 4

Heater position	$\frac{E\alpha T_{ocr} b^2 t}{\pi^2 D}$	T^*_{ocr} °C.
c = b (centre)	5.7588	107
$c = \frac{3}{4}b$	6.20675	115
$c = \frac{b}{2}$	8.0305	149
$c = \frac{b}{4}$	13.3566	248

* Based on a plate, b = 11.5 in., a = 23.5 in., ν = 0.313,

$\alpha = 23.2 \times 10^{-6}/°C.$

TABLE 5

Theoretical Buckle Forms: Odd case - symmetrical heating

$$\omega = \sum_{m=1,3,5}^{\infty} \sum_{n=1,3,5}^{\infty} a_{mn} \cos \frac{m\pi x}{2a} \cos \frac{n\pi y}{2b}$$

Aspect Ratio	a_{mn}								
	a_{11}	a_{31}	a_{51}	a_{13}	a_{33}	a_{53}	a_{15}	a_{35}	a_{55}
0.5	1.000	.03083	-	.31027	.01066	-	.03943	-	-
0.75	1.000	.03981	-	.1084	.003881	-	.005701	-	-
1.0	1.000	.05751	-	.06653	.002664	-	.002057	-	-
1.5	1.000	.1229	-	.03813	.003883	-	-	-	-
2.0	1.000	.3245	.002315	.003013	.001573	-	-	-	-
2.25	1.000	.7949	.1267	.02862	.04723	.014041	-	.001542	-
2.40	.6531	1.000	.2041	.01808	.06012	.01949	-	.001823	-
2.5	.4191	1.000	.2259	.01116	.05863	.01989	-	.001697	-
3.0	.00411	1.000	.2969	-	.04679	.01915	-	.001122	-
3.5	.07608	1.000	.3745	-	.03778	.01952	-	-	-
4.0	-.09561	1.000	.5240	-.003714	.03186	.02392	-	-	-
4.5	-.1036	1.000	.9029	-.003782	.02777	.03800	-	-	-

TABLE 6

Theoretical Buckle Forms: Even case - symmetrical heating.

$$\omega = \sum_{m=2,4,6}^{\infty} \sum_{n=1,3,5}^{\infty} a_{mn} \sin \frac{m\pi x}{2a} \cos \frac{n\pi y}{2b}$$

Aspect Ratio	a_{mn}								
	a_{21}	a_{41}	a_{61}	a_{23}	a_{43}	a_{63}	a_{25}	a_{45}	a_{65}
2.0	1.000	.1997	-.00143	.05208	.01294	.00157	.00130	-	-
2.5	1.000	.2639	-.00369	.03819	.01291	.00191	-	-	-
3.0	1.000	.4021	.01210	.03141	.01886	.00380	-	-	-
3.5	.4778	1.000	.2557	.01145	.05059	.02052	-	.00133	-
4.0	.01551	1.000	.3668	-.00163	.04397	.02261	-	.00102	-
4.5	-.08759	1.000	.4604	-.00407	.03743	.02381	-	-	-

TABLE 7

Theoretical Buckle Forms. Asymmetrical heating. Aspect ratio = 2.04.

$$\omega = \sum_{m=1,3,5}^{\infty} \sum_{n=1,2,3}^{\infty} a_{mn} \cos \frac{m\pi x}{2a} \sin \frac{n\pi y}{2b}$$

Heater Position	a_{mn}								
	a_{11}	a_{31}	a_{51}	a_{12}	a_{32}	a_{52}	a_{13}	a_{33}	a_{53}
$c = b$	1.000	.3684	.03125	-	-	-	-	-	-
$c = \frac{3}{4}b$	1.000	.3652	.02961	.03100	.03177	.00509	-.02681	-.01426	-
$c = \frac{b}{2}$	1.000	.4070	.03385	.05595	.07145	.01099	-.01921	-	-
$c = \frac{b}{4}$	1.000	.6456	.06896	.06776	-.1618	-.02450	-.01043	+.01468	-.01245

(b) Evaluation of the critical temperature using the polynomial form of stress distribution

Having obtained an alternative form for the stress function (1b) using the Rayleigh-Ritz method, it is worthwhile to evaluate the critical buckling temperature of a plate using this form in the buckling calculations. The value of critical temperature obtained can then be compared directly with the results of the previous analysis (2a). Also, an assessment can be made of the suitability of the Rayleigh-Ritz method used in the analysis for the stresses when this form is used in buckling calculations.

Following out the same procedure as in the previous analysis (2a), the application of the Galerkin method to equation 2.31, using the distribution of stresses given by equation 2.29, leads to a set of linear simultaneous equations. If the terms a_{11}, a_{31} and a_{13} are retained in the series for the deflected form of the plate, then the set of linear simultaneous equations can be written in matrix form. For a plate of aspect ratio of 1.566, the coefficients of the equations have the following values:-

$$\begin{bmatrix} 15.76 & 21.91 & 14.76 \\ 0.4916 & 1.323 & 0.776 \\ 1.342 & 3.227 & 7.355 \end{bmatrix} \begin{bmatrix} a_{11} \\ a_{13} \\ a_{31} \end{bmatrix} = \frac{100}{E \alpha T_{ocr} b^2 t / \pi^2 D} \begin{bmatrix} a_{11} \\ a_{13} \\ a_{31} \end{bmatrix} \quad \ldots \quad 2.45$$

The numerical evaluation of the above matrices to give the lowest value of the critical temperature parameter was again carried out using an iterative method already referred to. Applying the above procedure to equation 2.45, the lowest value of the critical temperature parameter is

$$\frac{E\alpha T_{ocr} b^2 t}{\pi^2 D} = 5.41 \qquad \ldots\ldots\ldots\ldots \quad 2.46$$

and the relative values of the deflection coefficients, a_{mn}, are:-

$$\begin{bmatrix} a_{11} \\ a_{13} \\ a_{31} \end{bmatrix} = \begin{bmatrix} 1.000 \\ 0.0351 \\ 0.132 \end{bmatrix} \qquad \ldots\ldots\ldots\ldots \quad 2.47$$

Some idea of the convergence of the critical temperature parameter in this case can be gained from Table 8.

If this value of critical temperature parameter is compared with the value in Table 2, for a plate of the same aspect ratio, it can be seen that the agreement between the values is very close.

Thus the methods used in this section provide an alternative approach to the buckling problem.

Although the methods used in this section give reasonable

TABLE 8

Terms retained	$\frac{E\alpha T_{ocr} b^2 t}{\pi^2 D}$
a_{11}	6.35
a_{11} a_{31}	5.64
a_{11} a_{31} a_{13}	5.41

results, the amount of numerical effort required is considerably greater than that of former methods. This arises from the form of stress function used which results in cross-product terms appearing in the buckling calculations. Using the single product type of stress function, this type of complication does not arise.

3. Use of Deuce Computer

For each particular case, either equation 2.37, 2.38 or 2.39 must be solved to determine the smallest value of the critical temperature parameter.

It has been shown that at least three terms in the equation for the deflected form must be considered in order to obtain a reasonably accurate value of the critical buckling temperature.

The amount of numerical work involved is dependent on the number of terms taken in the deflected form. If more than three terms are taken the amount of numerical work rapidly increases. With this point in mind, and also the desire to take sufficient number of terms in the equation for the deflected form to cover all values of aspect ratio of interest, it was decided to use an electronic digital computer to carry out the numerical analyses. The effort required in the construction of the programme does not increase proportionately to the number of terms taken in the deflected form.

To indicate the amount of numerical work involved, the first simultaneous equation has been written out in full, with nine terms taken in the deflected form.

From many considerations, especially from the point of view of programme construction, it appeared that Alpha-Code, an auto-code system, would be suitable for evaluating the coefficients in the nine simultaneous equations.

$$\frac{1}{E\alpha T_{ocr} b^2 t/\pi^2 D} \; a_{11}\left\{\frac{1}{4}\left(\frac{a}{b}+\frac{b}{a}\right)\right\}^2 =$$

$$a_{11}\left\{-A_{11}(B_1 I_{11} + B_2 J_{11} + F_{11}) - \frac{a^2}{b^2} C_{11}(D_1 I_{11} + D_2 J_{11}) + 2\frac{a}{b} B_{11}(D_3 G_{11} + D_4 K_{11})\right\}$$

$$+ a_{31}\left\{-3^2 A_{11}(B_1 I_{31} + B_2 J_{31} + F_{31}) - \frac{a^2}{b^2} C_{11}(D_1 I_{31} + D_2 J_{31}) + 2 \times 3\frac{a}{b} B_{11}(D_3 G_{31} + D_4 K_{31})\right\}$$

$$+ a_{51}\left\{-5^2 A_{11}(B_1 I_{51} + B_2 J_{51} + F_{51}) - \frac{a^2}{b^2} C_{11}(D_1 I_{51} + D_2 J_{51}) + 2 \times 5\frac{a}{b} B_{11}(D_3 G_{51} + D_4 K_{51})\right\}$$

$$+ a_{13}\left\{-A_{31}(B_1 I_{11} + B_2 J_{11} + F_{11}) - \frac{a^2}{b^2} 3^2 C_{31}(D_1 I_{11} + D_2 J_{11}) + 2 \times 3\frac{a}{b} B_{31}(D_3 G_{11} + D_4 K_{11})\right\}$$

.....

$$+ a_{55}\left\{-5^2 A_{51}(B_1 I_{51} + B_2 J_{51} + F_{51}) - 5^2 \frac{a^2}{b^2} C_{51}(D_1 I_{51} + D_2 J_{51}) + 2.5.5\frac{a}{b} B_{51}(D_3 G_{51} + D_4 K_{51})\right\}$$

The numerical evaluation was carried out on the computer in several distinct steps. Firstly, the constants B_1, B_2, D_1, D_2, D_3 and D_4 were evaluated for a particular size of plate. The next step was concerned with the evaluation of the constants C_1 to C_8 using equation 5.62. In this case the nine different values of C_1, C_2 etc. were computed in the following logical order. For the values of $m = 1, 3, 5$, $p = 1, 3, 5$, the order was:-

$$C_1^{11}, C_2^{31} \ldots\ldots C_1^{35}, C_1^{55}; \quad C_2^{11} \ldots\ldots C_2^{55}, \text{ etc.},$$

the index indicating the value of m and p respectively.

Using these values of C_1, C_2, etc., the integrals I_{mp}, J_{mp}, G_{mp} and K_{mp}, were evaluated from the formulaes given by equations 5.58, 5.59 and 5.56 and 5.60 in Appendix 4 for values of $m = 1, 3, 5$ and $p = 1, 3, 5$ in precisely the same sequence as for the previous constants. Following this set of integrals, the integrals A_{nq}, B_{nq} and C_{nq} were evaluated from the formulaes given by equations 5.41, 5.42 and 5.43 again for values of $n = 1, 3, 5$ and $q = 1, 3, 5$.

In the final stages of the computation, the numbers representing B_1, B_2 ..... I_{mp}, ... C_{nq}, etc. were picked up in the sequence specified by equations 2.37, 2.38 or 2.39 to give the numerical values of the eighty one coefficients of the nine linear simultaneous equations.

The evaluation of the critical buckling temperature in the case of asymmetrical heating was complicated by a discontinuity existing

in the temperature function at the point y = c. Separate functions representing the integrals A_{nq}, B_{nq} and C_{nq} were required on each side of the point of discontinuity. In the previous analyses, simple formulae were deduced giving the values of these integrals over the range of integration. As a result of the above complication, no simple formulae could be found, and therefore numerical procedures were used to evaluate these integrals over the range of integration of 0 to 2.

The Deuce Computer makes use of Simpson's Rule to carry out numerical integration. In this case, 80 intervals were taken over this range of integration.

In order that the coefficients, a_{mn}, have values other than zero in the above set of simultaneous equations, the determinant must be equal to zero. This condition leads to the solution giving the nine values of the critical temperature parameter, the lowest value being the only one of practical significance.

It has already been mentioned that an iterative procedure can be used to give the largest value or by inversion the smallest value of the critical temperature parameter.

A standard General Interpretive Programme (G.I.P.) exists for this procedure and makes use of the following standard bricks.

LL097 - read good guess (initial vector)

LR02A - read binary matrix (the 81 coefficients arranged in binary matrix form)

LL042 - iterate

LL052 - punch result

This procedure can be represented in block form as follows:-

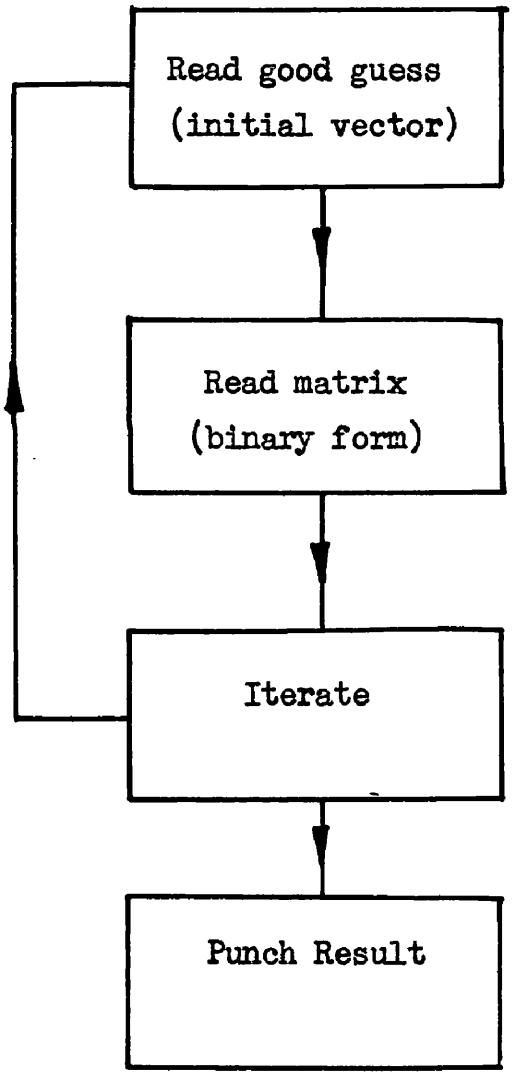

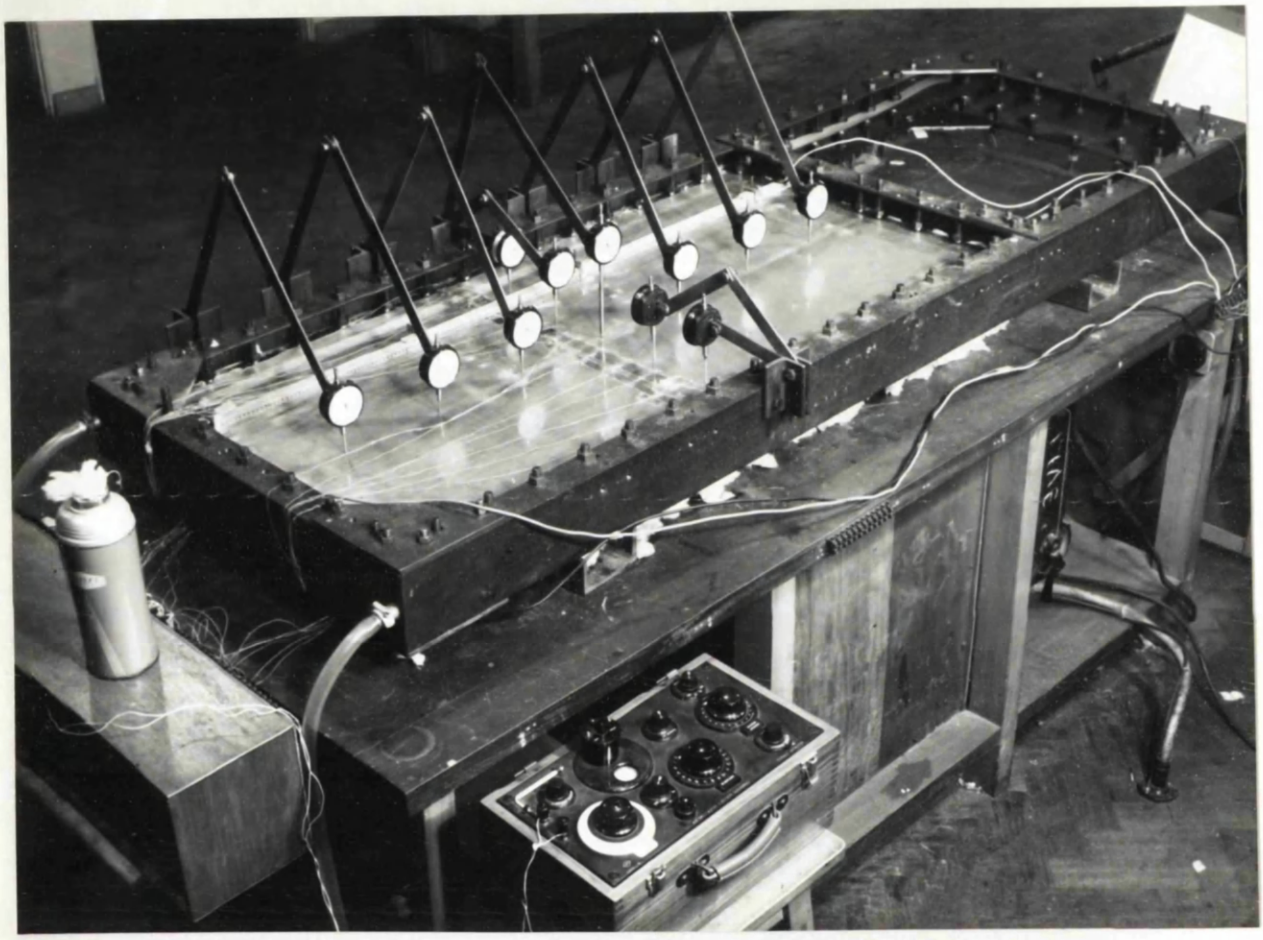

Figure 40: Supporting frame with test plate in position.

PART III. EXPERIMENTAL WORK

A range of experimental work was carried out to verify all aspects of theoretical analyses. It included:-

1) The measurement of the initial irregularities of the plates.
2) The measurement of the temperature distributions over the lateral surface of the plate.
3) The measurement of plate centre, or maximum deflection with increase in temperature differential.
4) The experimental determination of the critical buckling temperature.
5) The determination of the modes of plate buckling.

Owing to the effect of the temperature on apparatus material and measuring instruments, new techniques were devised before routine experimental work was carried out. Many of these new techniques were based on the use of 'Araldite', a synthetic epoxy resin. Advantage was taken of its cold setting properties to avoid thermal distortions in the plate which would have been set up if conventional welding had been used.

Since it is easy to reproduce experimentally, a 'tent-like' temperature distribution over the lateral surface of the plate was chosen. This type of temperature distribution can be obtained in a plate with a line source of heat and two equal heat sinks at the longitudinal edges. If the plate is adequately lagged over its surfaces, then the flow of

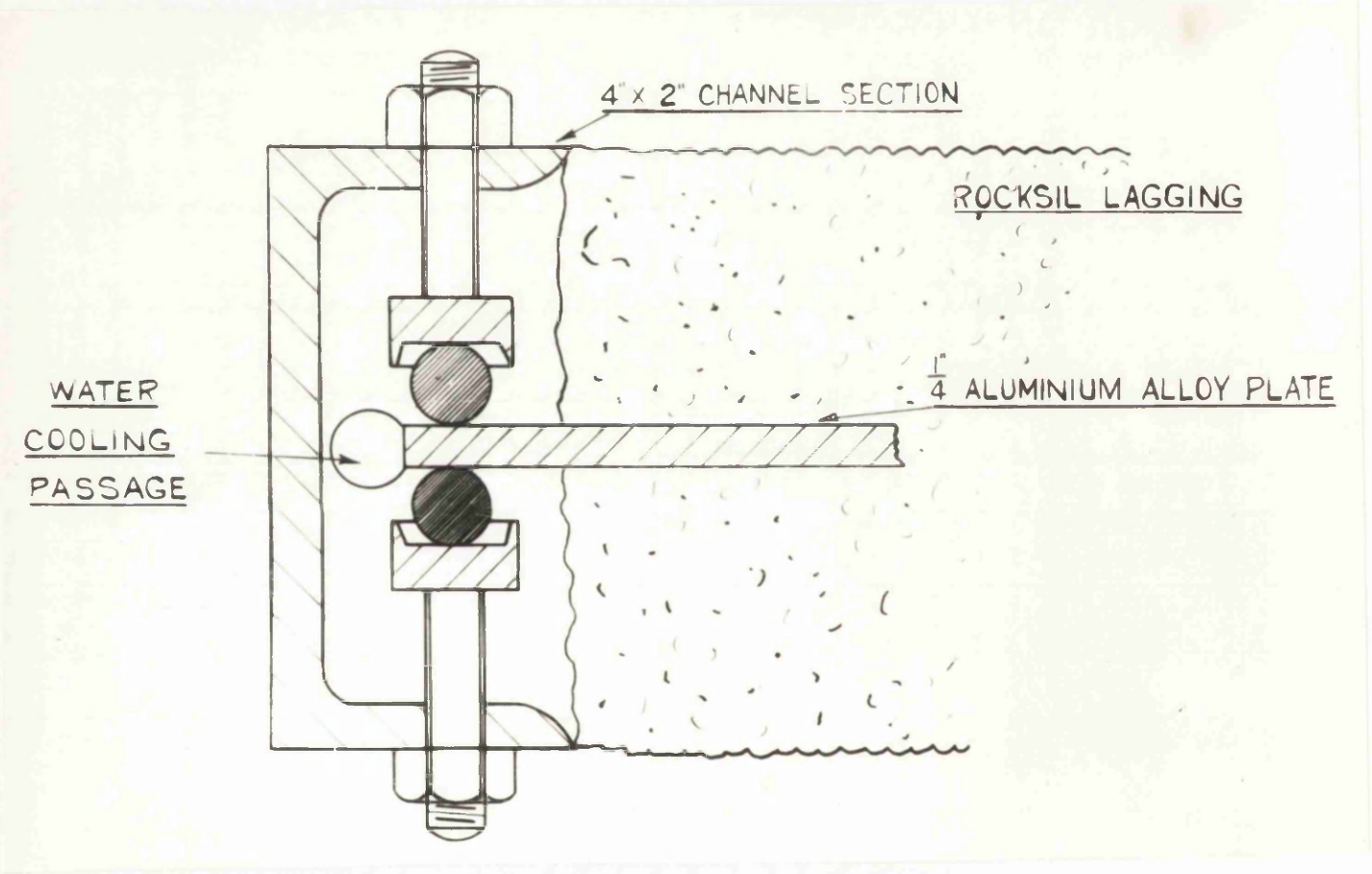

Figure 41: Details of line support.

heat from the source to the sinks will be by conduction through the plate material; the convection and radiation effects will be negligible.

From the laws of conduction of heat through solids, it follows that the plate will be subjected to a 'tent-like' distribution of temperature over its lateral surfaces, and that the variation of temperature through the plate thickness will be constant.

For convenience, the experimental work was divided into two parts. The first part consisted of a series of tests carried out on a comprehensive range of T.I.224 aluminium alloy plates of constant width of 24 in. and $\frac{1}{4}$ in. thickness with variations in lengths from 2 ft. to 6 ft. in increments of 6 in. In each test the line source of heat was in the centre position, $c = b$.

The second part of the experimental work was concerned with a series of tests carried out on a single 4 ft. x 2 ft. x $\frac{1}{4}$ in. aluminium alloy plate subject to a variety of asymmetrical 'tent-like' temperature distributions.

Five different types of temperature distributions were investigated corresponding to the line source of heat in the $c = b$, $c = \frac{3}{4}b$, $c = 5/8b$, $c = b/2$ and $c = 3/8b$ positions.

Experimental Appliances

The essential features of the experimental apparatus are shown in figures 40 and 41.

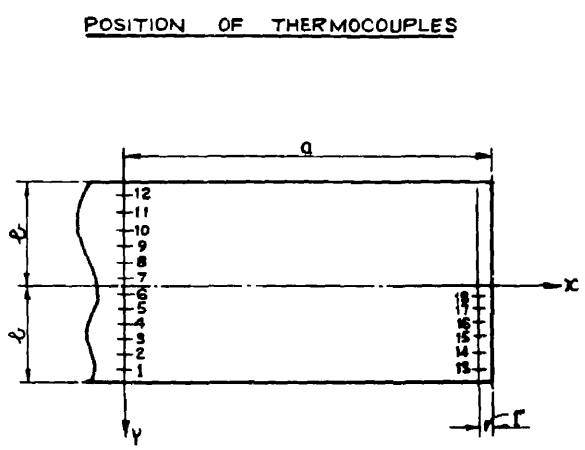

Figure 42: Location of thermocouples.

The experimental set-up consisted of a rectangular steel framework which supported the test plates in a manner assumed in the theoretical analysis. The frame, whose length and breadth were 6 ft. 2 in. and 2 ft. 2 in. respectively, was constructed of 4" x 2" x 3/8" channel section. An adjustable cross-piece was fitted to accommodate plates ranging from 2 ft. to 6 ft. in length.

To reproduce experimentally simple support conditions assumed in the theoretical analyses, the edge supports of the plate consisted of closely spaced ½" steel balls located on each side of the plate using 7/16" diameter bolts with recessed heads, as shown in figure 41. Spaced at 3-inch intervals along the edges of the plate, the bolts which were screwed into the channel section gave a good approximation to simple line support conditions.

As already mentioned, a 'tent-like' temperature over the lateral surface of the plate was induced by a line source of heat along a longitudinal line and cooling the two longitudinal edges.

A good approximation to a line source of heat was obtained using electric heating elements constructed from half-inch width asbestos strip wound with nichrome wire.

By means of aluminium bridge pieces previously attached to the plate with Araldite cement, the heaters were clamped on each side of the plate.

Cooling of the plate was effected by passing water at room

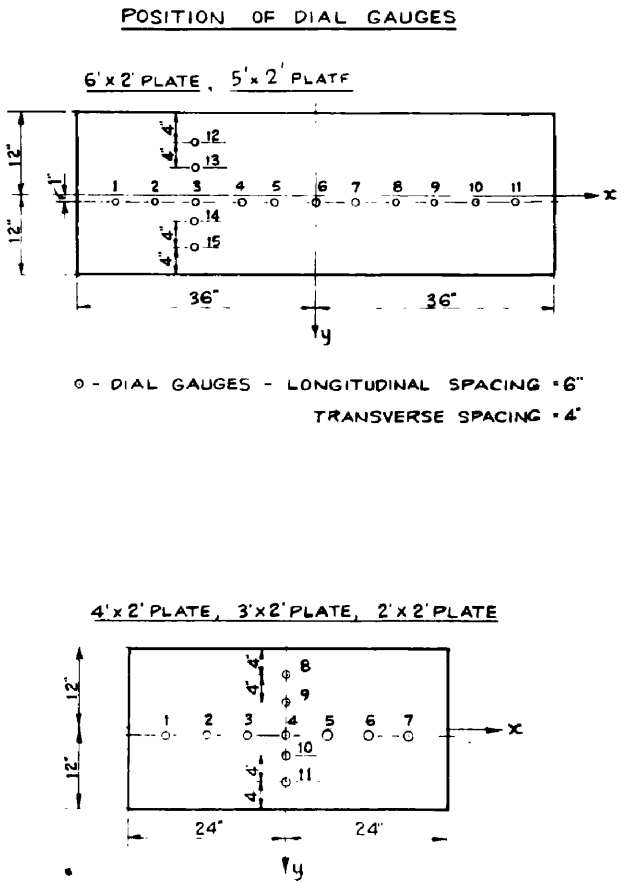

Figure 43: Location of dial gauges.

temperature through ½" diameter, 0.009" wall thickness aluminium tubes cemented to the longitudinal edges with Araldite cement. The flow of cooling was adjusted so that temperature distribution in the longitudinal direction was essentially constant.

To avoid fluctuation in the mains voltage, which could cause a variation of the heat supplied to the plate, constant voltage transformers were employed to reduce the fluctuation of mains voltage to within $\pm \frac{1}{2}$ volt.

The power supplied to the upper and lower heaters, and in consequence the temperature differential across the surface of the plate, was varied by including a 'variac' infinitely variable transformer in the circuit. As the lateral surfaces of the plate were well lagged it was found unnecessary to peen the thermocouple junctions into the plate material. It was also found that Vaeron-Eureka thermocouples attached to the plate with Araldite cement, used in conjunction with a Cambridge Portable Potentiometer, were suitable for the measurement of the temperature distributions across the lateral surfaces of the plate. Figure 42 shows the position of the temperature measurement stations on the test plate.

The buckled form of the test plates was determined by measuring the lateral deflections of the plate using dial gauges of the 0.001 in. per division type positioned along transverse and longitudinal lines, as shown in figure 43.

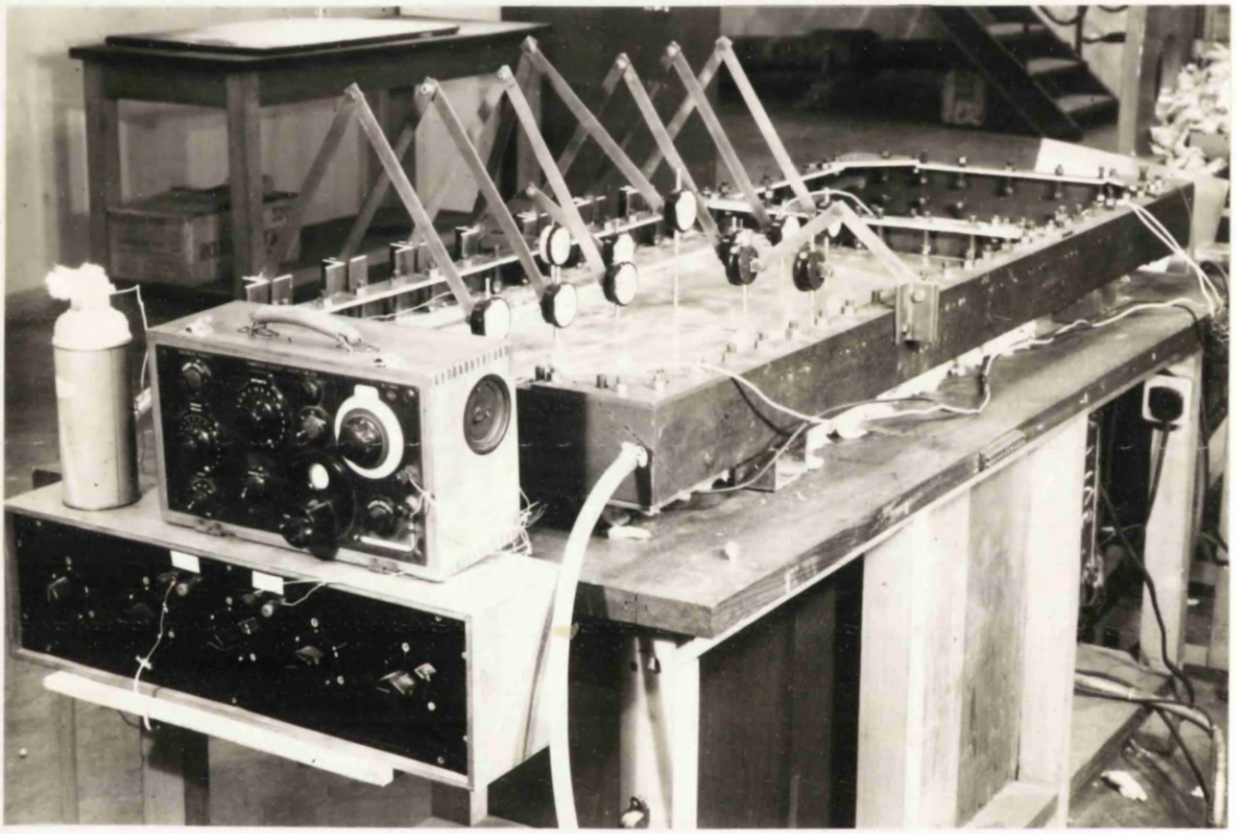

Figure 44: Supporting frame with details of instrumentation.

Experimental Procedure

Before the plate was inserted into the framework, the thermocouples and the heating elements were fixed into the desired position.

The plate was then inserted into the framework and located in position using the ball supporting screws. Connections to the thermocouple switching unit, as shown in figure 44, were made and the dial gauges set into their correct positions. Finally, connections were made to the cooling water tubes.

After allowing the plate to reach thermal equilibrium (approximately two hours) readings of temperature and lateral deflection were taken. This procedure was repeated with increasing values of plate temperature differential up to a maximum value of approximately 100°C.

Experimental Results

The following results were obtained directly from the thermocouple and lateral deflection readings:-

a) The experimental temperature distributions.

b) The growth of centre or maximum lateral deflection of the plate with increasing temperature differential.

c) The deflected form of the plate.

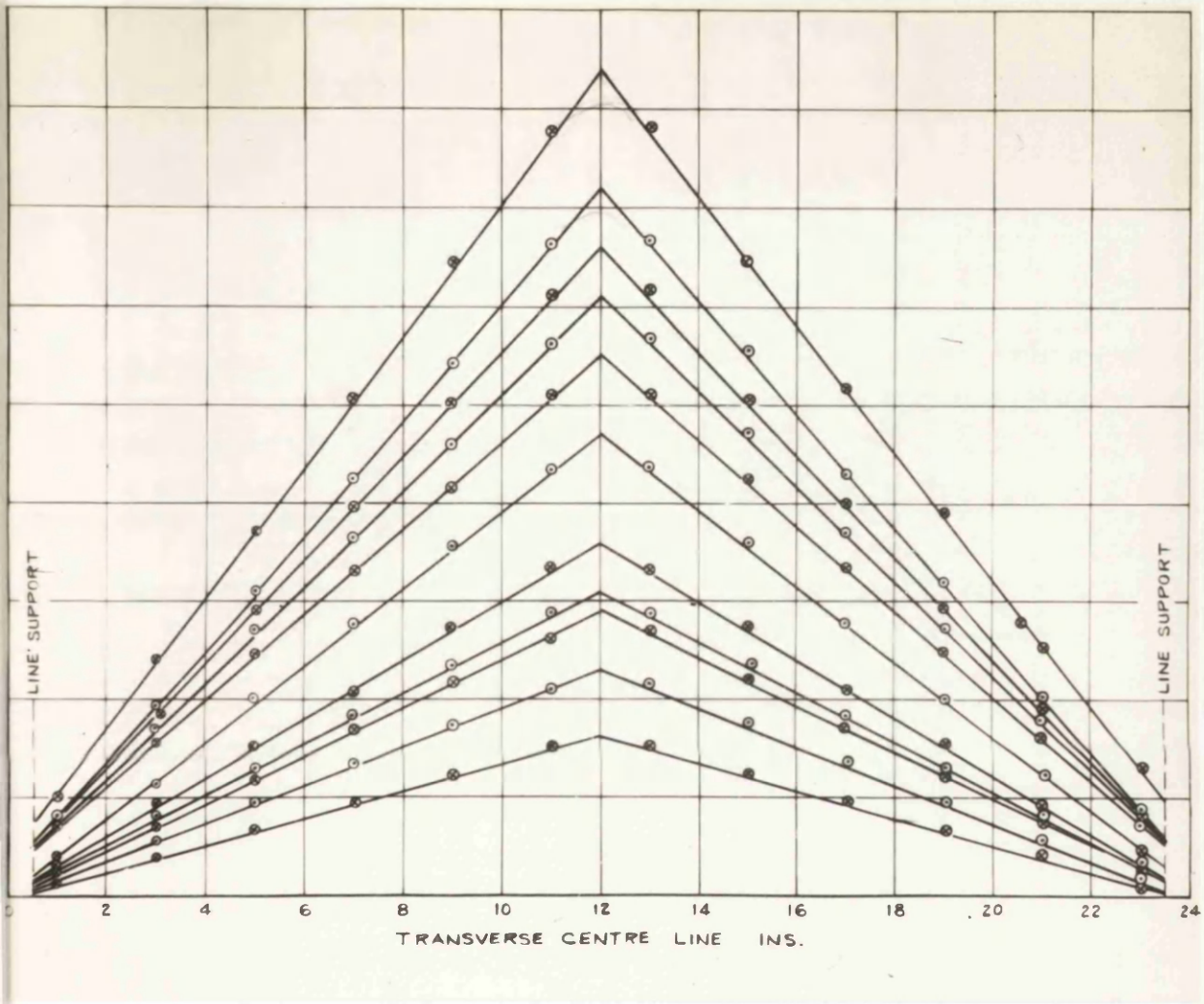

Figure 45: Measured temperature distribution, symmetrical case, c = b.

a) The temperature distributions were obtained by plotting the converted thermocouple for the various stations. A straight line drawn through the test points was used to predict the temperature at the centre line of the heater. Subtracting the temperature at the line supports, from this value, the plate temperature differential, T_o, was found. The temperature distribution of all the cases considered are shown in figures 45 to 49. It can be seen that the test points define a straight line variation, permitting the temperature at the centre line of the heater to be assessed.

The deviation of points close to the heater can be attributed to the finite width of the heater. No measurable difference in the temperature was noted throughout the thickness of the plate. The temperature along the longitudinal axis was virtually constant; for all tests the variation did not exceed $\pm$ 1°C.

b) Figure 50 shows a typical growth of centre deflection with increasing temperature differential plot for a 4' x 2' x $\frac{1}{4}$" plate symmetrically heated.

Owing to the initial irregularities in the plate and the stretching of the mid-plane the onset of buckling is one of gradual development rather than of sudden occurrence predicted by theory. Thus the direct determination of the critical buckling temperature presents considerable difficulties. These can be overcome by the application of the Southwell-Lundguist plot which predicts the critical temperature, providing the variation of plate deflection with temperature is known.

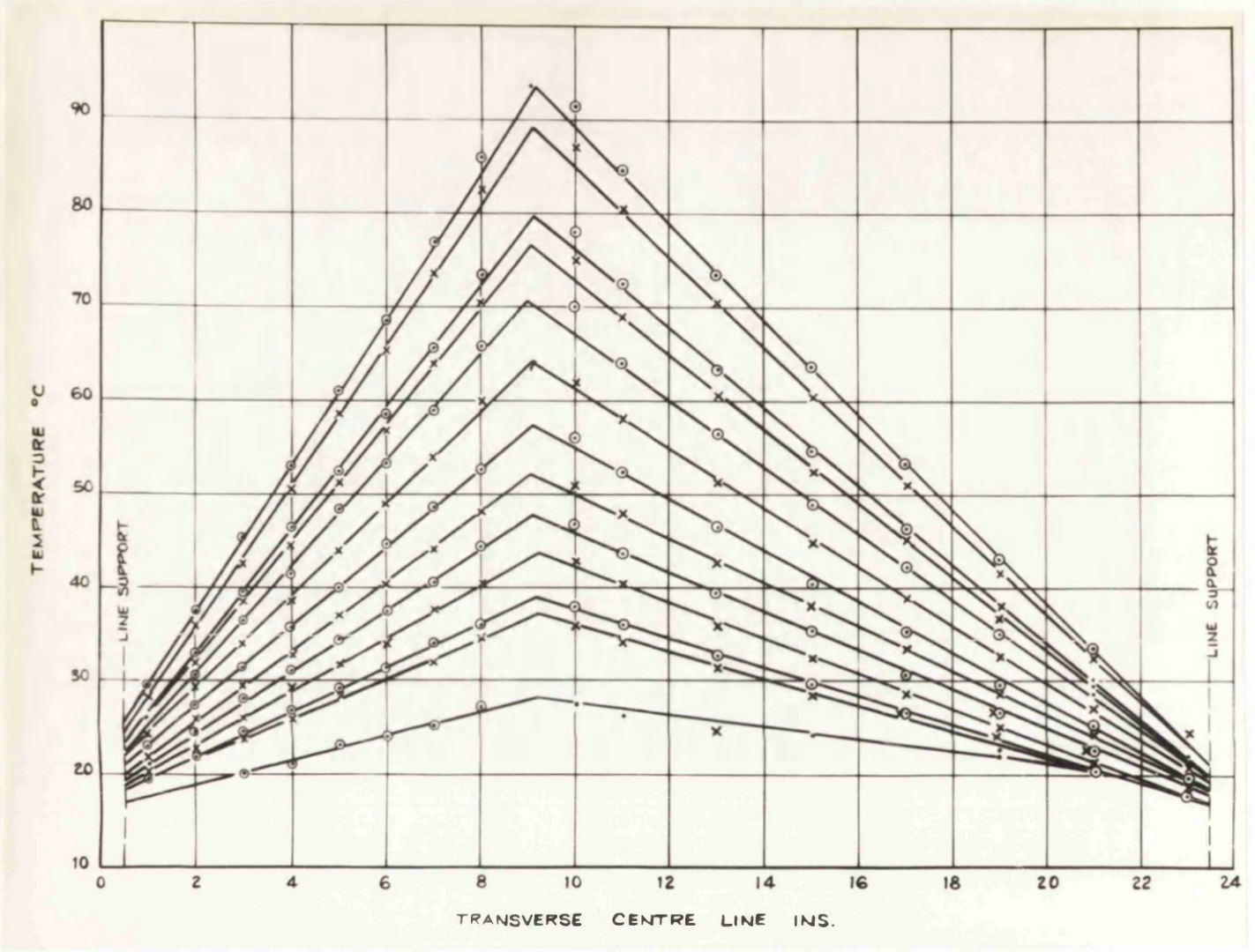

Figure 46: Measured temperature distribution, asymmetrical case, c = 3/4 b.

It should be noted that the Southwell-Lundguist plot has been derived on the assumption that the load deflection curve is a rectangular hyperbola, asymptotic to the critical buckling load.

In a flat plate this assumption would only be satisfied if the mid-plane of the plate remained unstressed at the onset of buckling. However, the stretching of the mid-plane does occur in the practical case which contributes additional strength to the plate in the post-buckling range. This means that after buckling has taken place, the plate will sustain a load greater than the critical load.

Nevertheless the critical load on critical temperature can be predicted, providing values up to the knee of the temperature-deflection curves are used in the Southwell-Lundguist plot. A typical plot is shown in figure 51, from which the critical temperature can be deduced from the slope of the straight line.

c) The experimental deflected form which gives the buckle pattern of the plates is shown in figures 54 to 64. It can be seen that irrespective of the longitudinal mode of buckling, the transverse mode of buckling is always one half wave.

Summary of Results

The effective aspect ratio measured between line supports and the maximum initial imperfections in the plate are given in Table 9.

Table 10 presents the value of the critical temperature for

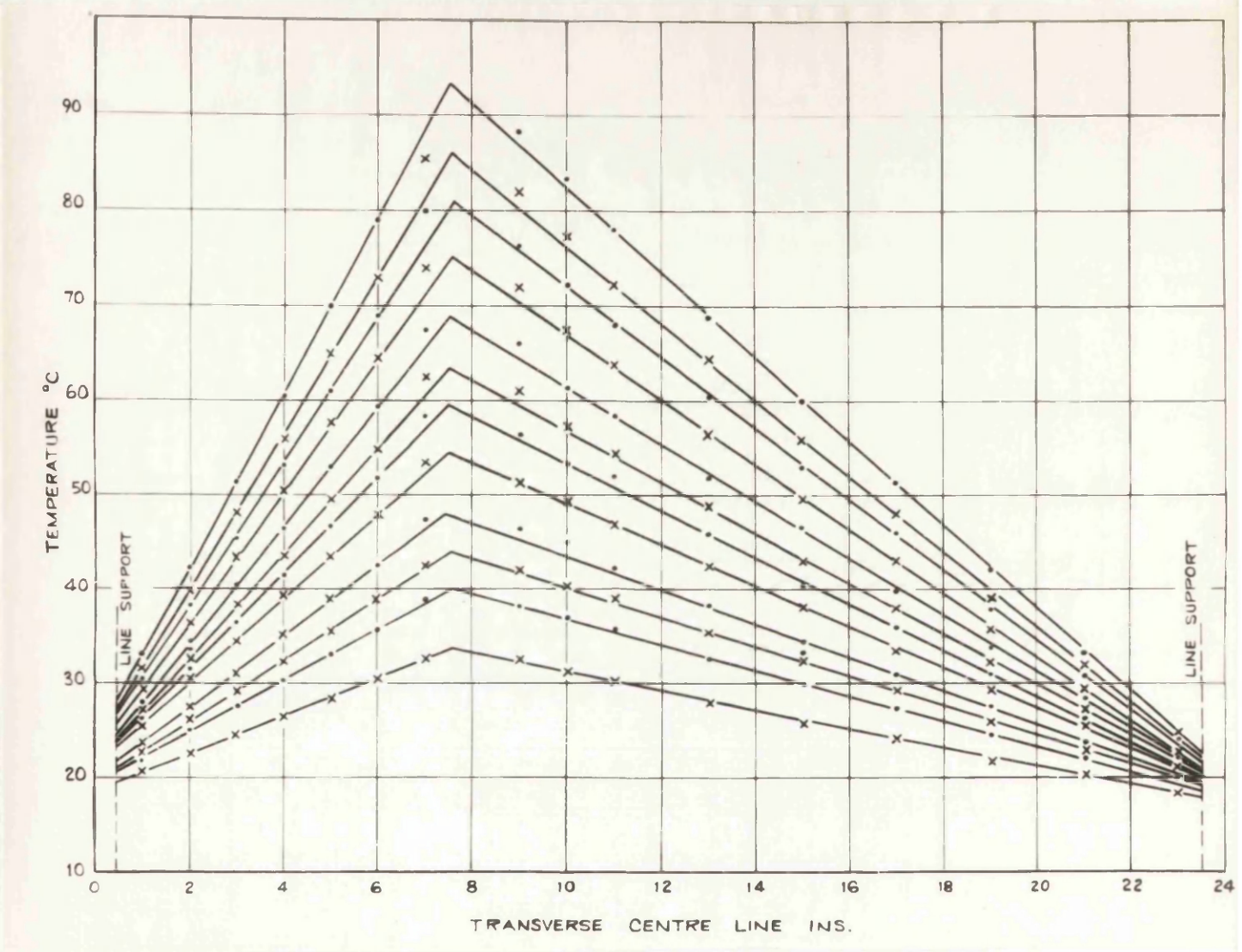

Figure 47: Measured temperature distribution, asymmetrical case, c = 5/8b.

plates of various aspect ratio with the heater in the symmetrical position.

Table 11 presents the values of the critical temperatures for the 4 ft. x 2 ft. plate for various degrees of asymmetrical heating.

Material Properties

As a result of tensile tests carried out on specimens of T.I.224 aluminium alloy, the average value of Poisson's Ratio was found to be $\nu = 0.313$ (full details are given in Appendix 6). The value of the linear coefficient of expansion of the above alloy was given by the manufacturer and confirmed by tests carried out by the National Physical Laboratory as

$$\alpha = 23.2 \times 10^{-6}/^{\circ}C.$$

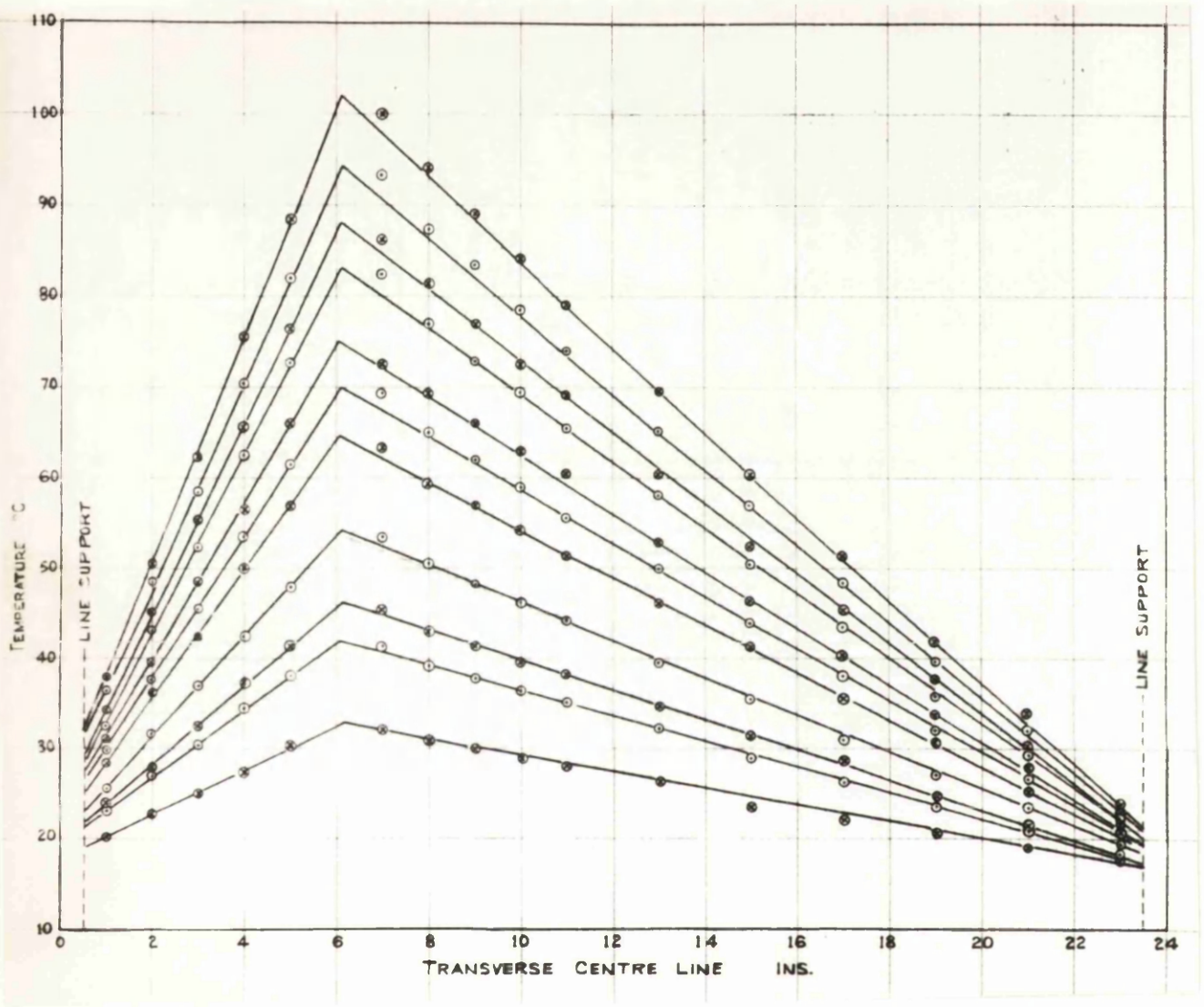

Figure 48: Measured temperature distributions, asymmetrical case, c = b/2.

TABLE 9

Overall Size	Effective Length	Effective Width	Aspect Ratio	Maximum Initial Imperfection
2' x 2'	23 in.	23 in.	1.0	0.08 in.
3' x 2'	35 in.	23 in.	1.52	0.05 in.
4' x 2'	47 in.	23 in.	2.04	0.085 in.
5' x 2'	59 in.	23 in.	2.56	0.03 in.
6' x 2'	71 in.	23 in.	3.09	0.03 in.

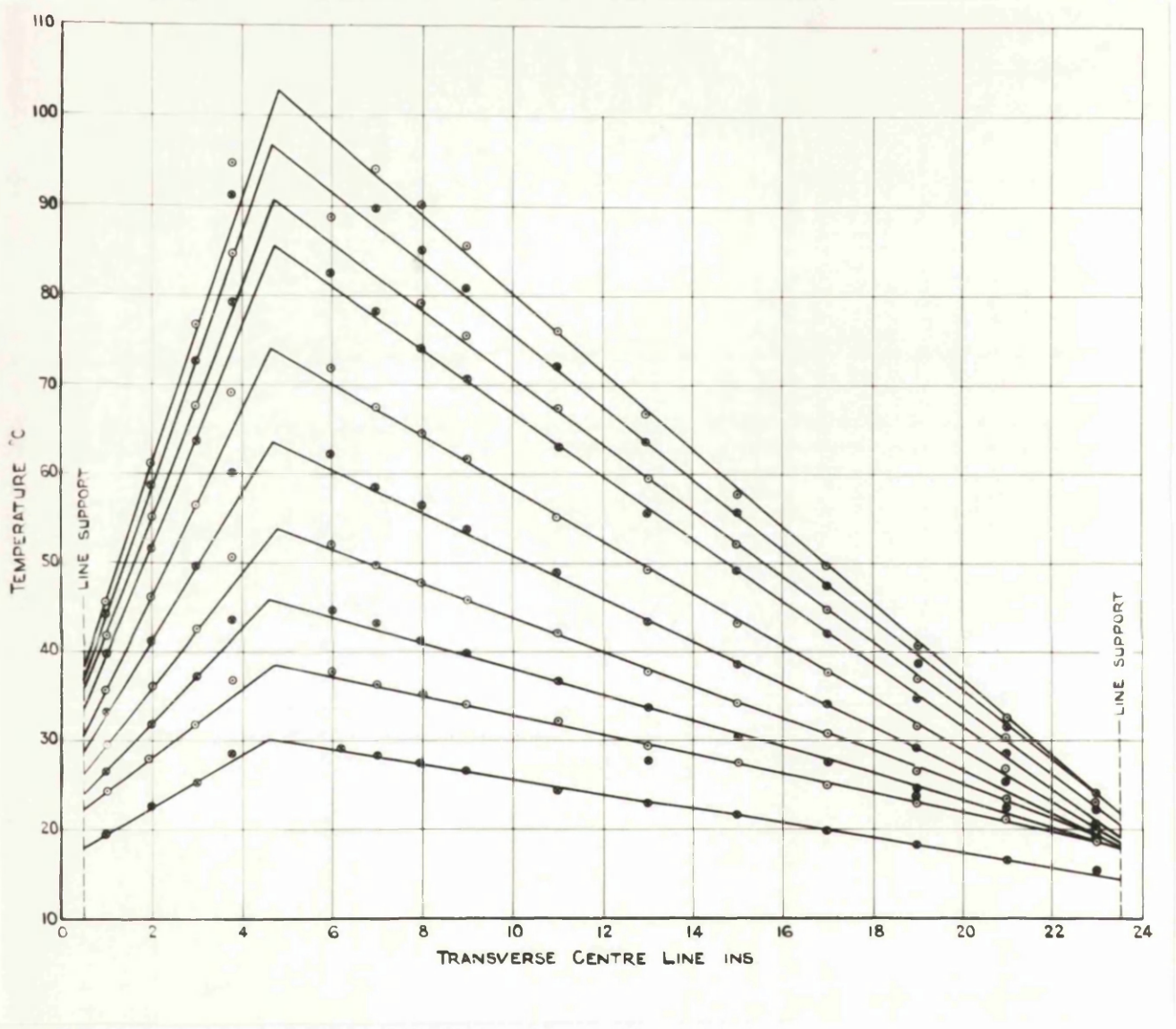

Figure 49: Measured temperature distribution, asymmetrical case, c = 3/8 b.

TABLE 10

Plate Length ft.	Aspect Ratio	T_{ocr} °C.	Mode of Longitudinal Buckling
2.0	1.0	168	One half wave
2.0	1.0	188	"
3.0	1.57	114	"
3.0	1.57	123	"
3.0	1.57	129	"
4.0	2.04	100	"
4.0	2.04	102	"
5.0	2.56	82.4	Two half waves
5.0	2.56	91.1	"
6.0	3.09	83.2	Three half waves
6.0	3.09	86.5	"

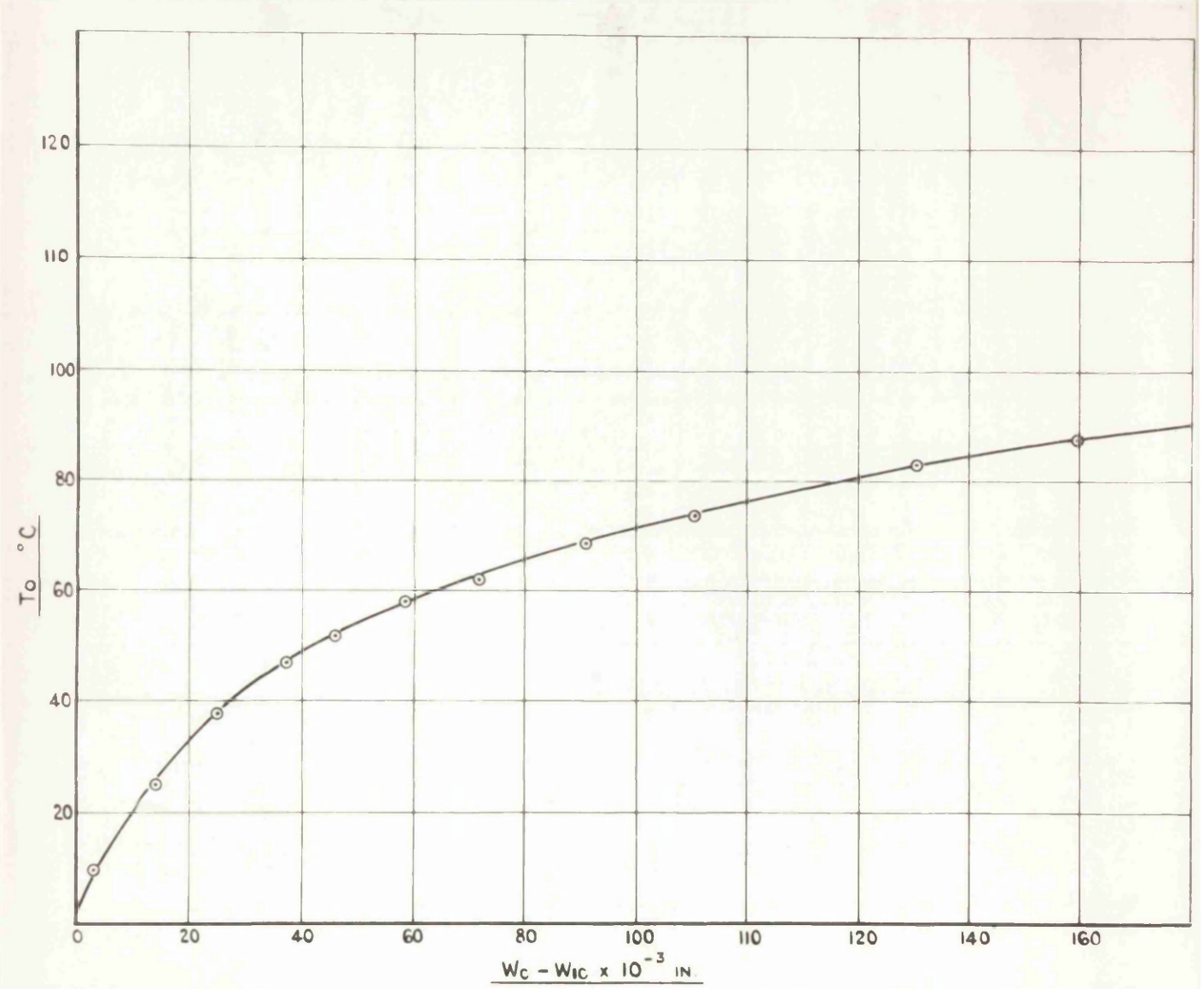

Figure 50: Typical growth of experimental plate centre deflection with increase in temperature differential. (4' x 2' plate symmetrically heated.)

TABLE 11

Aspect Ratio	Heater Position	T_{ocr} °C.	Mode of Longitudinal Buckling
2.04	c = b	100	One half wave
2.04	c = b	102	"
2.04	$c = \frac{3}{4}b$	117	"
2.04	$c = \frac{3}{4}b$	108	"
2.04	$c = \frac{5}{8}b$	136	"
2.04	$c = \frac{5}{8}b$	125	"
2.04	$c = \frac{b}{2}$	144	"
2.04	$c = \frac{b}{2}$	152	"
2.04	$c = \frac{3}{8}b$	176	"

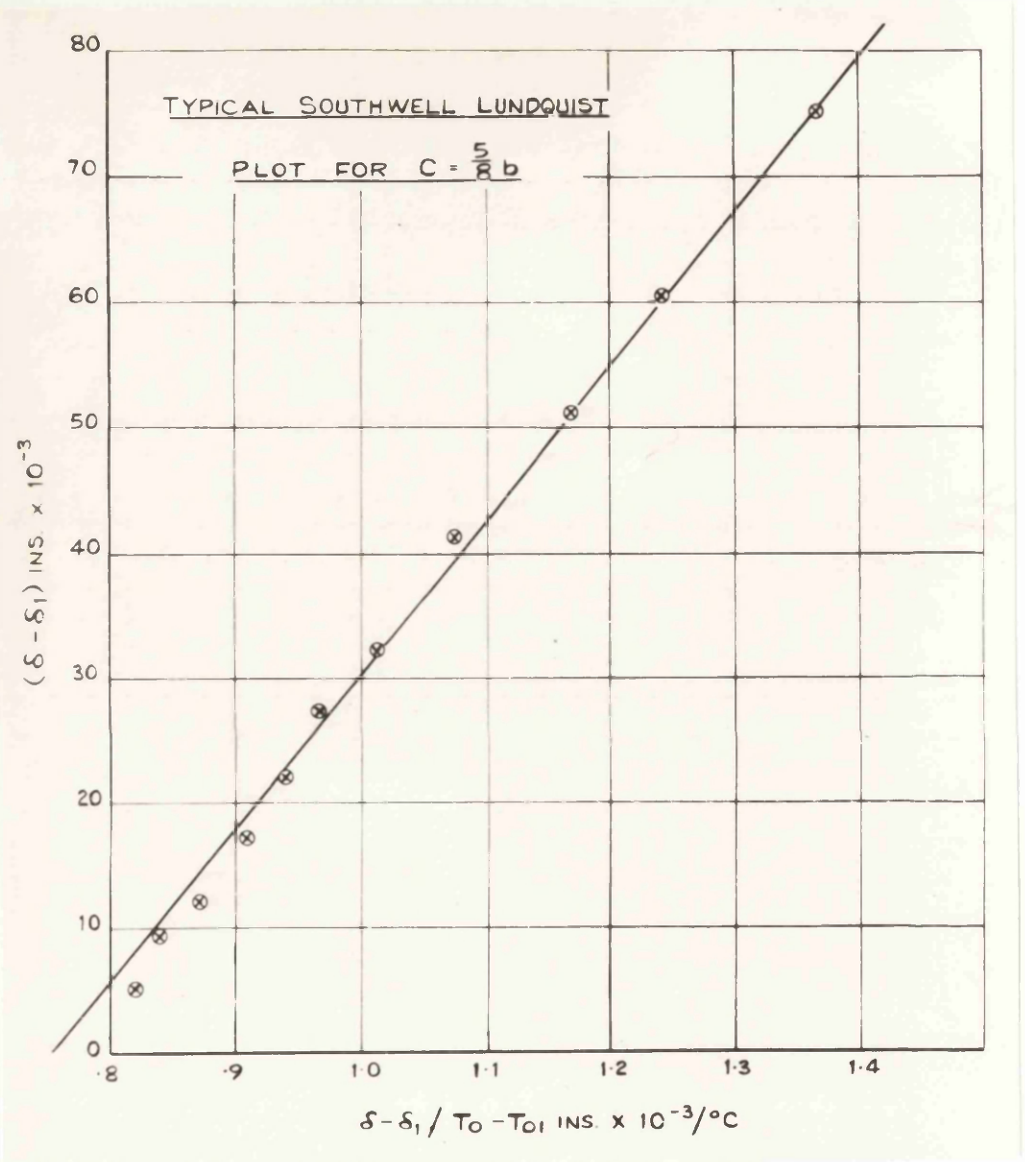

Figure 51: Typical Southwell-Lundguist plot.

PART IV. CRITICAL DISCUSSION

In Part II of the thesis a variety of methods has been presented for the evaluation of the critical buckling temperature of a plate subjected to 'tent-like' temperature distributions. It is considered relevant to focus attention, in the first instance, on the relative merits of the methods employed.

Table 12 compares the value of the critical temperature parameter obtained for a plate of aspect ratio 1.566, symmetrically heated, using several different methods of solution.

Remarkably good agreement was obtained between the values of the critical temperature parameter for the different methods used in the analysis. Table 12 also shows that the Galerkin and the Rayleigh-Ritz methods are equivalent to each other providing the same deflected form of the plate is assumed in both analyses.

A comparison of equations 2.37 and 1.66, which have been used to evaluate the critical temperature parameter, shows that the Galerkin method gives the simplest form of solution and, in this case, is preferable to the Rayleigh-Ritz method.

Figure 52 shows the variation of the critical temperature parameter against plate aspect ratio obtained by the Galerkin method. Figure 53 indicates the corresponding variation of critical temperature with plate length for a constant plate width of 24 in., and its comparison with experimental values.

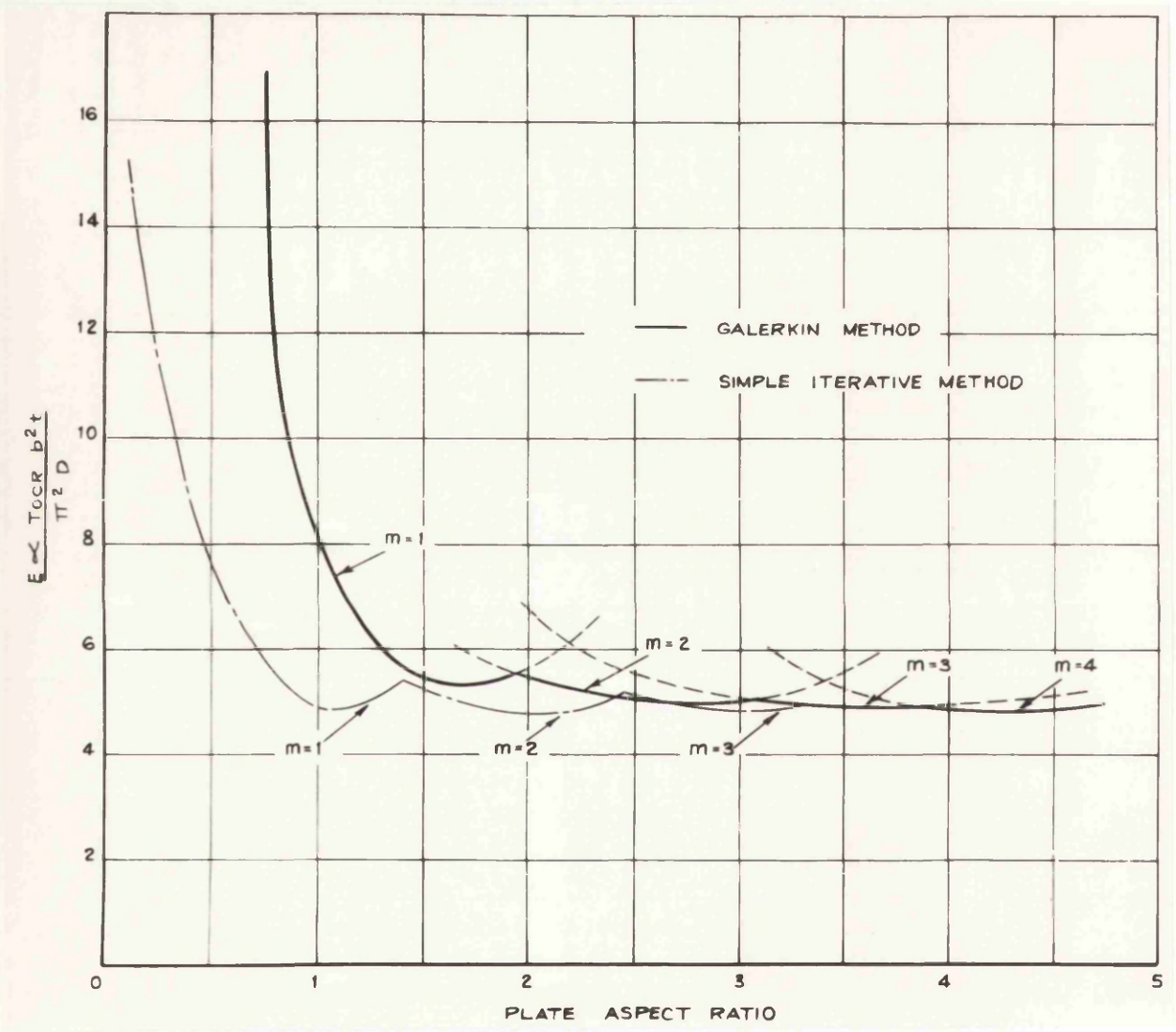

Figure 52: Theoretical variation of critical temperature parameter with aspect ratio for a plate subjected to a symmetrical 'tent-like' temperature distribution.

Good agreement was obtained between theoretical and experimental values, particularly for plates of aspect ratio greater than 1.5.

A rapid increase in the critical temperature was noted when the plate aspect ratio was less than 1.5. In this case it was inevitable that the agreement between experiment and theory would not be so close.

In short plates the condition that the edge stresses vanish necessitates a modification in the longitudinal direct stress and introduces transverse and shear stresses at points near the transverse ends. It is the effect of this redistribution of stresses in short plates which results in this rapid rise in the value of the critical temperature. This effect might have some practical significance.

In long plates the longitudinal direct stress (σ_x) approaches the infinite plate distribution of stress; thus the plate behaves as if it were a plate subjected to loads acting on the transverse ends of the plate, a case extensively treated by Timoshenko and others. Loading of this type causes a long plate to buckle into squares and for each mode of buckling, the load to initiate instability has the same minimum value. This condition is approached in the case of long plates with induced thermal stress due to 'tent-like' temperature distributions. For each mode of longitudinal buckling, the critical buckling temperature has the same minimum value. This is clearly shown in figure 52 for the series of curves corresponding to m = 3, 4, 5 etc., in which each of these curves is virtually tangential to a common minimum temperature line.

TABLE 12

When used	Stresses $\nabla^4\phi = -E\alpha\nabla^2 T$	Instability $D/t\,\nabla^4\omega = \sigma_x \frac{\partial^2\omega}{\partial x^2} + \sigma_y \frac{\partial^2\omega}{\partial y^2} + 2\tau_{xy} \frac{\partial^2\omega}{\partial x \partial y}$	$\frac{E\alpha T_{ocr} b^2 t}{\pi^2 D}$
1a and 2a	Kantorovitch Method	Galerkin Method	5.394
1b and 2b	Rayleigh-Ritz Method	Galerkin Method	5.41
Ref. 13	Kantorovitch Method	Rayleigh-Ritz Method	5.39

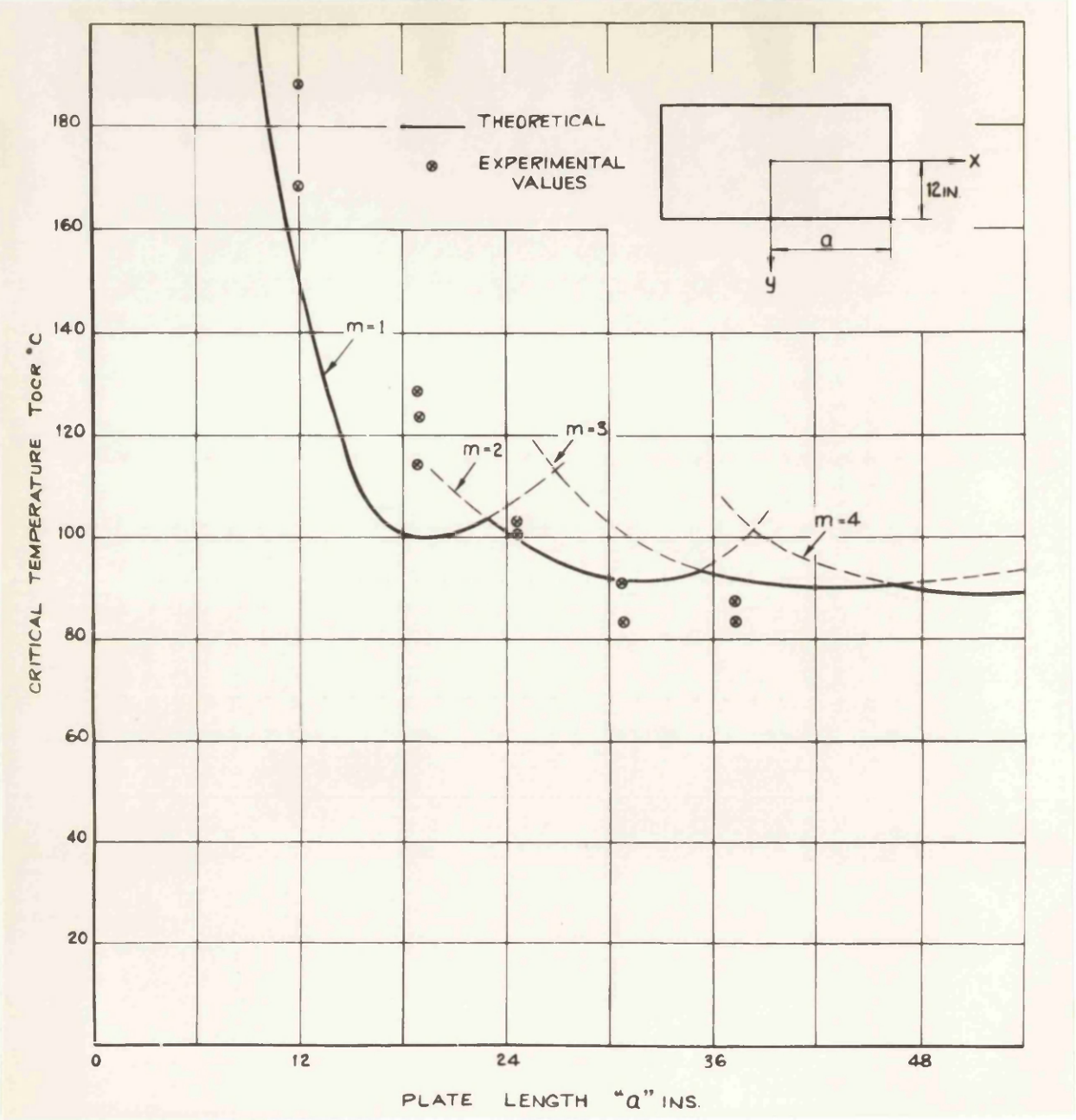

Figure 53: Comparison of theoretical and experimental values of critical temperature for a plate subjected to a symmetrical 'tent-like' temperature distribution.

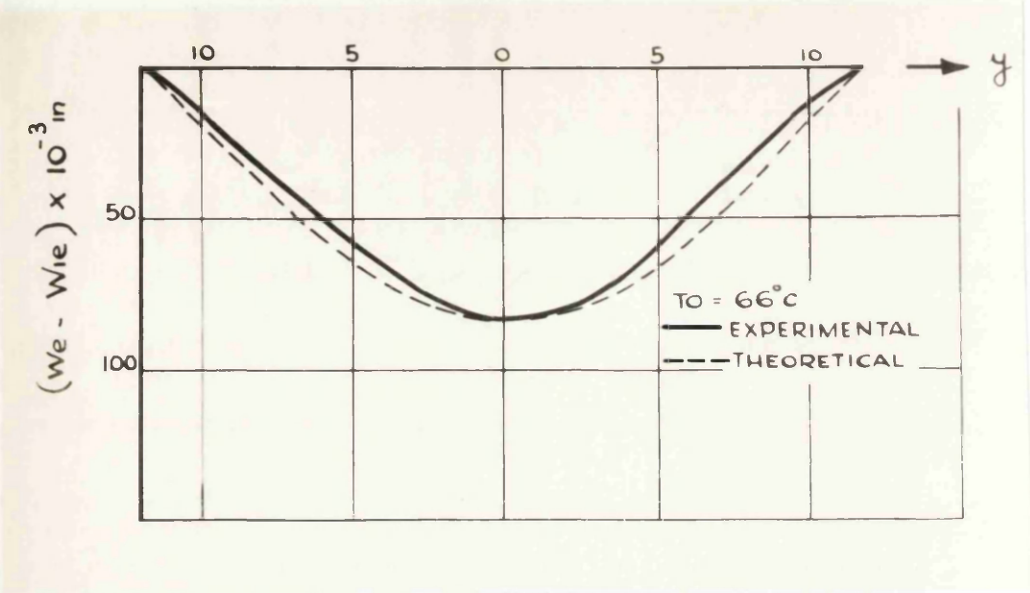

Figure 54: Transverse buckle pattern, 2 ft. x 2 ft. plate.

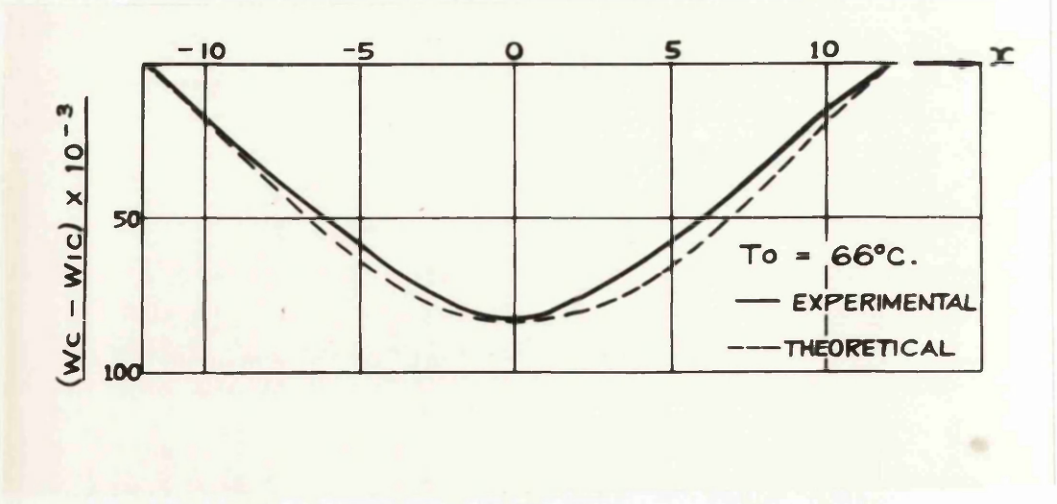

Figure 55: Longitudinal buckle pattern, 2 ft. x 2 ft. plate.

In passing it is interesting to compare the foregoing theoretical values of critical temperature parameter with the values obtained using a simple iterative method suggested by Kenedi[19,20]. In this method the assumption is made that the distribution of the longitudinal stress is the same as that of an infinite plate[4], and that the plate buckles into one half sine wave in the transverse direction and m half sine waves in the longitudinal direction. The above assumptions suggest that the buckling behaviour will be similar to the case of a plate subjected to compressive loads acting in the plane of the plate. This was found to be so.

For each mode of longitudinal buckling corresponding to m = 1, 2, 3 etc., a series of curves, shown in figure 52, was obtained. It was found that each individual curve had the same minimum value and occurred at a point where the number of longitudinal half waves equalled the aspect ratio of the plate.

In the more refined approach (2a), where the 'end-effects' are taken into account, this mode of plate behaviour occurred only in the case of long plates where the transverse and shear stresses near the ends are small compared with the longitudinal stress. Thus if the values of the critical temperature parameter obtained by the two methods are compared it can be seen from figure 52 that at large aspect ratios the values are nearly identical. A slight difference of 5% does exist between the two methods; the iterative method giving the higher value. This small difference is, no doubt, due to the assumed form of buckled

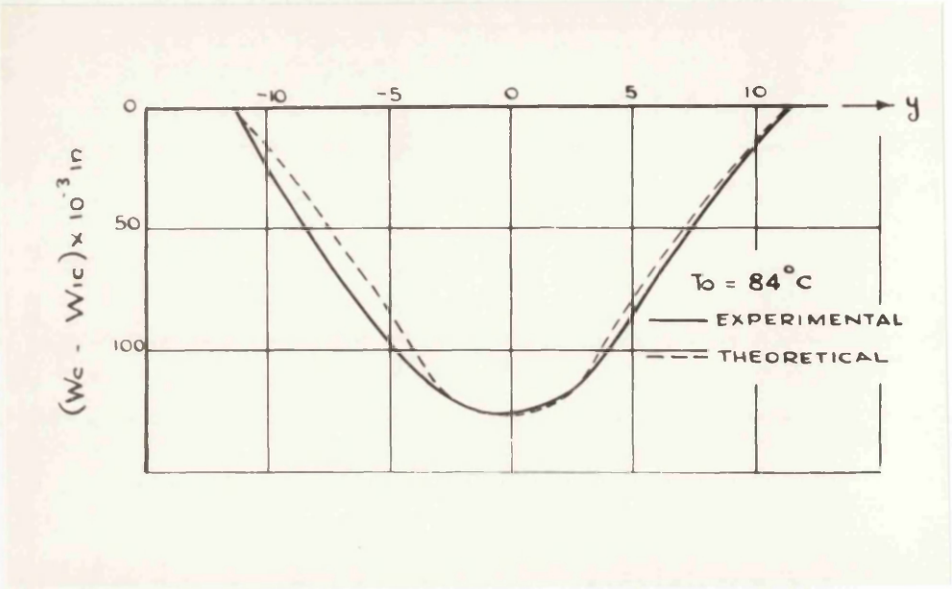

Figure 56: Transverse buckle pattern, 3 ft. x 2 ft. plate.

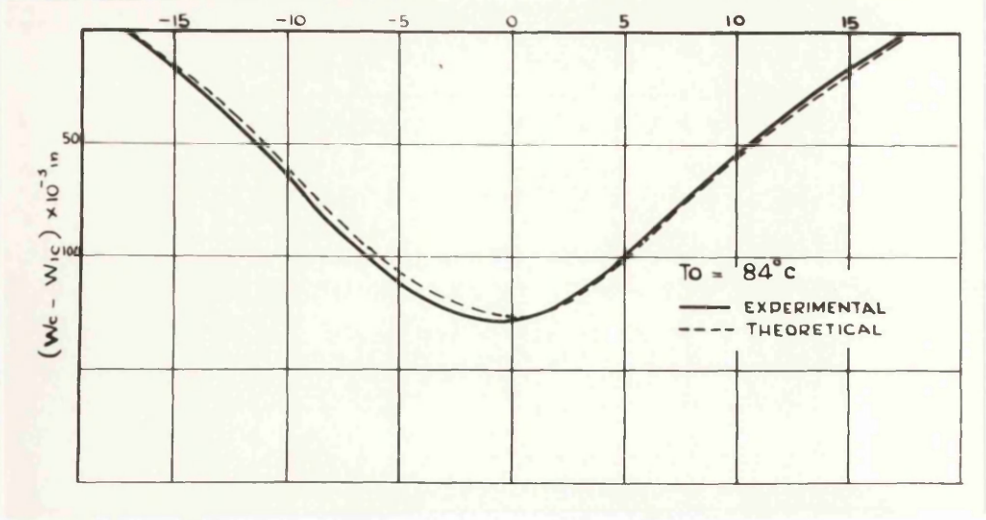

Figure 57: Longitudinal buckle pattern, 3 ft. x 2 ft. plate.

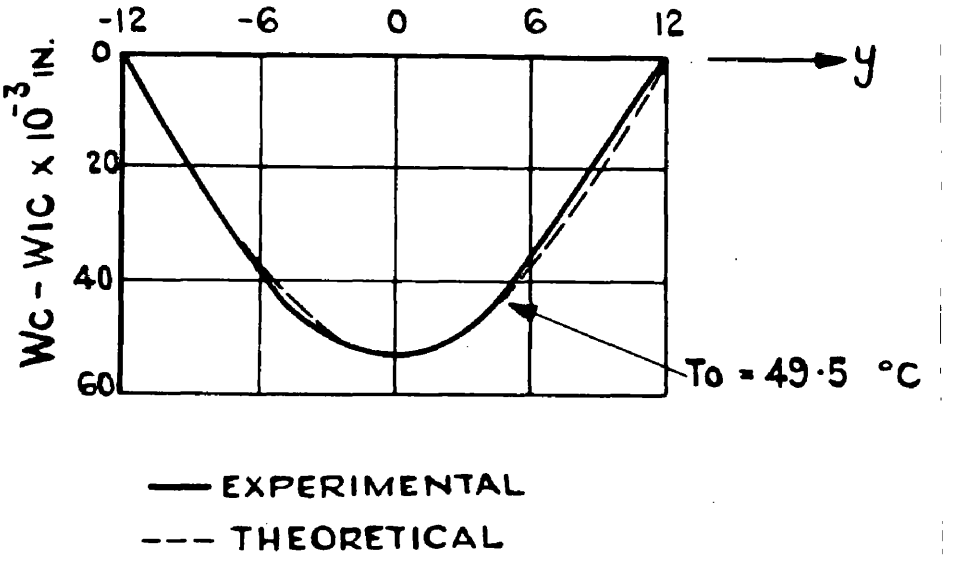

Figure 58: Transverse buckle pattern, 4 ft. x 2 ft. plate.

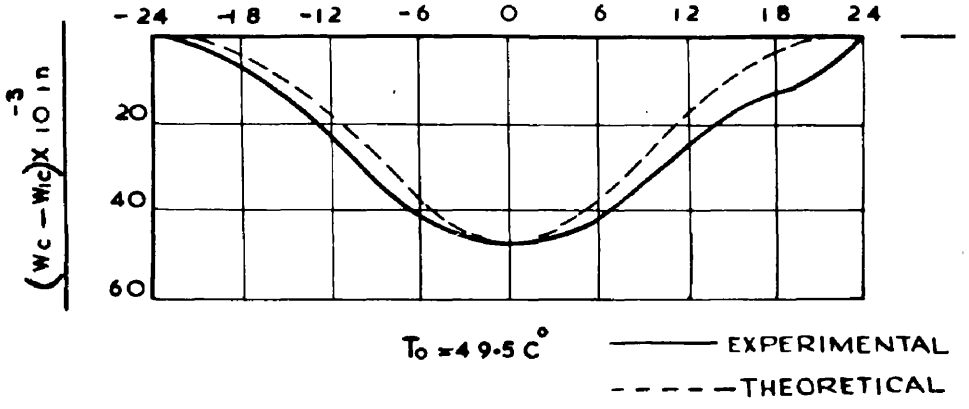

Figure 59: Longitudinal buckle pattern, 4 ft. x 2 ft. plate.

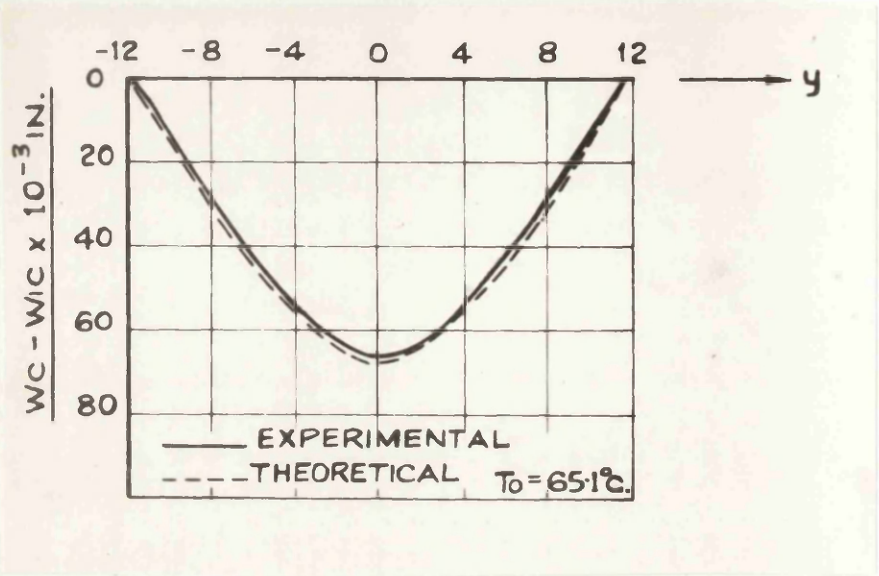

Figure 60: Transverse buckle pattern, 5 ft. x 2 ft. plate.

at x = +12 in. (See fig. 61)

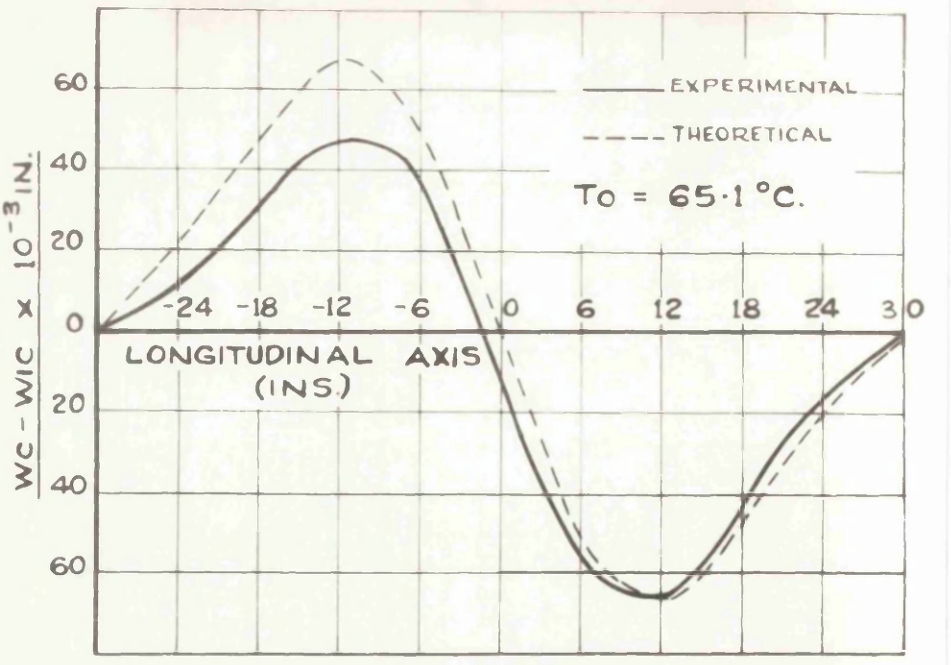

Figure 61: Longitudinal buckle pattern, 5 ft. x 2 ft. plate.

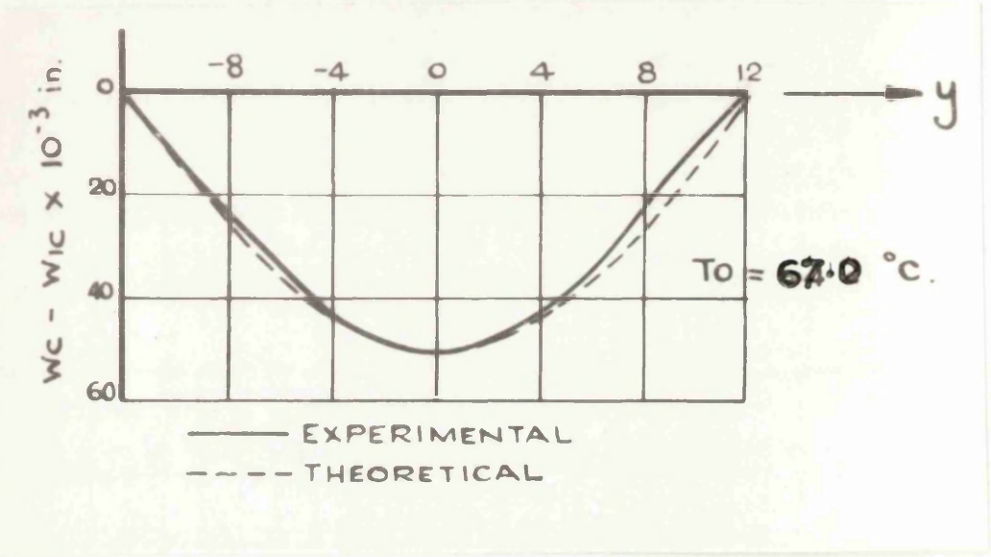

Figure 62: Transverse buckle pattern, 6 ft. x 2 ft. plate.

at x = +24 in. (See fig. 63)

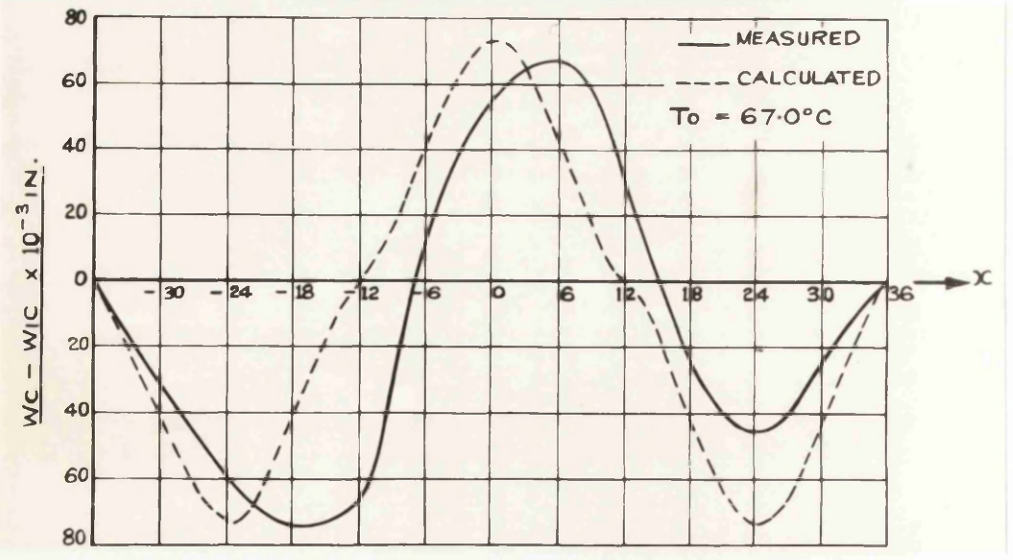

Figure 63: Longitudinal buckle pattern, 6 ft. x 2 ft. plate.

plate in each case. In the refined approach nine terms were taken in the series for the deflected form of the plate, whilst in the iterative method only one half sine wave was assumed in the longitudinal direction before the iterative process was carried out. A better approximation to the buckle pattern was effected by iterating once and this gave results, as already stated, which were in close agreement with the results of the previous analysis for plates of large aspect ratio.

In the theoretical analysis concerning the evaluation of the critical temperature it was shown that for a plate of aspect ratio of 1.566 that the deflection coefficients a_{11}, a_{31} and a_{13} were the only ones of significance, the others having a negligible effect on the final value of the critical temperature parameter.

At this point it is of interest to examine the significant deflection coefficients for plates of other aspect ratios. Table 5 shows that the coefficients a_{11}, a_{31} and a_{13} determine the deflected form of plates up to an aspect ratio of 2.25. In these cases, the coefficient, a_{11}, determines the overall deflected form; the other coefficients, a_{31} and a_{13}, only affecting the deflected form at points near the supports.

For plates of aspect ratio greater than 2.25, the coefficient a_{31} is predominant which implies that the deflected form of the plate will be three half waves in the longitudinal direction.

Table 6 shows that the change over from the two half wave mode

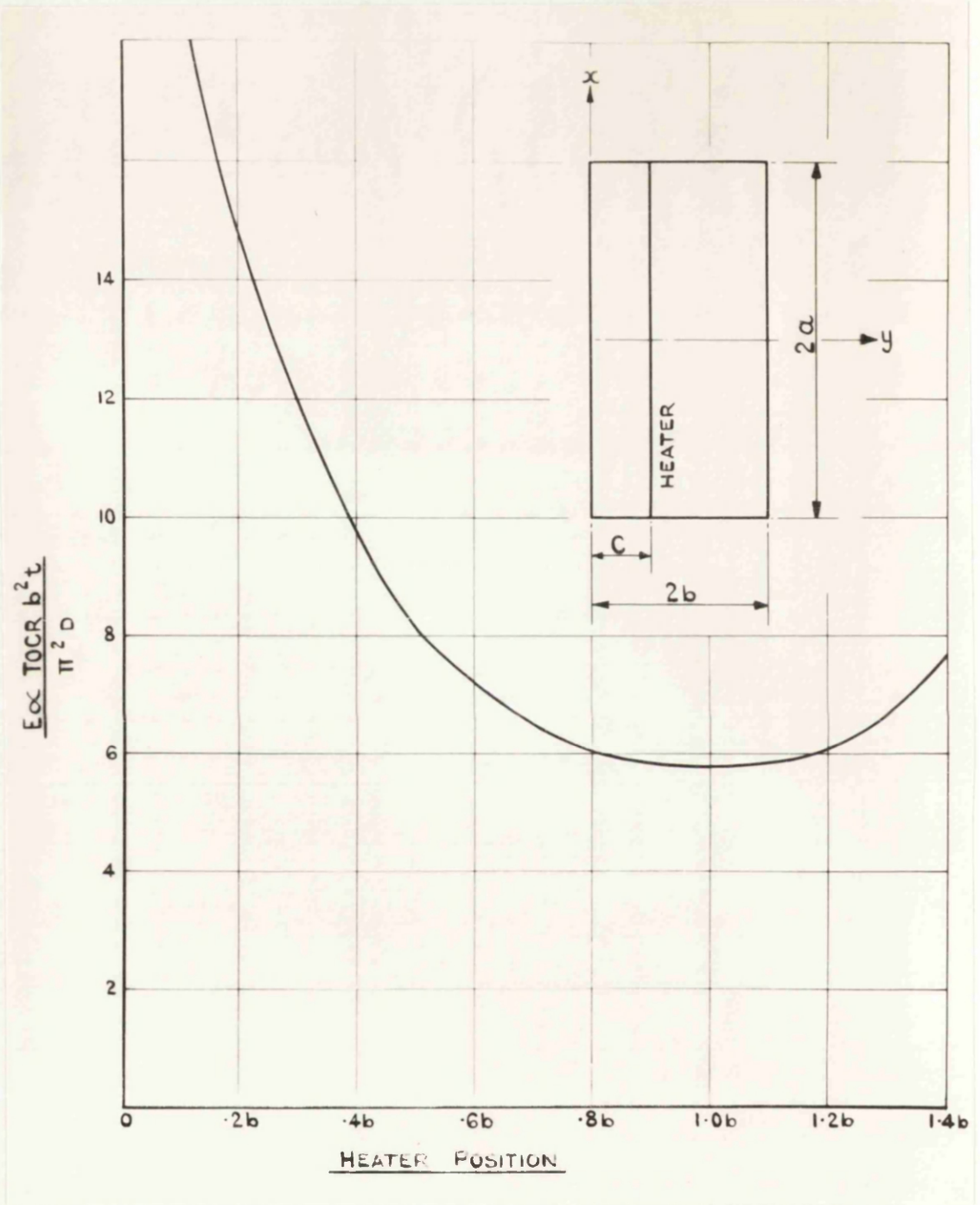

Figure 64: Variation of theoretical values of the critical temperature parameter with the degree of asymmetry of temperature distributions for a plate of aspect ratio 2.04.

of buckling to the four half wave mode takes place at an aspect ratio of 3.4. The complete behaviour of the buckling modes is summed up in figure 52, and shows that as the aspect ratio is increased there will be a progressive change from the one half wave mode to the two half wave mode and so on. In all the cases investigated the transverse mode of buckling was always one half wave. It should be noted that since the value of the deflection coefficients, a_{mn}, given by small deflection theory are indeterminate and only the ratios defined, the theoretical peak values have been chosen to coincide with the experimentally observed peak values. Figures 54 to 63 compare the theoretical buckle patterns with the experimental buckle patterns plotted from the dial gauge readings. It can be seen that the agreement between the theoretical and experimental buckle patterns is very close, thus confirming that the function chosen to represent the deflected form of the plate was of the correct type.

Thermal Buckling - Asymmetrical Temperature Distributions

The effect of the degree of asymmetry of the temperature distributions on the critical temperature parameter and critical temperature is clearly shown in figures 64 and 65. The most significant feature of these graphs is that the critical temperature has a minimum value for a particular size of plate when it is subjected to a symmetrical 'tent-like' temperature distribution. As the line source of heat is moved away from the central position, the resulting asymmetrical temperature distribution causes an increase in the value of the critical temperature. A limiting case is reached when the line source of heat/

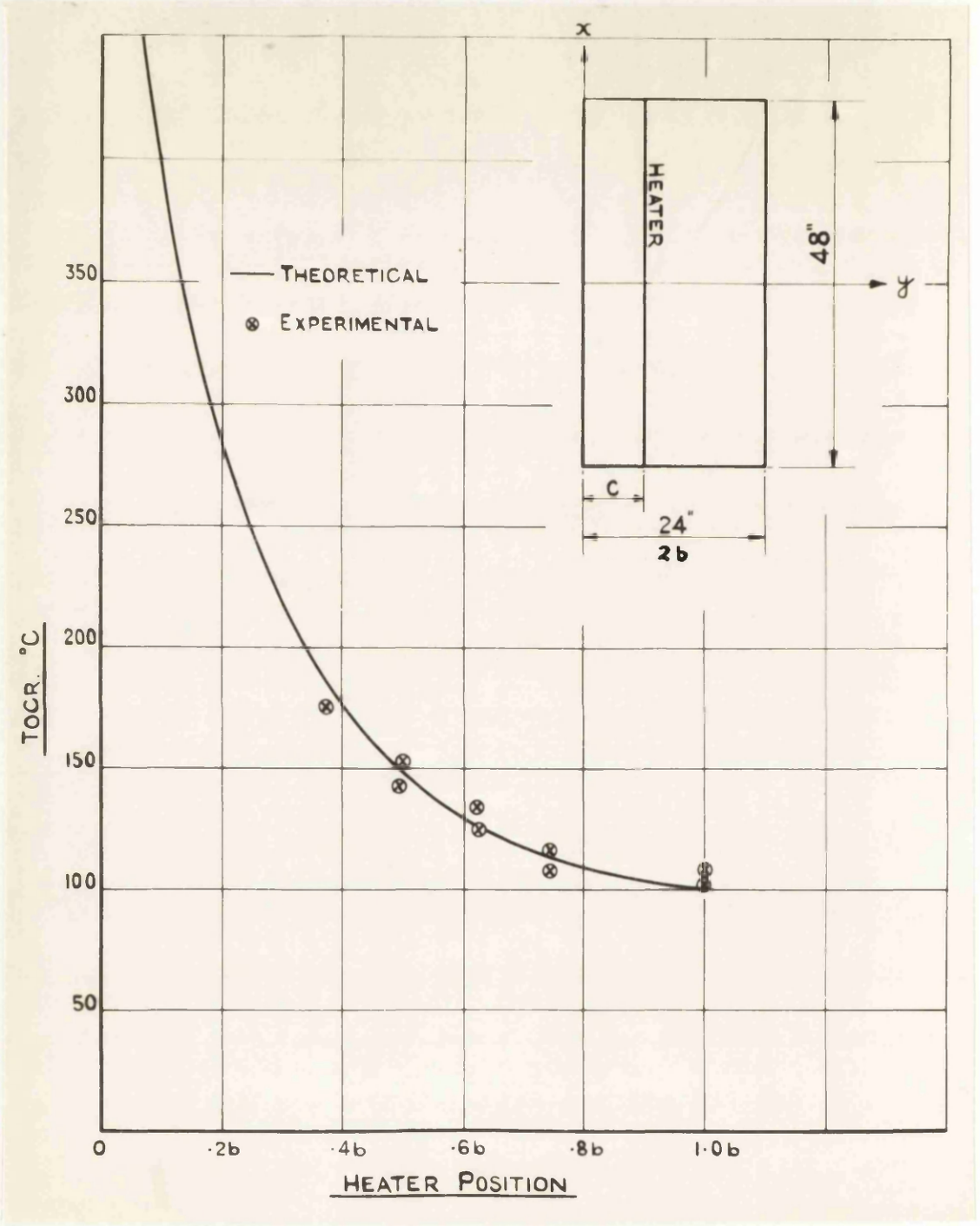

Figure 65: Comparison of experimental and theoretical values of critical temperature for a 4 ft. x 2 ft. plate subjected to an asymmetrical 'tent-like' temperature distribution.

is coincident with one of the longitudinal edges, the other edge being cooled as usual. In this case, although there is a linear temperature gradient across the surface of the plate, the stresses vanish since the strains corresponding to the free thermal expansion of each element, $\varepsilon_x = \varepsilon_y = \alpha T$, $\gamma_{xy} = 0$, satisfy the conditions of compatibility. Consequently, for this condition the critical temperature will be infinite.

Figure 65 shows experimental and theoretical values of critical temperature plotted as a function of the distance of the line source of heat from the origin. The agreement between theory and experiment is very good.

If attention is now turned to the deflected form of the plate, an examination of the vectors in Table 7 shows that only the vectors a_{11} and a_{13} influence the convergence of the critical temperature. Table 7 also shows that the vector a_{12}, which could affect the shape of the buckle pattern in the transverse direction and hence the position of the point maximum deflection, is very small compared with the dominant vector, a_{11}. Thus the shift of the point of maximum deflection is insignificant; a fact confirmed experimentally and shown in figure 66.

Post-Buckling Behaviour of Plates

In the concluding part of the review the post-buckling behaviour of plates was investigated with particular reference to the growth of plate centre deflection with increase in temperature differential.

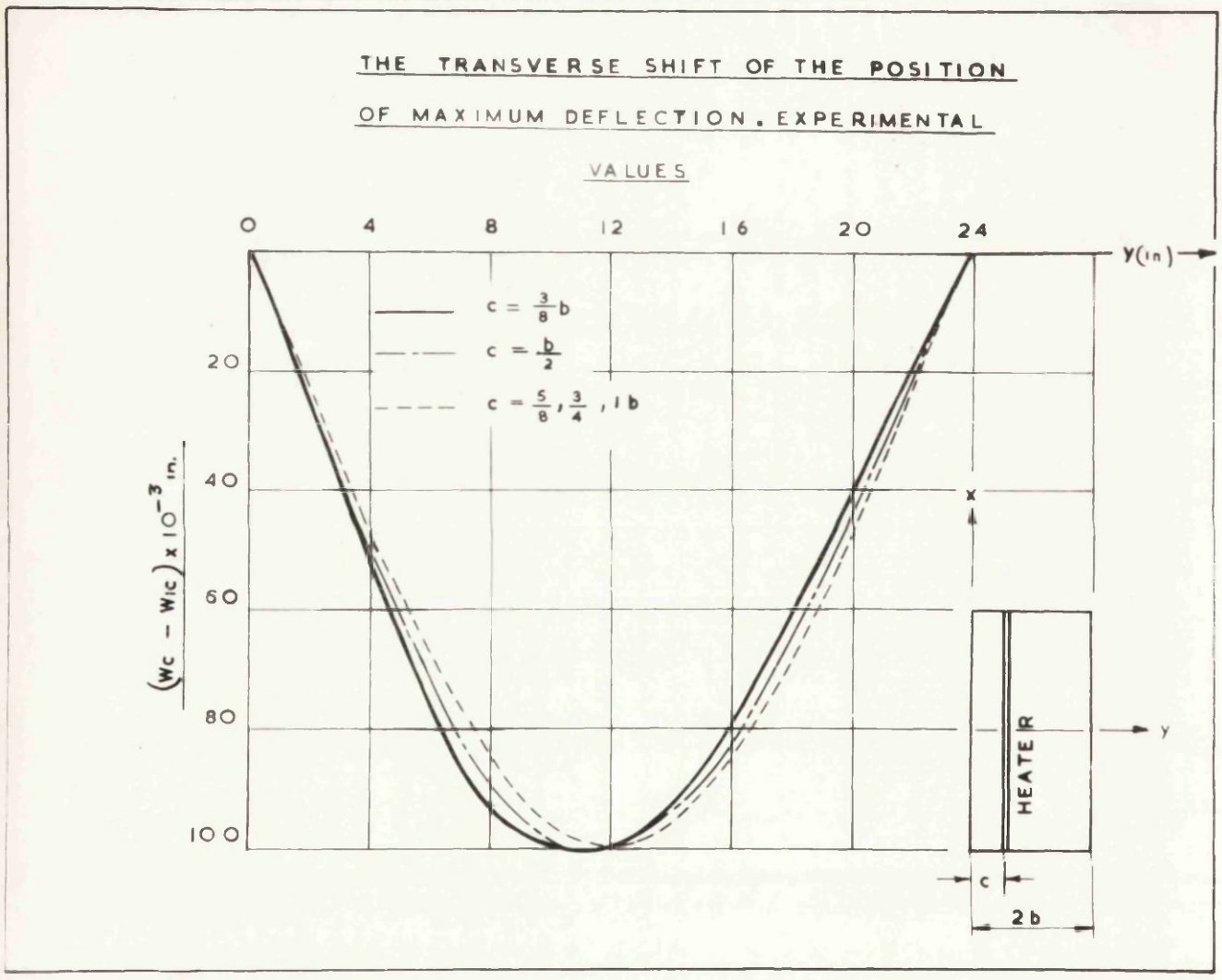

Figure 66: Experimental transverse buckle pattern of a 4 ft. x 2 ft. plate subjected to a variety of asymmetrical temperature distributions.

It was shown that the Von Kármán large deflection plate equations must be used if the stresses and deflections are required. Generally only an approximate solution to these equations can be obtained and even this is a very laborious procedure.

An alternative method for determining the growth of plate centre deflection from its initial value has been proposed by Gatewood[18] using the theory of mid-plane thermal strains. It has been shown that this method is very simple to apply and therefore it is worthwhile to compare the values of plate centre deflection using this method with the experimental values already obtained in the critical temperature experiments.

At first this comparison was carried out for a plate of aspect ratio 1.566 since the results in reference 13, obtained from an approximate solution of the large deflection equations, can also be presented on the same graph.

The experimental and theoretical results are shown graphically in figure 67. The theoretical curves based on the theory of mid-plane thermal strains are presented for various values of initial imperfections of a plate. Good agreement was obtained between experimental and theoretical values of plate deflection for a plate with a measured initial imperfection of 0.050 in. Also plotted on the same graph are the results obtained in reference 13 represented by the equation:-

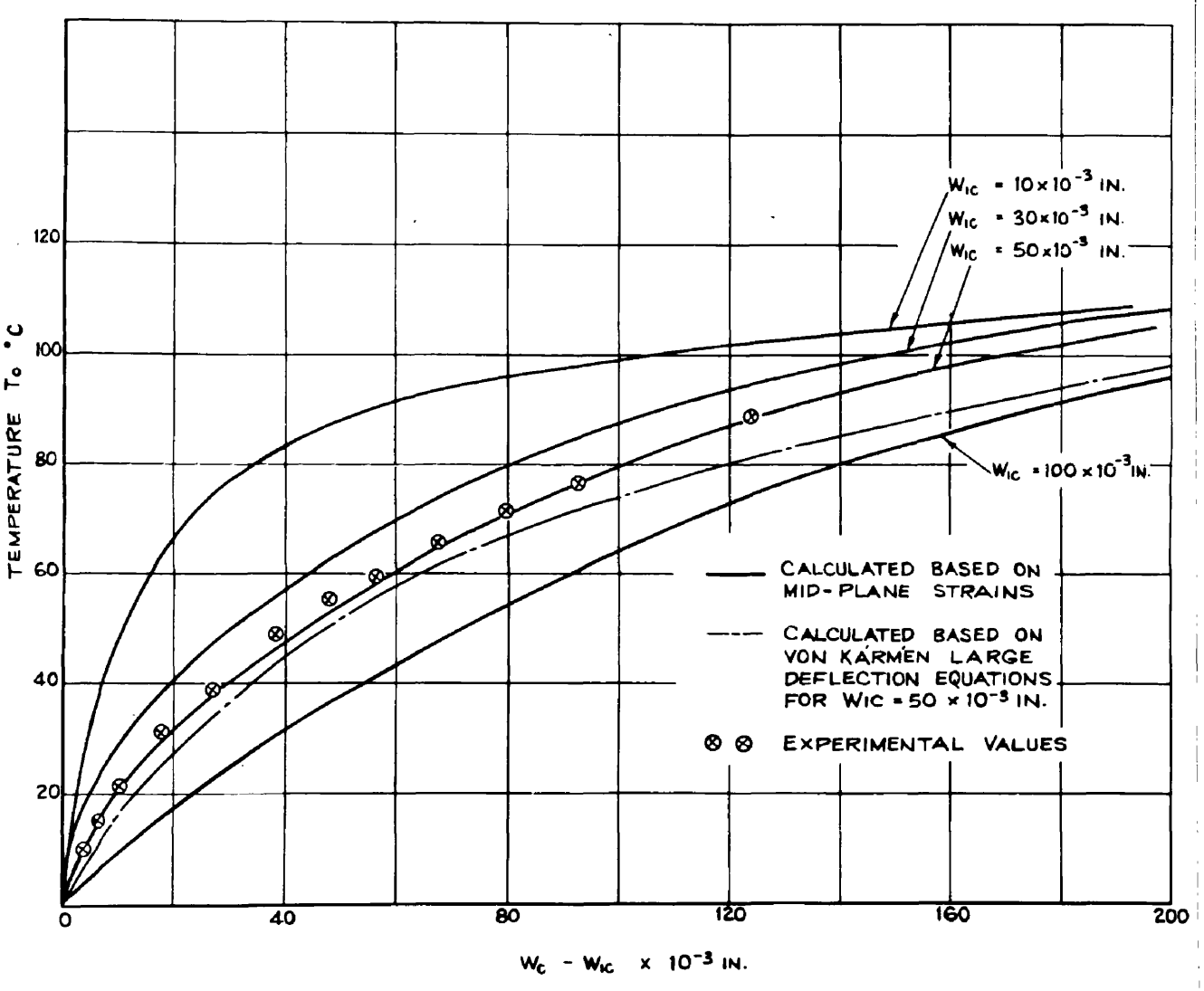

Figure 67: Calculated and experimental centre deflections of a 3 ft. x 2 ft. plate symmetrically heated.

$$T_o = 100\left(1 - \frac{W_{ic}}{W_c}\right) + 1.01\left(\frac{W_c^2 - W_{ic}^2}{t^2}\right) \qquad \ldots\ldots\ldots \quad 4.1$$

Again, good agreement exists between the experimental and theoretical values, based on a solution of equation 4.1.

Both theoretical methods may be expected to be fairly accurate when the initial deflected shape of the plate is similar to the first mode of buckling of the corresponding flat plate. This was found to be true for the 2 ft. x 2 ft., 3 ft. x 2 ft. and 4 ft. x 2ft. plate. In this range, figure 68 shows excellent agreement between experimental and theoretical values.

For longer plates, it is unlikely that the initial deflected shape will correspond to the predominant mode of buckling of the corresponding flat plate. It is for this reason that only fair agreement was obtained for the 5 ft. x 2 ft. and 6 ft. x 2 ft. plates.

In conclusion, it appears that the method of mid-plane strains is sufficiently accurate for practical purposes since in a design, only the average value of the initial imperfections will be known. Hence, using the above method some indication of the lateral deflection of a plate can be obtained if the temperature distribution of the plate is known.

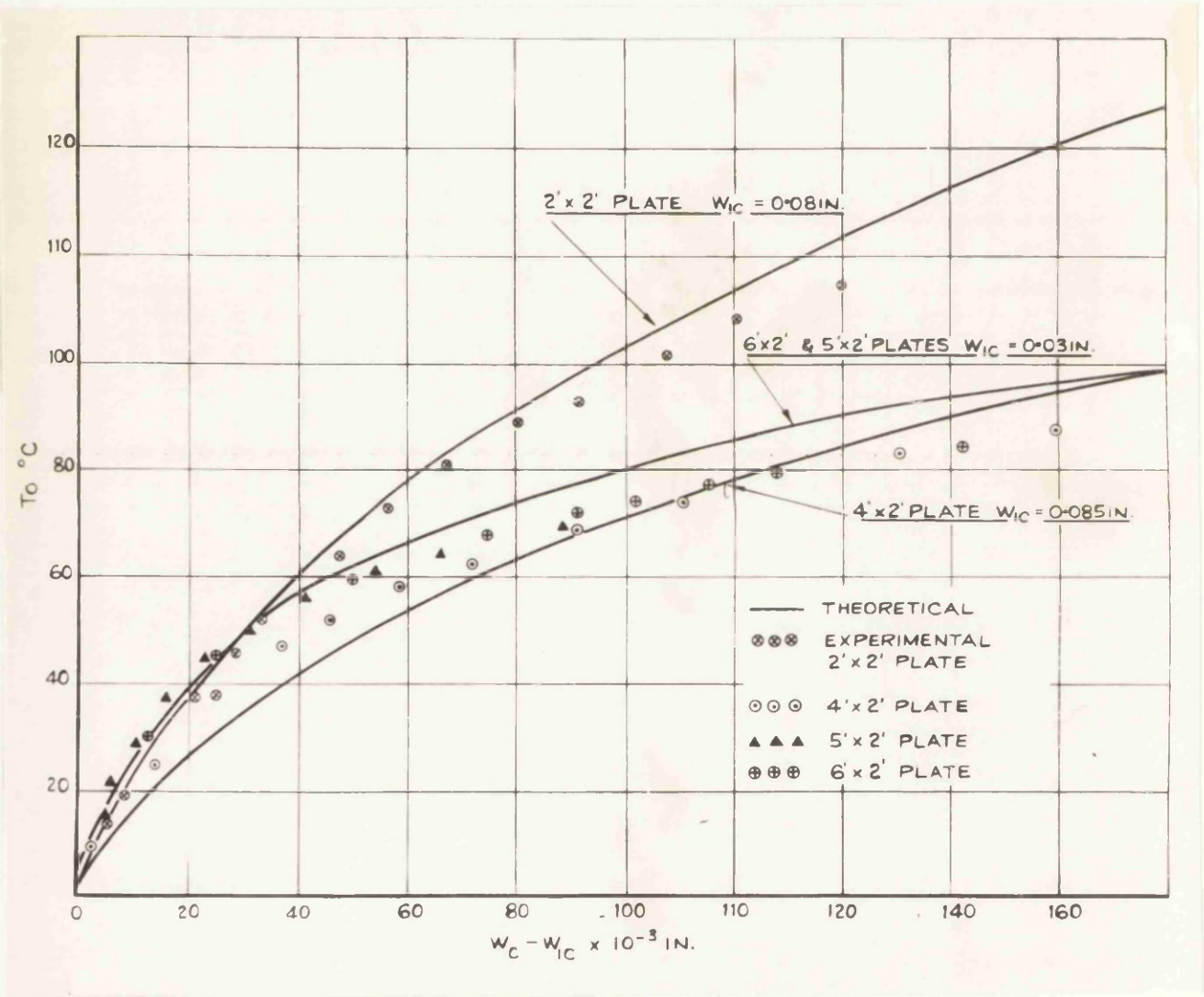

Figure 68: Calculated plate deflections, based on mid-plane strain theory and experimental plate deflections for plates of various aspect ratios subjected to symmetrical 'tent-like' temperature distributions.

SUMMARY OF CONCLUSIONS

The subject matter presented in the thesis may be summarised in broad outlines as follows:

1) The Galerkin method applied to the equation governing the stability of flat plates gives calculated values of critical temperatures which are in good agreement with experimental results.

2) It has been shown for the buckling problem that the Galerkin method is fully equivalent to the Rayleigh-Ritz method and leads to the same result if the same function is used to represent the deflected form of the plate.

3) Approximate methods for the determination of the thermal stress distribution based on minimum complementary energy concepts, appear to give consistent results in the evaluation of the critical buckling temperature.

4) The single product type of solution gives the stress function in the simplest functional form.

5) The 'end-effects' modify the distribution of thermal stresses in plates of small aspect ratio so as to cause a large increase in the value of critical temperature.

6) The critical temperature of a plate has a minimum value when the plate is symmetrically heated about a longitudinal centre-line.

7) The theoretical buckling patterns (buckling modes), determined from the small deflection theory plate equations, match very closely the experimental patterns when the peak magnitude of the modes is selected to be identical with the experimentally observed peak magnitude.

8) Values of plate centre deflection based on the theory of mid-plane strains compare favourably with the values obtained from an approximate solution of the Von Karman large deflection plate equation for values of temperature up to the critical temperature of an idealized flat plate.

9) Experimental values of plate centre deflections are in good agreement with the theoretical values derived from the large deflection plate equations and the mid-plane strain theory.

APPENDIX 1

Minimization of the Complementary Energy

The complementary energy of the heated plate can be expressed as:-

$$U^* = \frac{1}{2E} \int_{-a}^{a} \{A_1 g^2 + A_2 g''^2 - 2\nu A_3 g g'' + 2(1+\nu) A_4 g'^2 + 2E\alpha (A_6 X g + A_8 X g'')\} dx \qquad 5.1$$

where A_1 to A_8 are defined by equation 2.9.

Setting the first variation of U^*, i.e. δU^*, to zero by means of the calculus of variations, then the variation of complementary energy, term by term, is:-

First Term

$$\delta U^* = \frac{1}{E} \int_{-a}^{a} A_1 g \, \delta g \, dx$$

Second Term

$$\delta U^* = \frac{A_2}{E} \int_{-a}^{a} g'' \delta g'' dx = \frac{A_2}{E} \int_{-a}^{a} g'' \, \delta \left[\frac{dg'}{dx}\right] dx$$

$$= \frac{A_2}{E} \int_{-a}^{a} g'' d \left[dg'\right]$$

Integrating by parts yields

$$\delta U^* = \frac{A_2}{E} \left\{ \left[g'' \delta g' \right]_{-a}^{a} - \int_{-a}^{a} g''' \delta g' dx \right\}$$

$$\delta U^* = \frac{A_2}{E} \left\{ \left[g'' \delta g' \right]_{-a}^{a} - \int_{-a}^{a} g''' d\left[\delta g \right] \right\}$$

Integrating by parts again yields:-

$$\delta U^* = \frac{A_2}{E} \left\{ \left[g'' \delta g' \right]_{-a}^{a} - \left[g''' \delta g \right]_{-a}^{a} + \int_{-a}^{a} g'''' \delta g \, dx \right\}$$

<u>Third Term</u>

$$\delta U^* = - \frac{A_3 \nu}{E} \int_{-a}^{a} g \, \delta g'' dx - \frac{A_3 \nu}{E} \int_{-a}^{a} g'' \delta g \, dx$$

Integrating by parts taking the first expression first, yields

$$\delta U^* = - \frac{A_3 \nu}{E} \left\{ \left[g \delta g' \right]_{-a}^{a} - \int_{-a}^{a} g' \delta g' \, dx \right\}$$

Integrating by parts again yields

$$\delta U^* = \frac{A_3 \nu}{E} \left\{ - \left[g \, \delta g' \right]_{-a}^{a} + \left[g' \delta g \right]_{-a}^{a} - \int_{-a}^{a} g'' \, \delta g \, dx \right\}$$

and the second expression of the third term yields

$$\delta U^* = -\frac{A_3}{E} \int_{-a}^{a} g'' \delta g$$

Fourth Term

$$\delta U^* = \frac{2(1+\nu)A_4}{E} \int_{-a}^{a} g' \delta g' dx = \frac{2(1+\nu)A_4}{E} \int_{-a}^{a} g' d\left[\delta g\right]$$

Integrating by parts yields

$$\delta U^* = \frac{2(1+\nu)A_4}{E} \left\{ \left[g' \delta g \right]_{-a}^{a} - \int_{-a}^{a} g'' \delta g \, dx \right\}$$

Fifth Term

$$\delta U^* = \frac{E\alpha}{E} \int_{-a}^{a} A_6 X \delta g \, dx$$

Sixth Term

$$\delta U^* = \frac{E\alpha}{E} \int_{-a}^{a} A_8 X \delta g \, dx = \frac{E\alpha}{E} \int_{-a}^{a} A_8 X d \, \delta g'$$

Integrating yields

$$\delta U^* = \frac{E\alpha}{E} \left[A_8 X \quad \delta g' \right]_{-a}^{a}$$

Collecting terms gives

$$\delta U^{*} = 0 = \frac{1}{E}\int_{-a}^{a} \{A_1 g + A_2 g'''' - 2\left[A_4(1+\nu) + \nu A_3\right] g'' + E\alpha A_6 X\}\,\delta g\, dx$$

$$+ \frac{1}{E}\left[\{(\nu A_3 + 2(1+\nu)A_4)g' - A_2 g'''\}\,\delta g\right]_{-a}^{+a}$$

$$+ \frac{1}{E}\left[\{A_2 g'' - \nu A_3 g' + E\alpha A_8 X\}\,\delta g'\right]_{-a}^{a} \quad \ldots\ldots\ldots \quad 5.2$$

The boundary conditions at $x = \pm a$, where $\sigma_x = \tau_{xy} = 0$, require that g and g' vanish at these points and that $A_3 = -A_4$ and $A_5 = 0$.

Using these conditions, the term under the integral sign in equation 5.2 reduces to:-

$$A_2 g'''' - 2A_4 g'' + A_1 g + E\alpha A_6 X = 0 \quad \ldots\ldots\ldots \quad 5.3$$

and the terms in the square brackets are equal to zero for the above boundary conditions. Thus the approximate solution is independent of Poisson's ratio ν.

APPENDIX 2

The relationship, $A_1 = -A_6 E\alpha$, provides a valuable check when the coefficients of equation 5.3 are being evaluated.

The proof of this relationship is as follows:

since $A_1 = \int_{-b}^{b} f''^2 dy$, then integrating by parts gives

$$A_1 = \left[f'f'' \right]_{-b}^{b} - \int_{-b}^{b} ff''' dy \qquad \ldots\ldots\ldots \quad 5.4$$

Note that the contents in the square brackets are zero.

Integrating by parts again:-

$$A_1 = \left[- ff''' \right]_{-b}^{b} + \int_{-b}^{b} ff'''' dy \qquad \ldots\ldots\ldots \quad 5.5$$

noting that the quantity in the square brackets is zero.

In a similar manner, the expression for A_6 is integrated by parts twice to give:-

$$A_6 = \int_{-b}^{b} f'' Y dy = \int_{-b}^{b} f Y'' dy \qquad \ldots\ldots\ldots \quad 5.6$$

For a plate infinite in the 'x' direction the stress is a function of y only; therefore the biharmonic equation 2.2 reduces to:-

$$f'''' = -E \alpha Y'' \qquad \ldots\ldots\ldots \quad 5.7$$

Substituting for f'''' in the equation for the integral A_1, this yields

$$A_1 = -E \alpha A_6 \qquad \ldots\ldots\ldots \quad 5.8$$

APPENDIX 3

Derivation of the stress functions for the symmetrical case (c = b), and the asymmetrical cases, c = $\frac{3}{4}$b, $\frac{1}{2}$b, $\frac{1}{4}$b

Symmetrical Case

Reference 10 suggests that a good choice for the function f is a stress function for an infinite plate.

Using the coordinate system shown in figure 21, then

$$\sigma_{x_\infty} = f'' = E\alpha T_o(y/b - \frac{1}{2}) \quad \text{for} \quad 0 \leq y \leq b \qquad \ldots\ldots\ldots \quad 5.9$$

Integrating equation 5.9 twice gives the function f together with two arbitrary constants of integration

$$f = E\alpha T_o \left(\frac{y^3}{6b} - \frac{y^2}{4} + S_1 y + S_2\right) \qquad \ldots\ldots\ldots \quad 5.10$$

Equation 5.10 is valid in one quadrant only and therefore conditions at y = -b are not applicable.

The conditions of symmetry can be used, however, which gives:-

$$f'(0) = f(b) = f'(b) = 0 \qquad \ldots\ldots\ldots \quad 5.11$$

The condition, f'(0), is implied in equation 2.12 (zero stress resultant along any axis parallel to the y axis) and therefore the remaining

boundary conditions are used to determine S_1 and S_2.

After solving for S_1 and S_2, the function becomes:-

$$f = \frac{b^2}{12} \left\{1 - 3\left(\frac{Y}{b}\right)^2 + 2\left(\frac{Y}{b}\right)^3\right\} E \alpha T_o \qquad \ldots\ldots\ldots \quad 5.12$$

Integrals A_1, A_2, A_4 and A_6 can now be evaluated to give the coefficients of the resulting linear differential equation:-

$$13b^4 g'''' - 84b^2 g'' + 420g = 420 \qquad \ldots\ldots\ldots \quad 5.13$$

The complementary solution of this equation can be assumed to be of the form:-

$$g_c = Pe^{mx} \qquad \ldots\ldots\ldots \quad 5.14$$

Substituting this assumed form in equation 5.13, the auxiliary equation

$$13b^4 m^4 - 168b^2 m^2 + 420 = 0 \qquad \ldots\ldots\ldots \quad 5.15$$

is obtained, having roots

$$\begin{aligned} m_1 &= \frac{1}{b}(2.1113 + 1.10752j) \; ; \quad m_2 = \bar{m}_1 \\ m_3 &= \frac{1}{b}(-2.1113 - 1.10752j) \; ; \quad m_4 = \bar{m}_3 \end{aligned} \qquad \ldots\ldots\ldots \quad 5.16$$

where the bar denotes conjugate quantities.

Thus it follows that the complementary solution can be written as:-

$$g = e^{2.1113\frac{x}{b}}\left\{P_1 e^{1.10752j\frac{x}{b}} + P_2 e^{-1.10752j\frac{x}{a}}\right\}$$

$$+ e^{-2.1113\frac{x}{b}}\left\{P_3 e^{-1.10752j\frac{x}{b}} + P_4 e^{1.10752j\frac{x}{a}}\right\} \quad \ldots\ldots \quad 5.17$$

After some simplification, this can be written as:-

$$g_c = C_1 \sinh rx \sin sx + C_2 \cosh rx \cos sx$$

$$+ C_3 \cosh rx \sin sx + C_4 \sinh rx \cos sx \quad \ldots\ldots\ldots \quad 5.18$$

where $r = 2.1113/b$ and $s = 1.10752/b$. C_1 to C_4 are four arbitrary constants to be found from the boundary conditions at $x = \pm a$.

By inspection the particular integral of equation 5.13 is

$$g_p = -\frac{A_6 E a}{A_1} = 1 \quad \ldots\ldots\ldots \quad 5.19$$

Hence the complete solution of equation 5.13 is

$$g = 1 + C_1 \sinh rx \sin sx + C_2 \cosh rx \cos sx$$

$$+ C_3 \cosh rx \sin sx + C_4 \sinh rx \cos sx \quad \ldots\ldots\ldots \quad 5.20$$

where the constants C_1, C_2, C_3 and C_4 are determined from the condition that $g = g' = 0$ at $x = \pm a$ which yields:-

$$C_1 = \frac{r \sinh ra \cos sa - s \cosh ra \sin sa}{r \sin sa \cos sa + s \sinh ra \cosh ra}$$

..... 5.21

$$C_2 = -\frac{r \cosh ra \sin sa + s \sinh ra \cos sa}{r \sin sa \cos sa + s \sinh ra \cosh ra}$$

Using equation 2.1 in conjunction with equations 5.12 and 5.20 the stresses in the plate are given by:-

$$\sigma_x = \frac{E \alpha T_o}{2} \left(\frac{2y}{b} - 1\right)(1 + C_1 \sinh rx \sin sx + C_2 \cosh rx \cos sx)$$

$$\sigma_y = \frac{E \alpha T_o b^2}{12} \left(2\left(\frac{y}{b}\right)^3 - 3\left(\frac{y}{b}\right)^2 + 1\right)(C_7 \sinh rx \sin sx + C_8 \cosh rx \cos sx)$$

$$\tau_{xy} = -\frac{E \alpha T_o b}{2} \left(\left(\frac{y}{b}\right)^2 - \left(\frac{y}{b}\right)\right)(C_5 \sinh rx \cos sx + C_6 \cosh rx \sin sx)$$

where

$$C_5 = C_1 s + C_2 r \qquad C_7 = C_1(r^2 - s^2) - 2C_2 r.s$$

$$C_6 = C_1 r - C_2 s \qquad C_8 = 2C_1 r.s + C_2(r^2 - s^2)$$

..... 5.22

Asymmetrical Cases

In these cases the temperature is no longer symmetrical about the longitudinal axis of the plate. This means that one half of the plate must be analysed instead of one quadrant analysed in the symmetrical cases. The ordinary differential equation for the g function is of the same form but with different numerical coefficients.

Since one half of the plate must be considered in the analysis, it is necessary to derive separate expressions for the f function on each side of the point of discontinuity of the temperature function.

The derivation of the f functions can be found using similar methods to those used in the symmetrical cases. In this instance it is more convenient to use the coordinate system defined in figure 22.

As in the symmetrical case the distribution of thermal stresses in a long plate can be found by suppressing the free thermal expansion of each plate element by applying a compressive stress, $-E\alpha T$. As in the symmetrical cases considered, tensile stresses must be applied at the transverse edges to ensure that the edges remain stress free.

Owing to the asymmetry of the temperature distributions there will be a resultant moment as well as a resultant force action set up. Thus the longitudinal stress, σ_x, at a point removed from the ends will be:-

$$\sigma_x = -E\alpha T + \tfrac{1}{2}E\alpha T_o + \frac{3(b-y)}{2b^3} \times \text{Bending Moment} \qquad \ldots\ldots\ldots \quad 5.23$$

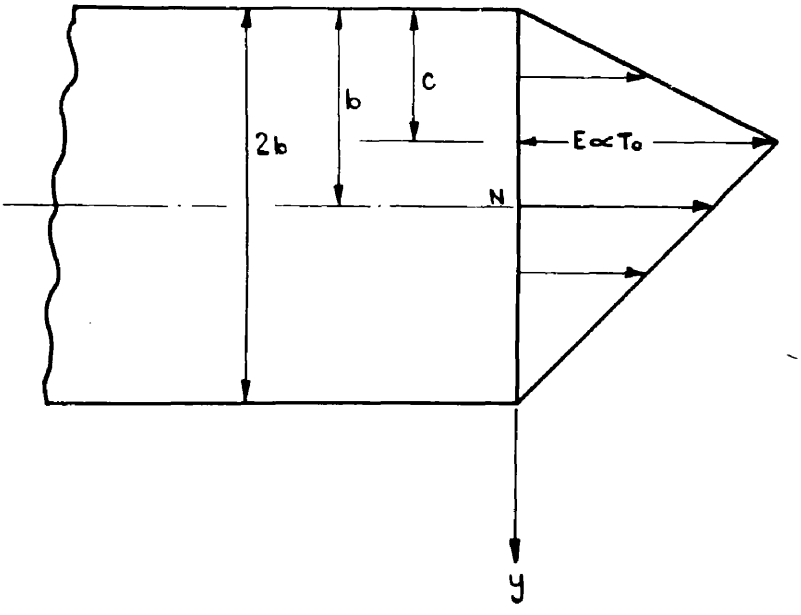

Figure 69: Tensile edge stresses, +E∝T, applied at transverse edges of the plate.

The bending moment on the plate about the axis N-N is:

$$BM = E\alpha T_o \left\{\frac{c}{2}\left(\frac{c}{3} + b - c\right) - \left(\frac{2b-c}{2}\right)\left(\frac{2b-c}{3} - b + c\right)\right\} \quad \text{(figure 69)}$$

which reduces to

$$BM = E\alpha T_o \frac{b}{3}(b - c) \qquad \ldots\ldots\ldots \quad 5.24$$

The longitudinal stress in the plate is therefore

$$\sigma_x = f'' = -E\alpha T + \tfrac{1}{2}E\alpha T_o + \frac{(b-c)(b-y)}{2b^2} E\alpha T_o \qquad \ldots\ldots\ldots \quad 5.25$$

As already mentioned, separate expressions for f must be derived on each side of the discontinuity occurring in the temperature function, and the algebraic analysis is simplified if the f function is evaluated for the particular cases of $c = \frac{3}{4}b$, $\frac{1}{2}b$ and $\frac{b}{4}$.

Particular case, $c = b/2$

The analysis for this case is given in full; the other cases are evaluated in a similar manner.

For the domain bounded by $0 < y < \frac{b}{2}$, the temperature distribution can be expressed as

$$T = T_o \, 2y/b \qquad \ldots\ldots\ldots \quad 5.26$$

and for the domain bounded by $\frac{b}{2} < y < 2b$,

$$T = \frac{4b - 2y}{3b} T_o \qquad \ldots\ldots\ldots \quad 5.27$$

Thus

$$f_1'' = E\alpha T_o \left\{-\frac{2y}{b} + \frac{1}{2} + \frac{b-y}{4b}\right\} \text{ valid for } 0 < y < \frac{b}{2} \qquad \ldots\ldots\ldots \quad 5.28$$

Integrating equation 5.28 twice yields

$$f_1' = E\alpha T_o \left\{-\frac{y^2}{b} + \frac{y}{2} + \frac{by - y^2/2}{4b} + S_1\right\} \qquad \ldots\ldots\ldots \quad 5.29$$

and

$$f_1 = E\alpha T_o \left\{-\frac{y^3}{3b} + \frac{y^2}{4} + \frac{by^2/2 - y^3/6}{4b} + S_1 y + S_2\right\} \qquad \ldots\ldots\ldots \quad 5.30$$

At the boundary $y = 0$, f_1 and $f_1' = 0$, which gives $S_1 = S_2 = 0$;

$$\text{hence} \qquad f_1 = E\alpha T_o \left\{\frac{3y^2}{8} - \frac{9}{24}\frac{y^3}{b}\right\} \qquad \ldots\ldots\ldots \quad 5.31$$

For the domain bounded by $b/2 < y < 2b$

$$f_2' = E\alpha T_o \left\{-\int_o^{b/2} \frac{2y}{b}\,dy - \int_{b/2}^{y} \frac{4b - 2y}{3b}\,dy + \int_o^{y} \left(\frac{1}{2} + \frac{b-y}{4b}\right)dy\right\}$$

i.e.

$$f_2' = E\alpha T_o \left\{-\left[\frac{y^2}{b}\right]_o^{b/2} - \left[\frac{4y}{3} - \frac{y^2}{3b}\right]_{b/2}^{y} + \frac{y}{2} + \frac{by - y^{2/2}}{4b} + S_3\right\}$$

which reduces to

$$f_2' = E\alpha T_o\left\{\frac{b}{3} - \frac{4y}{3} + \frac{y^2}{3b} + \frac{y}{2} + \frac{by - y^{2/2}}{4b} + S_3\right\} \quad \ldots\ldots\ldots \quad 5.32$$

Integrating again gives

$$f_2 = E\alpha T_o\left\{\int_o^{b/2} -\frac{y^2}{2b}\,dy + \int_{b/2}^{y}\left(\frac{b}{3} - \frac{4y}{3} + \frac{y^2}{3b}\right)dy + \int_o^{y}\left(\frac{y}{2} + \frac{by - y^{2/2}}{4b}\right)dy + S_3 y + S_4\right\}$$

i.e.

$$f_2 = E\alpha T_o\left\{-\frac{b^2}{18} + \frac{by}{3} - \frac{7y^2}{24} + \frac{5y^3}{72b} + S_3 y + S_4\right\} \quad \ldots\ldots\ldots \quad 5.33$$

The boundary conditions at $y = 2b$ are $f_2 = f_2' = 0$, which gives $S_3 = S_4 = 0$; hence

$$f_2 = E\alpha T_o\left\{-\frac{b^2}{18} + \frac{by}{3} - \frac{7y^2}{24} + \frac{5y^3}{72b}\right\} \quad \ldots\ldots\ldots \quad 5.34$$

Integral represented by A_1 is defined as $\int_o^{2b} f''^2\,dy$. Since f'' is not continuous over the whole range of integration, the integration must, in this case, be carried between the limits 0 to b/2 and from b/2 to 2b and then the two results added together to give the value of A_1.

i.e. $$A_1 = \int_o^{b/2} f_1''^2\,dy + \int_{b/2}^{2b} f_2''^2\,dy \quad \ldots\ldots\ldots \quad 5.35$$

In a similar manner, integrals represented by A_2, A_4 and A_6 can be

evaluated. For the case of c = b/2, the following values were obtained:-

$$A_1 = 0.124999(E\alpha T_o)^2 \qquad A_4 = 0.00937500b^3(E\alpha T_o)^2$$

$$A_2 = 0.00284598b^5(E\alpha T_o)^2 \qquad A_6 = -0.125000(E\alpha)^2 T_o$$

Substituting these values in equation 5.3, the following linear differential equation is obtained:-

$$2.84598b^4 g'''' - 18.750b^2 g'' + 125.000g = 125.000 \quad \ldots\ldots\ldots \quad 5.36$$

Using the same procedure as for the symmetrical case, similar equations for the stresses are obtained. They are:-

$$\sigma_x = E\alpha T_o\left\{\frac{3}{4} - \frac{9y}{4b}\right\}\{1 + C_1 \sinh rx \sin sx + C_2 \cosh rx \cos sx\}$$

$$\sigma_y = E\alpha T_o\left\{\frac{3y^2}{8} - \frac{9y^3}{24b}\right\}\{C_7 \sinh rx.\sin sx + C_8 \cosh rx \cos sx\}$$

$$\tau_{xy} = -E\alpha T_o\left\{\frac{3y}{4} - \frac{9y^2}{8b}\right\}\{C_5 \sinh rx \cos sx + C_6 \cosh rx \sin sx\}$$

valid for $0 < y < b/2$

$$\sigma_x = E\alpha T_o\left\{\frac{-7}{12} + \frac{5y}{12b}\right\}\{1 + C_1 \sinh rx \sin sx + C_2 \cosh rx \cos sx\}$$

$$\sigma_y = E\alpha T_o\left\{-\frac{b^2}{18} + \frac{by}{3} - \frac{7y^2}{24} + \frac{5y^3}{72b}\right\}\{C_7 \sinh rx \sin sx + C_8 \cosh rx \cos sx\}$$

$$\tau_{xy} = -E\alpha T_o\left\{\frac{b}{3} - \frac{7y}{12} + \frac{5y^2}{24b}\right\}\{C_5 \sinh rx \cos sx + C_6 \cosh rx \sin sx\}$$

valid for $b/2 < y < 2b$ $\quad \ldots\ldots\ldots \quad 5.37$

where C_1, C_2, C_5, C_6, C_7 and C_8 are defined in precisely the same manner as for the symmetrical cases.

Summary of Asymmetrical Cases

For convenience, the forms of the temperature f, f' and f'' functions and values of integrals A_1 etc. are given in tabular form in Tables 13, 14 and 15.

Thus the stresses in the plate are:-

$$\sigma_x = f''g \; ; \; \sigma_y = fg'' \text{ and } \tau_{xy} = -f'g' \quad \ldots\ldots\ldots \quad 5.38$$

where g is defined by the equation

$$g = 1 + C_1 \sinh rx \sin sx + C_2 \cosh rx \cos sx \quad \ldots\ldots\ldots \quad 5.39$$

TABLE 13

Case	Domain bounded by	Temperature function
$c = \frac{3}{4}b$	$0 < y < \frac{3}{4}b$	$T = T_o \frac{4y}{3b}$
	$\frac{3}{4}b < y < 2b$	$T = T_o \left(\frac{8b - 4y}{5b}\right)$
$c = \frac{b}{2}$	$0 < y < \frac{b}{2}$	$T = T_o \frac{2y}{b}$
	$\frac{b}{2} < y < 2b$	$T = T_o \left(\frac{4b - 2y}{3b}\right)$
$c = \frac{b}{4}$	$0 < y < \frac{b}{4}$	$T = T_o \frac{4y}{b}$
	$\frac{b}{4} < y < 2b$	$T = T_o \left(\frac{8b - 4y}{7b}\right)$

TABLE 14

Values of Integrals, A_1, A_2, A_4 and A_6, etc.

Case	$\frac{A_1 X}{b(E\alpha T_o)^2}$	$\frac{A_2 X}{b^4(E\alpha T_o)^2}$	$\frac{A_4 X}{b^3(E\alpha)^2 T_o^2}$	$\frac{A_6 X}{b(E\alpha)^2 T_o}$	$\frac{r}{b}$	$\frac{s}{b}$
$c = \frac{3}{4}b$	0.1562500	0.00451224	0.0146484	-0.1562500	2.136696	1.148515
$c = \frac{b}{2}$	0.124999	0.00284598	0.00937500	-0.125000	2.22727	1.29097
$c = \frac{b}{4}$	0.0729166	0.00094468	0.003190167	-0.0729166	2.46601	1.64447

TABLE 15

Case	Domain	function $f'' \times EcT_o$	function $f' \times EcT_o$	function $f \times EcT_o$
$c = \frac{3}{4}b$	$0 < y < \frac{3}{4}b$	$\frac{5}{8} - \frac{35}{24}\frac{y}{b}$	$\frac{5}{8}y - \frac{35}{48}\frac{y^2}{b}$	$\frac{5}{16}y^2 - \frac{35}{144}\frac{y^3}{b}$
	$\frac{3}{4}b < y < 2b$	$-\frac{39}{40} + \frac{27}{40}\frac{y}{b}$	$\frac{3}{5}b - \frac{39}{40}y + \frac{27}{80}y^2/b$	$-\frac{3b^2}{20} + \frac{3by}{5} - \frac{39}{80}y^2 + \frac{9}{80}\frac{y^3}{b}$
$c = \frac{b}{2}$	$0 < y < \frac{b}{2}$	$\frac{3}{4} - \frac{9}{4}\frac{y}{b}$	$\frac{3}{4}y - \frac{9}{8}\frac{y^2}{b}$	$\frac{3}{8}y^2 - \frac{9}{24}\frac{y^3}{b}$
	$\frac{b}{2} < y < 2b$	$-\frac{7}{12} + \frac{5}{12}\frac{y}{b}$	$\frac{b}{3} - \frac{7}{12}y + \frac{5}{24}\frac{y^2}{b}$	$-\frac{b^2}{18} + \frac{by}{3} - \frac{7y^2}{24} + \frac{5y^3}{72b}$
$c = \frac{b}{4}$	$0 < y < \frac{b}{4}$	$\frac{7}{8} - \frac{35}{8}\frac{y}{b}$	$\frac{14}{16}y - \frac{35}{16}\frac{y^2}{b}$	$\frac{7}{16}y^2 - \frac{35}{48}\frac{y^3}{b}$
	$\frac{b}{4} < y < 2b$	$-\frac{15}{56} + \frac{11}{56}\frac{y}{b}$	$\frac{b}{7} - \frac{30}{112}y + \frac{33}{336}\frac{y^2}{b}$	$-\frac{4b^2}{336} + \frac{by}{7} - \frac{15y^2}{112} + \frac{11}{336}\frac{y^3}{b}$

TABLE 16

Case	K_1	K_2
$c = b$	2.11130	1.107520
$c = \frac{3}{4}b$	2.13669	1.148515
$c = \frac{b}{2}$	2.22727	1.29097
$c = \frac{b}{4}$	2.46601	1.64447

TABLE 17

Case	Domain	Stress function ϕ
$c = b$	$0 < y < b$	$\frac{b^2}{12} E\alpha T_o\left(1 - 3\left(\frac{y}{b}\right)^2 + 2\left(\frac{y}{b}\right)^3\right)\left(B_1 \sinh R_1 \frac{x}{a} \sin R_2 \frac{x}{a} + B_2 \cosh R_1 \frac{x}{a} \cos R_2 \frac{x}{a} + 1\right)$
$c = \frac{3}{4}b$	$0 < y < \frac{3}{4}b$	$b^2 E\alpha T_o\left(\frac{5}{16}\left(\frac{y}{b}\right)^2 - \frac{35}{144}\left(\frac{y}{b}\right)^3\right)\left(B_1 \sinh R_1 \frac{x}{a} \sin R_2 \frac{x}{a} + B_2 \cosh R_1 \frac{x}{a} \cos R_2 \frac{x}{a} + 1\right)$
	$\frac{3}{4}b < y < 2b$	$b^2 E\alpha T_o\left(-\frac{3}{20} + \frac{3}{5}\frac{y}{b} - \frac{39}{80}\left(\frac{y}{b}\right)^2 + \frac{9}{80}\left(\frac{y}{b}\right)^3\right)\left(B_1 \sinh R_1 \frac{x}{a} \sin R_2 \frac{x}{a} + B_2 \cosh R_1 \frac{x}{a} \cos R_2 \frac{x}{a} + 1\right)$
$c = \frac{b}{2}$	$0 < y < \frac{b}{2}$	$b^2 E\alpha T_o\left(\frac{3}{8}\left(\frac{y}{b}\right)^2 - \frac{9}{24}\left(\frac{y}{b}\right)^3\right)\left(B_1 \sinh R_1 \frac{x}{a} \sin R_2 \frac{x}{a} + B_2 \cosh R_1 \frac{x}{a} \cos R_2 \frac{x}{a} + 1\right)$
	$\frac{b}{2} < y < 2b$	$b^2 E\alpha T_o\left(-\frac{1}{18} + \frac{y}{3b} - \frac{7}{24}\left(\frac{y}{b}\right)^2 + \frac{5}{72}\left(\frac{y}{b}\right)^3\right)\left(B_1 \sinh R_1 \frac{x}{a} \sin R_2 \frac{x}{a} + B_2 \cosh R_1 \frac{x}{a} \cos R_2 \frac{x}{a} + 1\right)$
$c = \frac{b}{4}$	$0 < y < \frac{b}{4}$	$b^2 E\alpha T_o\left(\frac{7}{16}\left(\frac{y}{b}\right)^2 - \frac{35}{48}\left(\frac{y}{b}\right)^3\right)\left(B_1 \sinh R_1 \frac{x}{a} \sin R_2 \frac{x}{a} + B_2 \cosh R_1 \frac{x}{a} \cos R_2 \frac{x}{a} + 1\right)$
	$\frac{b}{4} < y < 2b$	$b^2 E\alpha T_o\left(-\frac{4}{336} + \frac{1}{7}\frac{y}{b} - \frac{15}{112}\left(\frac{y}{b}\right)^2 + \frac{11}{336}\left(\frac{y}{b}\right)^3\right)\left(B_1 \sinh R_1 \frac{x}{a} \sin R_2 \frac{x}{a} + B_2 \cosh R_1 \frac{x}{a} \cos R_2 \frac{x}{a} + 1\right)$

APPENDIX 4

Buckling Calculations

The constants in equations 2.37, 2.38 and 2.39 are defined as follows:-

$$B_1 = \frac{K_1 \sinh R_1 \cos R_2 - K_2 \cosh R_1 \sin R_2}{K_1 \sin R_2 \cos R_2 + K_2 \sinh R_1 \cosh R_1}$$

$$B_2 = -\frac{K_1 \cosh R_1 \sin R_2 + K_2 \sinh R_1 \cos R_2}{K_1 \sin R_2 \cos R_2 + K_2 \sinh R_1 \cosh R_1}$$

$$K_1 = br \qquad K_2 = bs$$

$$D_1 = B_1(K_1^2 - K_2^2) - 2B_2K_1K_2$$

$$D_2 = B_2(K_1^2 - K_2^2) + 2B_1K_1K_2$$

$$D_3 = B_1K_2 + B_2K_1 \; ; \quad D_4 = B_1K_1 - B_2K_2$$

$$R_1 = K_1 \frac{a}{b} \; ; \quad R_2 = K_2 \frac{a}{b}$$

..... 5.40

where r and s are the roots of equation 2.15.

Other coefficients are:-

$$A_{nq} = \int_0^1 \left(\frac{y}{b} - \frac{1}{2}\right) \cos \frac{n\pi y}{2b} \cos \frac{q\pi y}{2b} \, d\left(\frac{y}{b}\right)$$

$$A_{nq} = -\frac{1}{\left(\frac{n-q}{2}\,\pi\right)^2} \quad \text{if } \left|\frac{n-q}{2}\right| \text{ is odd}$$

..... 5.41

$$A_{nq} = -\frac{1}{\left(\frac{n+q}{2}\,\pi\right)^2} \quad \text{if } \left|\frac{n-q}{2}\right| \text{ is even or zero}$$

$$B_{nq} = \frac{1}{2} \int_0^1 \frac{y}{b}\left(1 - \frac{y}{b}\right) \sin \frac{n\pi y}{2b} \cos \frac{q\pi y}{2b} \, d\left(\frac{y}{b}\right)$$

$$B_{nq} = \frac{1}{\left(\frac{n-q}{2}\,\pi\right)^3} \quad \text{if } \left|\frac{n-q}{2}\right| \text{ is odd}$$

..... 5.42

$$B_{nq} = \frac{1}{\left(\frac{n+q}{2}\,\pi\right)^3} \quad \text{if } \left|\frac{n-q}{2}\right| \text{ is even or zero}$$

$$C_{nq} = \frac{1}{12} \int_0^1 \left\{1 - 3\left(\frac{y}{b}\right)^2 + 2\left(\frac{y}{b}\right)^3\right\} \cos \frac{n\pi y}{2b} \cos \frac{q\pi y}{2b} \, d\left(\frac{y}{b}\right)$$

$$C_{nq} = \frac{1}{\left(\frac{n-q}{2}\,\pi\right)^4} \quad \text{if} \quad \left|\frac{n-q}{2}\right| \text{ is odd}$$

$$C_{nq} = \frac{1}{\left(\frac{n+q}{2}\,\pi\right)^4} \quad \text{if} \quad \left|\frac{n+q}{2}\right| \text{ is even} \qquad \ldots\ldots\ldots \quad 5.43$$

$$C_{nq} = \frac{1}{48} + \frac{1}{\left(\frac{n+q}{2}\,\pi\right)^4} \quad \text{if} \quad \left|\frac{n-q}{2}\right| \text{ is zero}$$

$$A'_{nq} = \int_0^{3/4} \frac{5}{24}\left(3 - 7\,\frac{y}{b}\right) \sin \frac{n\pi y}{2b} \sin \frac{q\pi y}{2b} \, d\left(\frac{y}{b}\right)$$

$$+ \int_{3/4}^{2} \frac{3}{40}\left(-13 + 9\,\frac{y}{b}\right) \sin \frac{n\pi y}{2b} \sin \frac{q\pi y}{2b} \, d\left(\frac{y}{b}\right)$$

valid for $c = {}^3/_4\, b$ 5.44

$$B'_{nq} = \int_0^{3/4} \frac{5}{48}\left(-6 + 7\frac{y}{b}\right)\frac{y}{b}\cos\frac{n\pi y}{2b}\sin\frac{q\pi y}{2b}\,d\left(\frac{y}{b}\right)$$

$$+ \int_{3/4}^{2} \frac{3}{80}\left\{-16 + 26\left(\frac{y}{b}\right) - 9\left(\frac{y}{b}\right)^2\right\}\cos\frac{n\pi y}{2b}\sin\frac{q\pi y}{2b}\,d\left(\frac{y}{b}\right)$$

valid for $c = {}^3/_4 b$ 5.45

$$C'_{nq} = \int_0^{3/4} \frac{5}{144}\left(9 - 7\frac{y}{b}\right)\left(\frac{y}{b}\right)^2\sin\frac{n\pi y}{2b}\sin\frac{q\pi y}{2b}\,d\left(\frac{y}{b}\right)$$

$$+ \int_{3/4}^{2} \frac{3}{80}\left\{-4 + 16\frac{y}{b} - 13\left(\frac{y}{b}\right)^2 + 3\left(\frac{y}{b}\right)^3\right\}\sin\frac{n\pi y}{2b}\sin\frac{q\pi y}{2b}\,d\left(\frac{y}{b}\right)$$

valid for $c = {}^3/_4 b$ 5.46

$$A'_{nq} = \int_0^{1/2} \frac{3}{4}\left(1 - 3\frac{y}{b}\right)\sin\frac{n\pi y}{2b}\sin\frac{q\pi y}{2b}\,d\left(\frac{y}{b}\right)$$

$$+ \int_{1/2}^{2} \frac{1}{12}\left(5\frac{y}{b} - 7\right)\sin\frac{n\pi y}{2b}\sin\frac{q\pi y}{2b}\,d\left(\frac{y}{b}\right)$$

valid for $c = b/2$ 5.47

$$B'_{nq} = \int_0^{1/2} \frac{3}{8}\left(3\frac{y}{b} - 2\right)\frac{y}{b}\cos\frac{n\pi y}{2b}\sin\frac{q\pi y}{2b}\,d\left(\frac{y}{b}\right)$$

$$+ \int_{1/2}^{2} \frac{1}{24}\left(-8 + 14\frac{y}{b} - 5\left(\frac{y}{b}\right)^2\right)\cos\frac{n\pi y}{2b}\sin\frac{q\pi y}{2b}\,d\left(\frac{y}{b}\right)$$

valid for $c = b/2$ 5.48

$$C'_{nq} = \int_0^{1/2} \frac{3}{8}\left\{\left(\frac{y}{b}\right)^2 - \left(\frac{y}{b}\right)^3\right\}\sin\frac{n\pi y}{2b}\sin\frac{q\pi y}{2b}\,d\left(\frac{y}{b}\right)$$

$$+ \int_{1/2}^{2} \frac{1}{72}\left\{-4 + 24\frac{y}{b} - 21\left(\frac{y}{b}\right)^2 + 5\left(\frac{y}{b}\right)^3\right\}\sin\frac{n\pi y}{2b}\sin\frac{q\pi y}{2b}\,d\left(\frac{y}{b}\right)$$

valid for $c = b/2$ 5.49

$$A'_{nq} = \int_0^{b/4} \frac{7}{8}\left(1 - 5\frac{y}{b}\right)\sin\frac{n\pi y}{2b}\sin\frac{q\pi y}{2b}\,d\left(\frac{y}{b}\right)$$

$$+ \int_{1/4}^{2} \frac{1}{56}\left(11\frac{y}{b} - 15\right)\sin\frac{n\pi y}{2b}\sin\frac{q\pi y}{2b}\,d\left(\frac{y}{b}\right)$$

valid for $c = b/4$ 5.50

$$B'_{nq} = \int_0^{1/4} \frac{7}{16}\left(-2 + 5\frac{y}{b}\right)\frac{y}{b}\cos\frac{n\pi y}{2b}\sin\frac{q\pi y}{2b}\,d\left(\frac{y}{b}\right)$$

$$+ \int_{1/4}^{2} \frac{1}{112}\left(-16 + 30\frac{y}{b} - 11\frac{y^2}{b^2}\right)\cos\frac{n\pi y}{2b}\sin\frac{q\pi y}{2b}\,d\left(\frac{y}{b}\right)$$

valid for $c = b/4$ 5.51

$$C'_{nq} = \int_0^{1/4} \frac{7}{48}\left(3 - 5\frac{y}{b}\right)\left(\frac{y}{b}\right)^2\sin\frac{n\pi y}{2b}\sin\frac{q\pi y}{2b}\,d\left(\frac{y}{b}\right)$$

$$+ \int_{1/4}^{2} \frac{1}{336}\left(-4 + 48\frac{y}{b} - 45\left(\frac{y}{b}\right)^2 + 11\left(\frac{y}{b}\right)^3\right)\sin\frac{n\pi y}{2b}\sin\frac{q\pi y}{2b}\,d\left(\frac{y}{b}\right)$$

valid for $c = b/4$ 5.52

$$D_{mp} = \int_0^1 \sinh R_1\frac{x}{a}\sin R_2\frac{x}{a}\sin\frac{m\pi x}{2a}\sin\frac{p\pi x}{2a}\,d\left(\frac{x}{a}\right)$$

$$D_{mp} = \sinh R_1\left\{C_1\cos\left(R_2 + \frac{m+p}{2}\pi\right) + C_2\cos\left(R_2 - \frac{m+p}{2}\pi\right)\right.$$

$$\left. - C_3\cos\left(R_2 + \frac{m-p}{2}\pi\right) - C_4\cos\left(R_2 - \frac{m-p}{2}\pi\right)\right\}$$

$$+ \cosh R_1\left\{- C_5\sin\left(R_2 + \frac{m+p}{2}\pi\right) - C_6\sin\left(R_2 - \frac{m+p}{2}\pi\right)\right.$$

$$+ C_7 \sin(R_2 + \frac{m-p}{2}\pi) + C_8 \sin(R_2 - \frac{m-p}{2}\pi)\}$$

valid for all integers of m and p 5.53

$$E_{mp} = \int_0^1 \cosh R_1 \frac{x}{a} \cos R_2 \frac{x}{a} \sin \frac{m\pi x}{2a} \sin \frac{p\pi x}{2a} \, d(\frac{x}{a})$$

$$E_{mp} = \cosh R_1 \{-C_1 \sin(R_2 + \frac{m+p}{2}\pi) - C_2 \sin(R_2 - \frac{m+p}{2}\pi)$$

$$+ C_3 \sin(R_2 + \frac{m-p}{2}\pi) + C_4 \sin(R_2 - \frac{m-p}{2}\pi)\}$$

$$+ \sinh R_1 \{-C_5 \cos(R_2 + \frac{m+p}{2}\pi) - C_6 \cos(R_2 - \frac{m+p}{2}\pi)$$

$$+ C_7 \cos(R_2 + \frac{m-p}{2}\pi) + C_8 \cos(R_2 - \frac{m-p}{2}\pi)\}$$

valid for all integers of m and p 5.54

$$F_{mp} = \int_0^1 \cos \frac{m\pi x}{2a} \cos \frac{p\pi x}{2a} \, d(\frac{x}{a}) = \int_0^1 \sin \frac{m\pi x}{2a} \sin \frac{p\pi x}{2a} \, d(\frac{x}{a})$$

$$F_{mp} = 0 \quad \text{if} \quad \left|\frac{m-p}{2}\right| \neq 0$$

$$F_{mp} = \frac{1}{2} \quad \text{if} \quad \left|\frac{m-p}{2}\right| = 0 \qquad \text{.....} \quad 5.55$$

$$G_{mp} = \int_0^1 \sinh R_1 \frac{x}{a} \cos R_2 \frac{x}{a} \sin \frac{m\pi x}{2a} \cos \frac{p\pi x}{2a} \, d\left(\frac{x}{a}\right)$$

$$G_{mp} = (-1)^{\frac{m-p}{2}} \{(C_1 - C_2 - C_3 + C_4) \sinh R_1 \cos R_2$$

$$- (C_5 - C_6 - C_7 + C_8) \cosh R_1 \sin R_2\}$$

valid for odd integers of m and p 5.56

$$G'_{mp} = \int_0^1 \sinh R_1 \frac{x}{a} \cos R_2 \frac{x}{a} \cos \frac{m\pi x}{2a} \sin \frac{p\pi x}{2a} \, d\left(\frac{x}{a}\right)$$

$$G'_{mp} = \sinh R_1 \{-C_1 \cos(R_2 + \frac{m+p}{2}\pi) + C_2 \cos(R_2 - \frac{m+p}{2}\pi)$$

$$+ C_3 \cos(R_2 + \frac{m-p}{2}\pi) - C_4 \cos(R_2 - \frac{m-p}{2}\pi)\}$$

$$+ \cosh R_1 \{C_5 \sin(R_2 + \frac{m+p}{2}\pi) - C_6 \sin(R_2 - \frac{m+p}{2}\pi)$$

$$- C_7 \sin(R_2 + \frac{m-p}{2}\pi) + C_8 \sin(R_2 - \frac{m-p}{2}\pi)\}$$

valid for all integers of m and p 5.57

$$I_{mp} = \int_0^1 \sinh R_1 \frac{x}{a} \sin R_2 \frac{x}{a} \cos \frac{m\pi x}{2a} \cos \frac{p\pi x}{2a} \, d\left(\frac{x}{a}\right)$$

$$I_{mp} = (-1)^{\frac{m-p}{2}} \{(C_1 + C_2 - C_3 - C_4) \sinh R_1 \cos R_2$$

$$- (C_5 + C_6 - C_7 - C_8) \cosh R_1 \sin R_2\}$$

valid for odd integers of m and p 5.58

$$J_{mp} = \int_0^1 \cosh R_1 \frac{x}{a} \cos R_2 \cos \frac{m\pi x}{2a} \cos \frac{p\pi x}{2a} \, d\left(\frac{x}{a}\right)$$

$$J_{mp} = (-1)^{\frac{m-p}{2}+1} \{(C_1 + C_2 - C_3 - C_4) \cosh R_1 \sin R_2$$

$$+ (C_5 + C_6 - C_7 - C_8) \sinh R_1 \cos R_2\}$$

valid for odd integers of m and p 5.59

$$K_{mp} = \int_0^1 \cosh R_1 \frac{x}{a} \sin R_2 \frac{x}{a} \sin \frac{m\pi x}{2a} \cos \frac{p\pi x}{2a} \, d\left(\frac{x}{a}\right)$$

$$K_{mp} = (-1)^{\frac{m-p}{2}} \{(C_1 - C_2 - C_3 + C_4) \cosh R_1 \sin R_2$$

$$+ (C_5 - C_6 - C_7 + C_8) \sinh R_1 \cos R_2\} \quad \ldots\ldots \quad 5.60$$

valid for odd integers of m and p

$$K'_{mp} = \int_0^1 \cosh R_1 \frac{x}{a} \sin R_2 \frac{x}{a} \cos \frac{m\pi x}{2a} \sin \frac{p\pi x}{2a} \, d\frac{x}{a}$$

$$K'_{mp} = \cosh R_1 \{- C_1 \sin(R_2 + \frac{m+p}{2}\pi) + C_2 \sin (R_2 - \frac{m+p}{2}\pi)$$

$$+ C_3 \sin (R_2 + \frac{m-p}{2}\pi) - C_4 \sin (R_2 - \frac{m-p}{2}\pi)\}$$

$$+ \sinh R_1 \{- C_5 \cos (R_2 + \frac{m+p}{2}\pi) + C_6 \cos (R_2 - \frac{m+p}{2}\pi)$$

$$+ C_7 \cos (R_2 + \frac{m-p}{2}\pi) - C_8 \cos (R_2 - \frac{m-p}{2}\pi)\}$$

valid for all integers of m and p $\quad \ldots\ldots\ldots$ 5.61

where

$$C_1 = \frac{1}{4} \frac{R_2 + \frac{m+p}{2}\pi}{R_1^2 + (R_2 + \frac{m+p}{2}\pi)^2}$$

$$C_2 = \frac{1}{4} \frac{R_2 - \frac{m+p}{2}\pi}{R_1^2 + (R_2 - \frac{m+p}{2}\pi)^2}$$

$$C_3 = \frac{1}{4} \frac{R_2 + \frac{m-p}{2}\pi}{R_1^2 + (R_2 + \frac{m-p}{2}\pi)^2}$$

$$C_4 = \frac{1}{4} \frac{R_2 - \frac{m-p}{2}\pi}{R_1^2 + (R_2 - \frac{m-p}{2}\pi)^2}$$

$$C_5 = \frac{1}{4} \frac{R_1}{R_1^2 + (R_2 + \frac{m+p}{2}\pi)^2}$$

$$C_6 = \frac{1}{4} \frac{R_1}{R_1^2 + (R_2 - \frac{m+p}{2}\pi)^2}$$

$$C_7 = \frac{1}{4} \frac{R_1}{R_1^2 + (R_2 + \frac{m-p}{2}\pi)^2}$$

$$C_8 = \frac{1}{4} \frac{R_1}{R_1^2 + (R_2 - \frac{m-p}{2}\pi)^2}$$

..... 5.62

APPENDIX 5

Determination of the stress function using the Rayleigh-Ritz method in conjunction with the principle of Minimum Complementary Energy

The complementary energy of a heated plate can be written as:-

$$U^* = \frac{1}{2E} \int_{-a}^{a} \int_{-b}^{b} \{\sigma_x^2 + \sigma_y^2 - 2\nu\,\sigma_x\sigma_y + 2(1+\nu)\tau_{xy} + 2E\alpha T(\sigma_x + \sigma_y)\}\,dxdy \quad \ldots\ldots\ldots \quad 5.63$$

For simply connected regions, the stress distribution has been shown to be independent of the elastic constants; thus:-

$$U^* = \frac{1}{2E} \int_{o}^{a} \int_{o}^{b} \{(\frac{\partial^2\phi}{\partial y^2})^2 + (\frac{\partial^2\phi}{\partial x^2})^2 + 2(\frac{\partial^2\phi}{\partial x\partial y})^2 + 2E\alpha T\,(\frac{\partial^2\phi}{\partial y^2} + \frac{\partial^2\phi}{\partial x^2})\}\,dxdy \quad \ldots\ldots\ldots \quad 5.64$$

The integration is carried out over one quadrant of the plate if a symmetrical temperature distribution is considered. It can be assumed that the stress function, satisfying the boundary conditions

$$\sigma_x = \tau_{xy} = 0 \text{ at } x = \pm a$$
$$\sigma_y = \tau_{xy} = 0 \text{ at } y = \pm b \quad \ldots\ldots\ldots \quad 5.65$$

can be expressed as:-

$$\phi = (x^2 - a^2)^2 (y^2 - b^2)^2 (\gamma_1 + \gamma_2 x^2 + \gamma_3 y^2 + \gamma_4 x^2 y^2) \quad \ldots\ldots\ldots \quad 5.66$$

Using the Rayleigh-Ritz procedure, the condition for minimum complementary energy of the plate is

$$\frac{\partial U^*}{\partial \gamma_1} = \frac{\partial U^*}{\partial \gamma_2} = \frac{\partial U^*}{\partial \gamma_3} = \frac{\partial U^*}{\partial \gamma_4} = 0 \quad \ldots\ldots\ldots \quad 5.67$$

This operation leads to four linear simultaneous equations for the parameters γ_1, γ_2, γ_3 and γ_4, viz:-

$$\left\{\frac{64}{7} + \frac{256}{49}k + \frac{64}{7}k^2\right\}\gamma_1 + \left\{\frac{64}{77} + \frac{64}{49}k^2\right\}\gamma_2 a^2 + \left\{\frac{64}{49} + \frac{64}{77}k^2\right\}\gamma_3 b^2$$

$$+ \left\{\frac{64}{539} + \frac{64}{539}k^2\right\}\gamma_4 b^2 a^2 = -\frac{9.5.5}{256 a^9 b^5} \int_0^a \int_0^b 2E\alpha T \frac{\partial}{\partial \gamma_1}\left(\frac{\partial^2 \phi}{\partial y^2} + \frac{\partial^2 \phi}{\partial x^2}\right) dx dy$$

$$\left\{\frac{64}{11} + \frac{64}{7}k^2\right\}\gamma_1 + \left\{\frac{192}{143} + \frac{256}{77}k + \frac{192}{7}k^2\right\}\gamma_2 a^2 + \left\{\frac{64}{77} + \frac{64}{77}k^2\right\}\gamma_3 b^2$$

$$+ \left\{\frac{192}{1001} + \frac{192}{77}k^2\right\}\gamma_4 b^2 a^2 = -\frac{9.7.5.5}{256 a^{11} b^5} \int_0^a \int_0^b 2E\alpha T \frac{\partial}{\partial \gamma_2}\left(\frac{\partial^2 \phi}{\partial y^2} + \frac{\partial^2 \phi}{\partial x^2}\right) dx dy$$

$$\left\{\frac{64}{7} + \frac{64}{11}k^2\right\}\gamma_1 + \left\{\frac{64}{77} + \frac{64}{77}k^2\right\}\gamma_2 a^2 + \left\{\frac{192}{7} + \frac{256}{77}k + \frac{192}{143}k^2\right\}\gamma_3 b^2$$

$$+\left\{\frac{192}{77}+\frac{192}{1001}k^2\right\}\gamma_4 b^2a^2 = -\frac{9.7.5.5}{256a^9b^7}\int_o^a\int_o^b 2E\alpha T\frac{\partial}{\partial\gamma_3}\left(\frac{\partial^2\phi}{\partial y^2}+\frac{\partial^2\phi}{\partial x^2}\right)dxdy$$

$$\left\{\frac{64}{11}+\frac{64}{11}k^2\right\}\gamma_1+\left\{\frac{192}{143}+\frac{192}{11}k^2\right\}\gamma_2a^2+\left\{\frac{192}{11}+\frac{192}{143}k^2\right\}\gamma_3b^2$$

$$+\left\{\frac{576}{143}+\frac{276}{121}k+\frac{576}{143}k^2\right\}\gamma_4 b^2a^2 = \frac{9.7.7.5.5}{256a^{11}b^7}\int_o^a\int_o^b 2E\alpha T\frac{\partial}{\partial\gamma_4}\left(\frac{\partial^2\phi}{\partial y^2}+\frac{\partial^2\phi}{\partial x^2}\right)dxdy$$

$$\text{where } k = \frac{b^2}{a^2} \qquad \ldots\ldots\ldots \quad 5.68$$

For a symmetrical 'tent-like' temperature distribution, the temperature in the first quadrant can be expressed as $T = T_o(1 - y/b)$. Substituting this equation in the above set simultaneous equations and then integrating, the values of the parameters can be found. In many cases it is more convenient to express the stress function in the following form:-

$$\phi = b^2E\alpha T_o\left(\frac{x^2}{a^2}-1\right)^2\left(\frac{y^2}{b^2}-1\right)^2\left(\beta_1+\beta_2\frac{x^2}{a^2}+\beta_3\frac{y^2}{b^2}+\beta_4\frac{x^2y^2}{a^2b^2}\right) \quad \ldots\ldots \quad 5.69$$

where β_1, β_2, β_3 and β_4 are non-dimensional parameters related to γ_1, γ_2, γ_3 and γ_4 by the equations:-

$$E\alpha T_o\beta_1 = \gamma_1a^4b^2 \qquad E\alpha T_o\beta_3 = \gamma_3a^4b^4$$

$$\ldots\ldots\ldots \quad 5.70$$

$$E\alpha T_o\beta_2 = \gamma_2a^6b^2 \qquad E\alpha T_o\beta_4 = \gamma_4a^6b^4$$

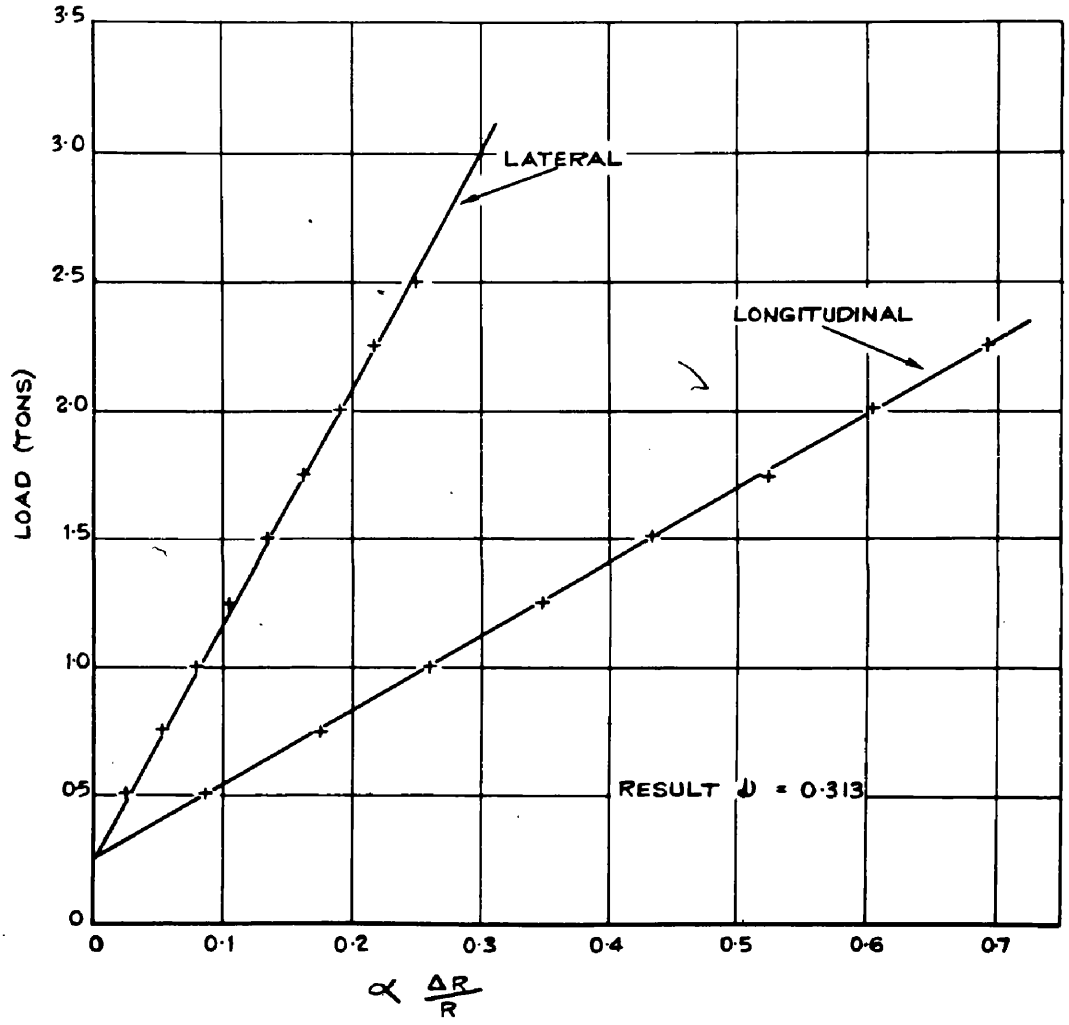

Figure 70: Mechanical Characteristics Poisson's Ratio.

APPENDIX 6

Material Characteristics and Properties

(1) Poisson's Ratio

Test pieces of TI.224 aluminium alloy were subjected to tensile loads in a 50 ton Denison Universal Testing Machine. Saunders-Roe $\frac{1}{2}$ in. electrical foil resistance strain gauges were fixed to the specimen in the longitudinal and transverse directions. Using a Strain Resistance Bridge, readings of increase of resistance and applied load were taken. Figure 70 shows typical readings of longitudinal and transverse strain plotted against applied load.

From the results of the tests the average value of Poisson's Ratio was found to be: $\nu = 0.313$.

(2) Calibration of Vacron-Eureka Thermocouples

The thermocouples were calibrated using a vacuum flask containing melting ice ($0^{\circ}C.$) to provide a cold source and a hypsometer with steam at $100^{\circ}C.$ to provide a hot source.

The e.m.f. generated between the hot and cold junctions was measured by a Cambridge Instrument Company portable potentiometer.

The calibration was repeated with the switches of the 'Thermal Buckling' apparatus incorporated in the circuit.

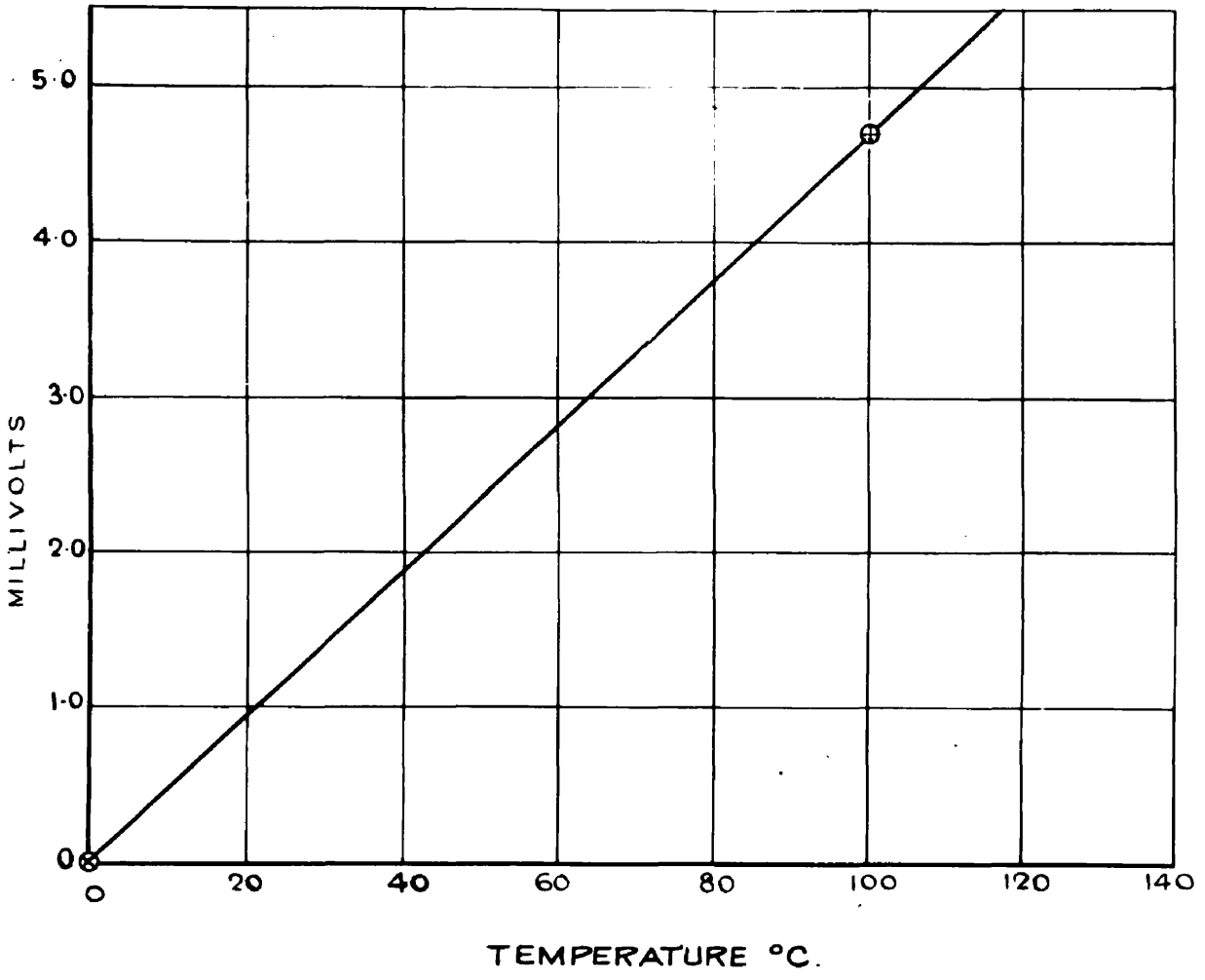

Figure 71: Thermocouple calibration curve.

Results: Temperature Differential = 100°C.

E.M.F. of thermocouple = 4.70 m.V.

A standard parabolic curve for a Vacron-Eureka junction was fitted after adjustments, between the two calibrated points. It was found that the deviation of the curve from the straight line joining these two points did not at any point exceed $-\frac{1}{4}$°C. For practical purposes, the straight line calibration was therefore adopted, (figure 71).

BIBLIOGRAPHY

1. DUHAMEL, J.M.C. — Memoire sur le calcul des actions moleculaires developpees par les changements de temperature dans les corps solides. Mem. inst. France, 5, 440-498 (1838).

2. NEUMANN, F.E. — Die Gesetze der Doppelbrechung des Lichts in Comprimirten oder ungleichformig erwarmten unkrystallinischen Korpern, Abhandl. koniglichen. Akad. Wiss. Berlin. Zweiter Teil. pp.1-254 (1841).

3. HOPKINSON, J. — On the stresses caused in an elastic solid by inequalities of temperature. Messenger Math. 8. 168-174 (1879).

4. TIMOSHENKO S. and GOODIER, J.W. — 'Theory of Elasticity' 2nd ed. McGraw-Hill Book Co. Inc., New York, 1951. pp.399-437.

5. DEN HARTOG, J.P. — Temperature stresses in flat plates. Journal Franklin Institute 1936. Vol. 222. pp.149-181.

6. KLOSNER, J. and FORRAY, M. — Buckling of simply supported plates under arbitrary symmetrical temperature distributions. Republic Aviation Corp. Report No. E-SAM-15, April 1956.

   An abridged form of this report is published in J. Aero. Sci. Vol. 25. 1958. pp.181-184.

7. MENDELSON, A. and HIRSCHBERG, M. — Analysis of elastic thermal stresses in thin plates with spanwise and chordwise variation of temperature and thickness. N.A.C.A. Technical Note 3778. Nov. 1956.

8. HORVAY, J. — The end problem of rectangular strips. Jour. App. Mechanics. Vol. 20. March 1953. p.87.

9. HORVAY, G. and BORN, J.S. — Tables of self-equilibrating functions. Jour. Maths. and Physics. Vol. 33. No. 4. Jan. 1955.

10. HELDENFELS, R. and ROBERTS, W. — Experimental and theoretical determination of thermal stresses in a flat plate. N.A.C.A. Technical Note 2769. Aug. 1952.

11. PORITSKY, H., JERRARD, R.P., JONES, N.M. and WEIDLER, S.E. — Thermal stresses in turbine buckets. DF-52GL27. Tech. Information Ser. Gen. Elect. Lab., General Electric Co., Schenectody (N.Y.). Feb. 18. 1952.

12. SINGER, J. — Distribution of Thermal Stresses in Solid Wings. W.A.D.C. Report No. 57-69. April 1957.

13. GOSSARD, M.L., SEIDE, P. and ROBERTS, W.M. — Thermal buckling of plates. N.A.C.A. Technical Note 2771. Aug. 1952.

14. SOKOLNIKOFF, I.S. — Mathematical Theory of Elasticity. 1st ed. McGraw-Hill Book Co. Inc. pp.281 and 313.

15. TIMOSHENKO, S. — Theory of Elastic Stability. McGraw-Hill Book Co. Inc. 1936. p.333. Art. 64.

16. TIMOSHENKO, S. and GOODIER, J.W. — Theory of Elasticity. 2nd ed. McGraw-Hill Book Co. Inc. New York 1951. Art. 23. pp.46-53.

17. VON KARMAN, T. and BIOT, M.A. — Mathematical Methods in Engineering. 1st ed. McGraw-Hill Book Co. Inc. 1940. pp.196-203.

18. GATEWOOD, B.E. — Thermal Stresses. McGraw-Hill Book Co. Inc. New York 1957. pp.200-201 and pp.175-179.

19. KENEDI, R.M., SMITH, W.S. and FAHMY, F.O. — Lightweight structures - research and application to economic design. Inst. of Eng. and Shipbuilders in Scotland, 1956.

20. BROWN, M.A.M. — Analytical and experimental investigation of the thermal buckling of flat plates. Thesis presented for the award of the Associateship of the Royal College of Science and Technology, Glasgow.

21. HEMP, W.S. — Fundamentals, principles and methods of thermo-elasticity. Aircraft Engineering. Vol. 26. 1954. pp.126-127.

ACKNOWLEDGEMENTS

The work presented in the thesis was carried out in the Laboratories of the Department of Mechanical, Civil and Chemical Engineering, The Royal College of Science and Technology, Glasgow.

The author wishes to express his thanks to the following members of the staff:-

Professor A.S.T. Thomson, D.Sc., Ph.D., A.R.C.S.T., M.I.C.E., M.I.Mech.E.

and

R.M. Kenedi, B.Sc., Ph.D., A.R.C.S.T., A.M.I.Mech.E., A.F.R.Ae.S.,

for permission to use the facilities of the College laboratories and workshops and their continued interest in the research project.